Very Large Telescope

SPHERE

User Manual

Reference	PDM-ESO-254263 VLT-MAN-SPH-14690-0430
Issue	P118
Status	20th public release (P118, phase 2)
Date of Issue	2026-11-24

Prepared *Z. Wahhaj, M. Jones, Célia Desgrange, R. de Rosa, F. Rodler, M. van den Ancker, H. Boffin, J. Olofsson.* *Early contributors: D. Mouillet, J. Girard, D. Mawet, J.Milli, A. Vigan, M. Kasper, R. Siebenmorgen and the SPHERE consortium*	***Date*** *2026-11-24*	***Signature***
Approved *S. Mieske*	***Date***	***Signature***
Released *A. Kaufer*	***Date***	***Signature***

The SPHERE consortium:

- Institut de Planétologie et d'Astrophysique de Grenoble, France (PI institute)
- Max-Planck-Institut für Astronomie, Heidelberg, Germany (co-PI institute)
- Laboratoire d'Astrophysique de Marseille, France
- Observatoire de Genève, Switzerland
- Laboratoire Lagrange, Nice, France
- The Italian National Institute for Astrophysics coordinated by the Osservatorio Astronomico di Padova, Italy
- Laboratoire d'Etudes Spatiales et d'Instrumentation en Astrophysique, Paris, France
- Eidgenössische Technische Hochschule (ETH) Zürich, Switzerland
- The Astronomical Institute Anton Pannekoek, University of Amsterdam, the Netherlands
- Office National d'Etudes et de Recherches Aérospatiales, Châtillon, France
- The Netherlands Research School for Astronomy (NOVA-ASTRON), the Netherlands
- The European Southern Observatory (ESO)

Change Record

Issue	**Section**	**Comments**
V95	All	First public draft
V95.1	8, Appendix	Added description of templates in Chapter 8 and associated tables in the Appendix.
V96.1	Many	Science Calibration Plan overview Beta ETC: + links IRDIS Astrometry IFS data reduction Inconsistencies Removed 4Q mask, Added ALC_YH_S mask Large NDIT Warning Added ZIMPOL saturation limits Comment on ND filters Warning about current ETC Clarification about provided flat field in IRDIS/LSS Updated IRDIS filters section Updated IFS dispersive elements information Added information on astrometry in Section 7 Several additions for LSS Corrected execution time calculation and overheads for IRDIFS observations IRDIS DPI mode Quality Assessment Low Wind Effect (LWE)
V97.1	Many	IRDIS_LSS mode offered in service if time critical (section 1.7) More information on the low wind effect (section 5.2) SPARTA files to review image quality now available in ESO archive (section 5.3) IRDIFS mode can now use BB_H filter. IRDIFS_EXT mode can now use BB_Ks filter (section 12.6) Getting calibration files from ESO archive (section 10.1)

Issue	**Section**	**Comments**

V99.0	Many	General reformatting Information on astrometric calibration More information on IRDIS DPI & link to the dedicated page
V100.0	5, 6, 7, 8, Appendix.	Table 4: R>11 GS are now offered in SM as well as SAM as a new setup for IRDI(F)S (all modes but LSS) Updated information on coronagraphic transmission (section A6), sky offsets (section 7.4), SPARTA files (section 5.3) and true north determination (section 8). SAM: Sparse Aperture Masking (several sections) GoTo acquisition template Rapid Response Modes (RRM) added. Sidereal constraints for meridian observations described.
V101.0		IRDIS/LSS mode with apodizer option. Correction on page 14 on SM Rmag limit. Correction on page 63/64 on astrometry/ orientation of North. Minor corrections on filters/coronagraphs/template listings in Appendix. Added recommendation to not use coronagraph for R > 11 in Sec 3 (Daniela Iglesias Project). IRDIS DPI will have dithering capability from P101. Templates with SAM masks updated in Appendix.
V102.0	3, 4, 5, 6, 9, A5.	Warning that spot at center of coronagraph does not show the stellar position (section 3.1.1). IRDIS DPI comment for ETC added (section 4). New grading scheme promoting importance of coherence time described (section 5.1) The vast improvement on the LWE effect problem described (section 5.2) Warning that sky offsets are cumulative for both IRDIFS and ZIMPOL (section 6). Added SAM mask position table in section 6. Reminder that IRDIS DPI problems with polarimetric efficiency occur only in field tracking. (section 6.1.8) Advice on 3 degree avoidance during meridian crossing and removing twilight constraint (section 6). IRDIS DPI template description updated to show dithering parameters (section 9). IRDIS linearity limit updated to 20000 ADU for all DITs (Appendix A1). IRDIS CI NB ghost images link to SPHERE web page added (section 6 and A5). IRDIS filters widths corrected to same values as on SPHERE web page (A5). Added image of new ghosts found in IRDIS in Appendix 5.
V103.1	5, 7, 9.	Further explanation of seeing and coherence time constraints used for phase 1, phase 2 and OB grading. Star hopping templates added for small jumps between stars (similar to GoTo): SPHERE_gen_acq_starhop, SPHERE_gen_acq_hopback (section 7, 9). Table 12 changed to reflect ATM categories. Link to OBJECT, AO files changed (section 5.3).
V104.1	3, 7	Further explanation of LSS mode, including PA offset and exposure time estimates Correction of mistakes Additional information on DPI Pupil tracking
V104.2	8, 7, Appendix A1.	Correction to the calibration plan. Strongly recommend that Flux and Center be included as separate templates before the main science templates. For DITs > 2 secs, IRDIFS exposures will not be changed up to 35K ADU (1% linearity) during observations. Users still asked to stay below 20K ADU when designing OBs.
V105.1	5, 7, 10.	Turbulence categories replace ATM conditions from P105 (Section 5 and 7). Star-hopping with RDI recommended as alternative to ADI (Section 7). IRDIS/DPI HWP control law improved (Section 7.1.8) IRDIS/DPI in pupil tracking offered in SM. New pipeline for polarimetry (Section 10.1.2). IRDIS/LSS N_S_LR_WS option removed for P105. Will return in P106.

V106.1	8.	Sign for PUPIL_offset in de-rotation equation corrected (section 8.1.3).
V106.2	7, Appendix A12.	For the star center observations (obs. Type=C), the WAFFLE pattern amplitude in all cases is calculated automatically and should be left as “AUTO” by default.
V107.1	3, 7.	Further details on faint star performance (section 3). Further details on Star-hopping RDI and special data reduction pipeline (section 7).
V111.1	1, 3, 9.	IRDIS LSS mode can be done in service without restrictions (section 1). Coronagraphs can be used for stars as faint as H=12 as new DTTS mode was implemented (section 3). Removed P45_135 polarizer options as these suffer from large polarization crosstalk (section 9, see van Holstein et al. 2020).
V113.1	5, 8, various.	Add specific recommendation of TCAT for faint star observations by Gmag (section 5). Made a correction removing the note that high and zero polarization standard stars are observed in IRDIS DPI mode every 30 days (section 8.1.1). Corrected various other typos in all sections.
V114.1	3, 7.	Section 3.1: Faint star performance text and figures updated. New figure on Strehl ratio vs PSF FWHM added. Added subsection on improved performance at G~11.5. Section 7.1: Star-hopping ref stars should have G mag within 1 mag of science star. Section 7.1.17.1: Zimpol Dithering explanation has been updated.
V118.1	Sections: 1–7, 10, 11, Appendix.	Section 1: Clarified noise regimes in high-contrast imaging. Improved descriptions of SDI and PDI and added relevant references. Section 2: Corrected references to instrument layout figures. Sections 3, 5 and 6: Clarified the use of Gaia G magnitudes for AO performance predictions, turbulence category recommendations and ZIMPOL limiting magnitudes. Section 3: Clarified the position angle correction required when preparing IRDIS/LSS OBs. Section 6: Clarified the possibility of requesting waivers for longer OBs in Service Mode. Appendix A6, A7, A8 and A9: Corrected notation, table entries and missing cross-references. Minor corrections to terminology, formatting, figure captions and typographical errors throughout the document.

LIST OF ACRONYMS

ADC	Atmospheric Dispersion Corrector
ADI	Angular Differential Imaging
AO	Adaptive Optics
APLC	Apodized Pupil Lyot Coronagraph
ATM	Atmospheric Turbulence Model
BB	Broadband
CI	Classical Imaging
CLC	Classical Lyot Coronagraph
CP	Common Path
DBI	Dual Band Imaging
DD	Double Difference
DIT	Detector Integration Time
DM	Deformable Mirror
DMS	Detector Motion Stage
DPI	Dual Polarization Imaging
DRH	Data Reduction and Handling
DTTP	Differential Tip Tilt Plate
DTTS	Differential Tip Tilt Sensor
ESP	Extra-Solar Planet
ETC	Exposure Time Calculator
FF	Flat-field
FLC	Ferro-electric Liquid Crystal
FoV	Field of View
FP	Focal Plane
HA	Hour Angle
HAR	High angular resolution
HF	High Frequency
HODM	High Order Deformable Mirror
HW	Hardware
HWP	Half Wave Plate
IFS	Integral Field Spectrometer
INS	Instrument Software
IRDIS	IR Differential Imaging Spectrometer
ITTM	Image Tip-Tilt Mirror
IWA	Inner Working Angle
LOCI	Locally Optimized Combination of Images
LRS	Low resolution spectroscopy
LSS	Long Slit Spectroscopy
LWE	Low Wind Effect
mas	milli-arcseconds
MRS	Medium Resolution Spectroscopy
NB	Narrowband
NCPA	Non Common-Path Aberrations
NDIT	Number of DIT
NGC	New Generation Controller
NIR	Near Infrared
NRM	Non-Redundant Masking, also called SAM (Sparse Aperture Masking)

PCA	Principal Component Analysis
PDI	Polarimetric Differential Imaging (data reduction technique applied for data obtained in DPI mode)
PCOM	Polarization Compensator
PSF	Point Spread Function
PTTM	Pupil Tip-Tilt Mirror
QWP	Quarter-Wave Plate
RDI	Reference Differential Imaging
RON	Readout Noise
RTC	Real-Time Computer
RTD	Real-Time Display
SAM	Sparse Aperture Masking, also called NRM (Non-Redundant Masking)
SAXO	Sphere AO for eXoplanet Observation
SC	Science Case
SD	Simple Difference
SDI	Spectral Differential Imaging
SNR	Signal to Noise Ratio
SP	Spectral type
SPHERE	Spectro-Polarimetric High contrast Exoplanet REsearch
SR	Strehl Ratio
tbc	to be confirmed
tbd	to be defined
WFE	WaveFront Error
WFS	WaveFront Sensor
ZIMPOL	Zurich Imaging POLarimeter
ZP	ZeroPoint

Table of contents

List of Acronyms 5

1. Introduction 10
SPHERE in a nutshell 10
High contrast imaging 11
Field and pupil rotation 12
Coronagraphy 12
Angular Differential Imaging (ADI) 13
Spectral Differential Imaging (SDI) 13
Sparse Aperture Masking (SAM) 14
Science case examples 15
Mode offering from P103 16

2. Technical description 17
Common Path Infrastructure (CPI) 17
IFS 18
IRDIS 19
ZIMPOL 20
2.1.1 Hardware 22
2.1.2 Instrumental polarization 23
2.1.3 Detectors 23
2.1.4 Imaging 24
2.1.5 Field of view 24
Instrument combinations 25

3. ADAPTIVE OPTICS Performance 26
SAXO preliminary representative performance 26
Faint star performance 27
Performance improvement at G ~ 11 mag 29
Coronagraphs not recommended for faint targets 29
IRDIS preliminary representative performance 30
3.1.1 IRDIS DBI 30
3.1.2 IRDIS LSS 31
3.1.3 IFS preliminary representative performance 33
3.1.4 ZIMPOL preliminary representative performance 35
3.1.5 SAM preliminary performance 36

4. Exposure time calculators 39

5. Quality assessment 40
5.1 Atmospheric Constraints 40
5.2 Low-wind effect (LWE) 42
5.3 Using SPARTA files to review image quality 43

6. SPHERE observing proposals 44
Observing modes 44
Rapid Response Modes 46
Coronagraphs and filters 46
Sparse Aperture Masks 46
AO limiting magnitudes 47
Telescope time 48

7. Preparing the observations 49
Phase 2 49
Observing constraints 49
Target acquisition templates 51

General user defined parameters for IRDIFS and IRDIS templates **51**
"GoTo" acquisition template **53**
"Starhop and Hopback" templates **53**
IRDIFS templates **55**
7.1.1 Observation templates and user-defined parameters 55
7.1.2 Calibrations 55
IRDIS Dual Band Imaging (DBI) **56**
7.1.3 Observation templates and user-defined parameters 56
7.1.4 Calibrations 56
IRDIS alone Classical Imaging (CI) **56**
7.1.5 Observation templates and user-defined parameters 56
7.1.6 Purpose and properties 56
7.1.7 Calibrations 56
IRDIS Dual Polarization Imaging (DPI) **56**
7.1.8 Instrumental polarization 56
7.1.9 Polarimetry in pupil-tracking mode: advantages and polarimetric efficiency 58
7.1.10 Observation templates and user-defined parameters 59
7.1.11 Calibrations 60
IRDIS alone Long Slit Spectroscopy (LSS) **60**
7.1.12 IRDIS/LSS: Observation templates and user-defined parameters 60
7.1.13 IRDIS/LSS: Purpose and properties 60
7.1.14 IRDIS/LSS: Calibrations 61
ZIMPOL polarimetric imaging **62**
7.1.15 ZIMPOL: Observation templates and user-defined parameters 62
7.1.16 ZIMPOL: P1 or P2 rotation modes for ZIMPOL polarimetry 63
7.1.17 ZIMPOL: Dithering, mosaicking 63
7.1.17.1 Dithering 63
7.1.17.2 Off-axis positions 64
7.1.18 Observing sequences for ZIMPOL polarimetry 64
7.1.18.1 Recommendations for sequences 64
7.1.18.2 Recommended sequences for different types of targets 65
7.1.19 ZIMPOL: polarimetric calibrations 65
ZIMPOL imaging **66**
7.1.20 ZIMPOL Imaging: Observation templates and user-defined parameters 66
7.1.21 ZIMPOL Imaging: Purpose and properties 66
7.1.22 ZIMPOL Imaging:Calibrations 67

8. Calibration plan SUMMARY **68**
Night-time calibrations **68**
8.1.1 Night-time calibrations provided by the observatory 68
8.1.2 Optional night-time calibrations 68
Day-time calibrations **68**
Astrometry **71**
8.1.3 Instrumental distortion and detector orientation in IRDIFS and IRDIFS_EXT 71
8.1.4 Plate scale and true north orientation 71

9. SPHERE Template parameters **73**
SPHERE Acquisition Templates **73**
SPHERE Observation Templates **73**

10. Data reduction **95**
Obtaining calibration files from the ESO archive **95**
IFS reduction cascade summary **95**
IRDIS reduction cascade summary **95**
10.1.1 DBI, classical imaging 95
10.1.2 IRDIS DPI 96

10.1.3 Long slit spectroscopy 96
ZIMPOL reduction cascade summary 96
10.1.4 Imaging 96
10.1.5 Polarimetry 97
AO performance monitoring 97

11. Overheads 98
Target acquisition 98
IRDIS and IFS observation overheads 98
ZIMPOL observation overheads 99

Appendix 101
A1. Detector properties 101
A1.1 IRDIS and IFS detectors 101
A1.2 ZIMPOL detectors 102
A2. System throughput 103
A3. Neutral densities 104
A3.1 CPI 104
A3.2 IFS 105
A3.3 IRDIS 105
A3.4 ZIMPOL 105
A4. IRDIS beam-splitter 106
A5. IRDIS filters 106
A6. NIR Coronagraphs 109
A6.1 ALC coronagraphs 110
A7. IFS dispersive components 112
A8. IRDIS dispersive components 112
A8.1 LSS 112
A8.2 Prism 112
A8.3 Grism 113
A9. Visible Coronagraphs 113
A10. ZIMPOL filters 114
A11. Polarimetric calibration components 117
A12. Waffle spots 117

1. INTRODUCTION

The aim of the SPHERE User Manual is to provide information on the technical characteristics of the instrument, its performance, observing, calibration and data reduction procedures.

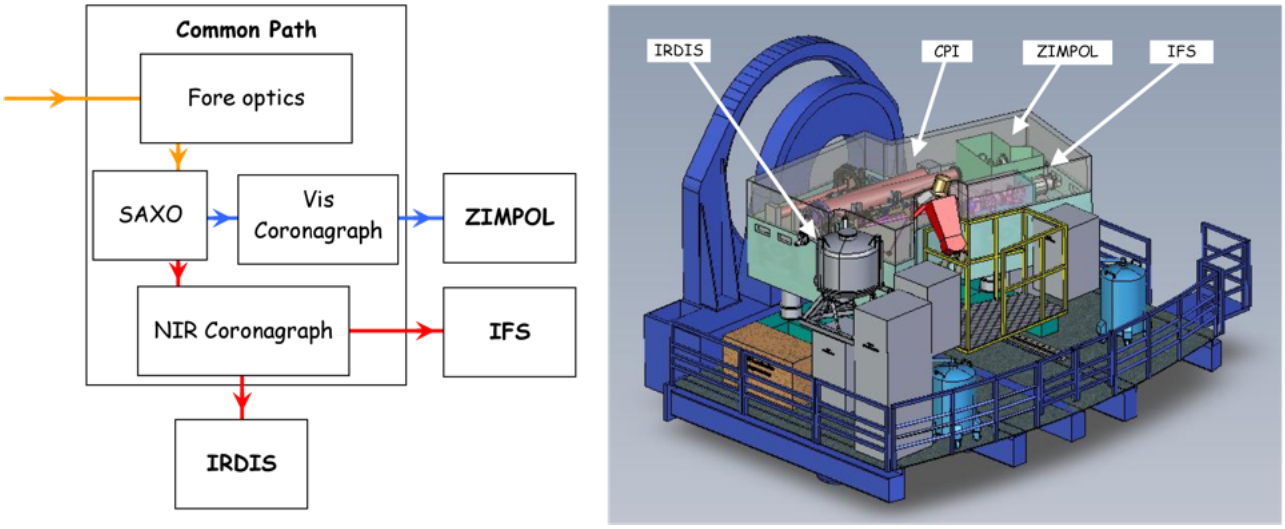

Figure 1: SPHERE sub-systems (left) including the common path (CPI) with adaptive optics system SAXO, coronagraphs, and sub-instruments IRDIS, IFS and ZIMPOL. Left: schematic view of the instrument on the Nasmyth platform.

SPHERE in a nutshell

The primary science goals of SPHERE are imaging, low-resolution spectroscopic, and polarimetric characterization of exoplanets. The instrument design is driven to provide highest image quality and contrast performance in a narrow field around bright targets observed in the visible or near infrared. SPHERE is installed at one of the UT3 Nasmyth foci of the VLT and consists of four subsystems:

CPI: The common path and infrastructure receives direct light from the telescope, and provides highly stabilized, AO-corrected, and coronagraphic beams to the three sub-instruments, described below.

IFS: The integral field spectrograph provides a data cube of 38 monochromatic images either at spectral resolution of R~50 between 0.95 - 1.35µm (Y-J) or at R~30 between 0.95 - 1.65µm (Y-H), see Table 1.

IRDIS: The infrared dual-band imager and spectrograph provides classical imaging (CI), dual-band imaging (DBI), dual-polarization imaging (DPI) in various filters, and long slit spectroscopy (LSS) either between 0.95 – 2.32µm, with resolving power of R~50 (LRS with 0".12 wide slit) or between 0.95 - 1.65µm with R~350 (MRS with 0".09 wide slit), see Table 2.

ZIMPOL: the Zurich imaging polarimeter provides near diffraction limited classical imaging and dual-polarization imaging (DPI) below 30 mas resolution in the visible, see Table 3.
Dichroic splitters allow simultaneous observations with IRDIS and IFS (IRDIFS modes).

Table 1: IFS

Observing mode	Integral field spectroscopy	
Spectral range	0.95–1.35 µm: R~50	0.95 – 1.65 µm: R~30
Sampling	(12.25 mas)^2 / spaxel (hexagonal grid), Nyquist at 0.95 µm. Resampled by the pipeline on a square with (7.4 mas)^2 / pixel.	

FOV	~ 1.73" x 1.73"
Detector type	Hawaii II RG 2048x2048
Coronagraph	None, or with classical or apodized pupil Lyot coronagraphs.
Stabilization	Pupil- or Field-stabilized
WFS	Visible light

Table 2: IRDIS

Observing modes	DBI, DPI, CI	LSS
Spectral range	0.95 – 2.32 µm: NB and BB filters	0.95 - 2.32 µm: R~50 0.95 - 1.65 µm: R~350
Sampling	$(12.25 \text{ mas})^2$ / pixel, Nyquist-sampled at 0.95 µm	
FOV	11" x 11"	11" slit
Detector type	Hawaii II RG 2048 x 1024	
Coronagraph	None, or with classical or apodized pupil Lyot coronagraphs.	Central blocking
Stabilization	Pupil- or Field-stabilized	Field-stabilized
WFS	Visible light	

Table 3: ZIMPOL

Observing modes	Imaging (I), differential polarimetric imaging (P1, P2)
Spectral range	500 – 900 nm in broad and narrowband filters
Sampling	$(7 \text{ mas})^2$ / pixel, diffraction-limited at λ >600 nm
FOV	3.5" x 3.5"
Detectors type	Two 4k × 2k pixel, back-illuminated, frame transfer CCD 220 (e2v CCD 44-82 bi) with 15µm × 15µm pixels, equipped with a stripe mask and a micro-lens array.
Linear polarization	Instrumental polarization <1%, polarimetric sensitivity < 0.1% with fast modulation, simultaneously on two CCDs
Coronagraph	None, or with classical Lyot coronagraphs
Stabilization	- Imaging: pupil or field-stabilized. - Polarimetry: field-stabilized, or fixed derotator with stable and minimized instrumental polarization.
WFS	Visible light shared between WFS and ZIMPOL: - Dichroic for R-band observation: (100% WFS outside R band / 100% R band to ZIMPOL) - Grey beam splitter: (20% WFS / 80% ZIMPOL), with the R-band AO limiting magnitude lowered by ~1.74 mag (from R ≈ 11 mag to R ≈ 9.3 mag for good/median AO performance)

High contrast imaging

When imaging a star one often aims at discovering companions or other faint structures around it. This requires removing the halo produced by the star. However, close to the star, there are point source structures called speckles that evolve over hour long timescales. Speckles are interference images of (atmospheric or instrumental) wavefront corrugations left uncorrected by the AO system, with a typical size of a resolution element (~λ/D). The sensitivity of an exposure is most often limited by these speckles. Subtracting them is the main goal in high contrast imaging. Speckles are a function of wavelength and change with time as optics and atmosphere change.

SPHERE combines various techniques to provide high contrast imaging, with excellent stellar PSF suppression and stability: a high density high frequency AO system that corrects turbulence and static optical aberrations, coronagraphy, and differential imaging, in which images at different wavelengths or polarization states are observed simultaneously (Figure 2).

The AO corrects the incoming wavefront up to ~20 cycles/aperture (20 = half the number of deformable mirror actuators across the pupil), corresponding to a radius = 20 λ/D in the image plane. Within this correction radius, the coronagraph efficiently suppresses the diffraction pattern down to a much fainter residual halo, which is associated with uncorrected wavefront errors. Within this radius, residual AO speckles and photon noise from the stellar halo can limit the sensitivity. Further out (>20 λ/D), the AO system still corrects the PSF of off-axis sources but does not contribute to the suppression of the stellar halo. Far from the star (beyond an arcsecond), the contrast depends on the filter width, number of detector reads and integration time rather than on AO correction (background and detector noise become increasingly important), so that at that location SPHERE performance behaves similar to previous instruments (e.g. NACO). Differential imaging techniques are then used to remove the residual stellar halo and/or speckles (see Section 1).

The stability of the PSF becomes critical when combining observations obtained at different times. This is important for angular differential imaging (ADI) or conventional PSF subtraction. The best PSF stability is obtained when observing in pupil-stabilized mode.

Field and pupil rotation

At the Nasmyth focus, both the pupil and the field rotate when tracking an object. The field rotation is the combination of the parallactic angle and altitude of the object. The pupil rotation is directly related to the altitude of the object being tracked. The SPHERE derotator allows stabilization of either the field or the pupil on the detector. See Figure 35 for examples of field rotation for different target declinations.

In *pupil-stabilized* observations the PSF variability is minimized because most of the optical elements do not move. The telescope pupil is also aligned with the Lyot stops of the instrument, which cover the M2 shadow and its spider arms. The pupil-stabilized mode provides the highest PSF stability and is recommended for coronagraphic observations and for high contrast imaging close to the star. The field rotates with the parallactic angle, enabling *angular differential imaging* (ADI). The center of rotation is the central star. One should then be aware of the trade-off between rotation rate and the smearing of off-axis PSF (see Exposure Time Calculator).

In *field-stabilized* mode, light from a specific location in the field of view falls on a particular location on the detector, throughout the observation. For SPHERE observations this is:

- Mandatory in long slit spectroscopy. The slit shall not rotate during the observation and is defined by the observer.
- Mandatory for ZIMPOL P2 polarimetric mode (see Table 9).
- Recommended when smearing of the image within a DIT becomes an issue (e.g. at larger separation). This may be caused by a long DIT, selected to reduce the RON, or by fast field rotation, while observing close to zenith.

Field-stabilized mode also ensures that a companion image would fall on the same detector pixels (lenslets for IFS). This reduces concern due to flat-fielding; this might improve stability of photometric time series.

For completeness, we mention that instrumental polarization is best understood when the derotator is static and hence does not move.

Coronagraphy

A coronagraph suppresses the coherent light coming from on-axis unresolved source (Figure 2). In SPHERE, all coronagraphs consist of a focal plane mask, followed by a pupil stop and sometimes preceded by an entrance pupil apodizer. SPHERE houses several coronagraphs to accommodate

different observational needs such as spectral range or inner working angle. Coronagraph choices and trade-offs are detailed in the Appendix.

Angular Differential Imaging (ADI)

ADI exploits the fact that the field and the pupil rotate with respect to each other. In pupil-stabilized mode, most speckles are caused by instrumental artifacts and are locked up in the pupil plane, whereas the object of interest, a companion or a disk, will rotate as the field rotates. This allows distinguishing the stellar halo from the object.

Spectral Differential Imaging (SDI)

Planets and the host star have different spectral features. This information can be used to suppress speckle noise. For this, one needs simultaneous images at two similar wavelengths at which the brightness of the planet varies, e.g. in and out of a molecular band. This method is called *spectral differential imaging* (SDI). This approach is used in IRDIS DBI. It can also be used with ZIMPOL imaging when different filters are used in ZIMPOL's two arms (e.g., Hα and continuum).
Simultaneous observation of several monochromatic images can be used to reduce the impact of speckles (Racine et al. 1999; Sparks and Ford, 2002). For a given observation, the location of a companion around a star is constant while the location of speckles from the star increases with wavelength and their intensity decreases. For a wide enough wavelength range this allows subtraction of the speckles. This process is known as *spectral deconvolution* (Thatte et al. 2007). This approach is used in IFS and in IRDIS LSS. Spectral deconvolution uses the wavelength dependence of the speckle pattern over a spectral range and is a form of spectral differential imaging.

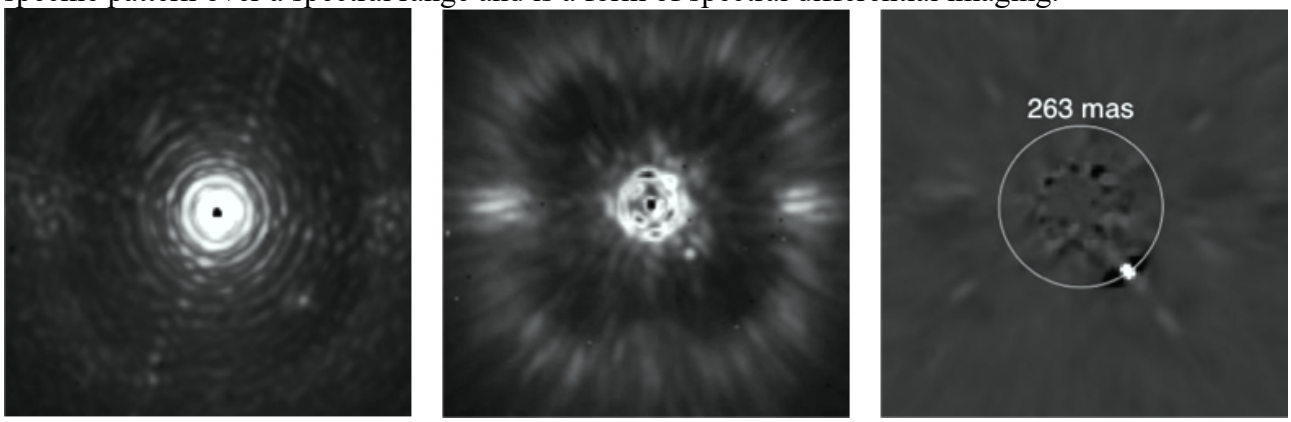

Figure 2: Illustration of the three pillars of high contrast imaging. Left: raw on-sky J-band PSF of SPHERE with IRDIS, showing the diffraction pattern resulting from the almost perfect correction provided by the extreme AO system up to 20 cycles per aperture, and so 20 λ/D in the image (this is half the number of actuators on the deformable mirror on a side). Middle: raw on-sky J-band coronagraphic image of Iota Sgr, illustrating the efficient removal of diffraction rings and pinned speckles by the coronagraph. Note the very visible AO correction radius. Outside the correction radius (r > 20 λ/D), the brighter halo results from the uncorrected wings of the seeing halo. Right: result of angular differential imaging (ADI) strategy, and post-processing using principal component analysis, cleaning the remaining speckles in the field after extreme AO and coronagraphy, revealing a faint off-axis companion.

Stars are often unpolarized, whereas circumstellar environments and planets may be highly polarized. This feature is used to increase the image contrast and is called *dual polarization imaging* (DPI). DPI is used in ZIMPOL polarimetric imaging and in IRDIS DPI. DPI refers to the observing mode; polarimetric differential imaging (PDI) is the associated data reduction technique.

Sparse Aperture Masking (SAM)

Sparse Aperture Masking (SAM) is one of the first extended modes offered to the community.
SAM is an interferometric technique for recovering high contrast structures at small angular separations. A small opaque pupil-plane mask with 1-meter circular sub-apertures (holes) turns a telescope into a Fizeau interferometer, changing the instrument PSF into an interference "snow flake" pattern.

The primary advantage of observing with SAM is the use of robust observables such as closure phase and kernel phase that are insensitive to residual wavefront errors, allowing high contrasts to be reached at angular separations where these effects typically dominate. Being an interferometric method, SAM allows measurements to be made beyond the Rayleigh diffraction limit, down to separations as small as 0.5λ/D. However, by blocking the majority (~90%) of the incoming light, SAM requires brighter targets (typ. R or H < 8 mag) and the use of longer exposure times. In addition, the field of view of SAM observations is typically limited to ~ 5-6 λ/D (250 mas at H-band) and the contrasts achieved are not comparable to those obtained at larger separations through other techniques (such as coronagraphy).

In summary, SAM is a useful "niche" technique for detecting companions and structures with moderate contrasts at or close to the diffraction limit.

From P100 and on, SAM is offered as a setup for the following modes:

- **IRDIS CI**
- **IRDIS DBI**
- **IRDIFS and IRFIS_EXT**
- **IRDIS DPI (similar to the SAMPOL mode on NACO)**
- **ZIMPOL I**

For IRDIS and IRDIFS, the 7-hole mask is introduced through the "IR coro/mask combination" (previously "IR Coronagraph"): N_SAM_7H.

For ZIMPOL, the 7-hole mask is introduced through the "IR coro/mask combination" (previously "Visible Coronagraph"): V_SAM_7H.

SAM always makes use of pupil tracking in order to keep the pupil (and telescope spiders) fixed with respect to the sparse sub-apertures as shown on Figure 3 for each given instrument.
The corresponding masks are located in the respective Lyot wheels.

The derotator angle is the same as for imaging and coronagraphy in pupil tracking and for this reason, SAM shares the same astrometric calibration (true north and plate scale). The POSANG keyword in P2 (which replaced P2PP from P101) does not have any effect when the tracking law is "PUPIL".

For SAM, the calibration files will be provided (flats, darks, backgrounds, etc.) accordingly to the standard IRDIS calibration plan. The basic reduction can be performed by the ESO pipeline but the interferometric analysis is left to the users.

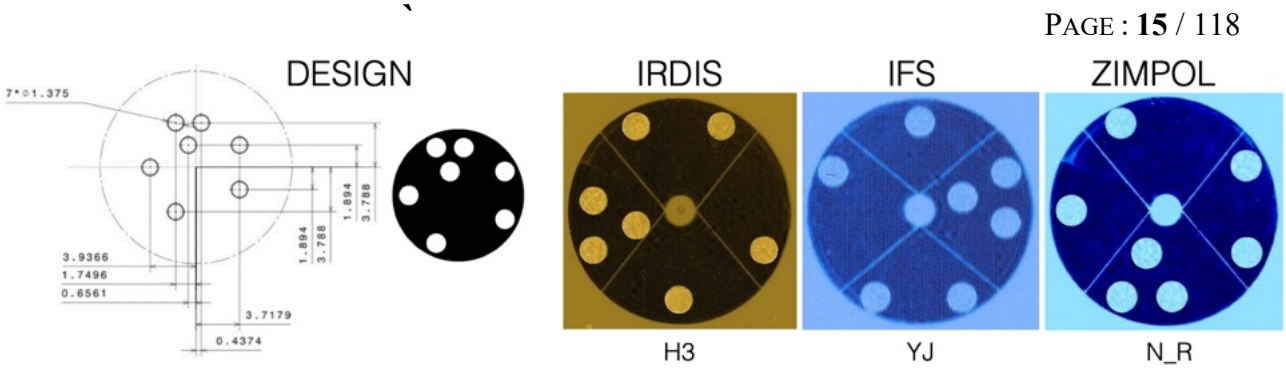

Figure 3: Layout of the SPHERE 7-hole aperture mask design projected on the 8m primary mirror. Each pair of holes (baseline) produces a set of interference fringes. The three images on the right are how the holes are located with respect to the full pupil of the telescope as seen by the 3 instruments. In the case of IRDIS, the mask has been mounted with a 90º offset and one of the holes is tangent with the telescope spider.

Science case examples

Besides imaging of exoplanets and companions around stars, there are other science opportunities opened by SPHERE.

1) The close environment around bright stars

Good/median AO performance is obtained for stars up to R = 11 mag (~9.3 for ZIMPOL with the BS_GREY) and much poorer performance but with relatively stable AO loops for stars as faint as R = 13. For fainter stars, AO loops will open quite often (see Section 6). The field of views (FOVs) are 1.73''x1.73" for IFS, 3.5''x3.5" for ZIMPOL and 11''x11" for IRDIS.

2) Circumstellar emission much fainter than the stellar halo

The suppression of the stellar PSF is for SPHERE much improved compared to previous instruments (e.g., NACO). This is in particular true at small separation angles from the star between 1 and 20 λ/D. Beside the high image quality and PSF stability of the instrument, there are dedicated data reduction techniques based on differential imaging to enhance the contrast of circumstellar emission further (ADI, PDI, SDI).

3) High angular resolution observations will support studies of stellar ejecta, binaries at small separations, stellar proper motions, solar system objects, etc.

Mode offering from P103

Table 4: Modes offered.

Observing Mode	Comment	Service/Visitor
IRDIFS	- Pupil-stabilized (default) or Field-stabilized	S+V
	- Coronagraph: N_ALC_YJH_S - SAM: N_SAM_7H	
	- Other coronagraphs	V
IRDIFS_EXT	- Pupil-stabilized (default) or Field-stabilized	S+V
	- Coronagraph: N_ALC_YJH_S - SAM: N_SAM_7H	
	- Other coronagraphs	V
IRDIS_DBI	- Pupil-stabilized (default) or Field-stabilized	S+V
	- Coronagraph: N_ALC_YJH_S, N_ALC_Ks with K-band filters - SAM: N_SAM_7H	
	- Other coronagraphs	V
IRDIS_CI	- Pupil-stabilized (default) or Field-stabilized	S+V
	- Coronagraph: N_ALC_YJH_S, N_ALC_Ks with K-band filters - SAM: N_SAM_7H	
	- Other coronagraphs	V
IRDIS_DPI	- Field-stabilized (default) - Coronagraph: N_ALC_YJ_S, N_ALC_YJH_S, N_ALC_Ks - Filters: broad band filters BB_J	S+V
	- Pupil-stabilized - Coronagraph: N_ALC_YJ_S, N_ALC_YJH_S, N_ALC_Ks - Filters: broad band filters BB_Y, BB_H, BB_Ks	S+V
	- SAM: N_SAM_7H (Pupil-stabilized)	V
IRDIS_LSS	Long Slit Spectroscopy in LRS and MRS	S+V
ZIMPOL_P1/P2	- Derotator: P1 (static) or P2 (Field-Stabilized) - Filters: combination of NB and BB filters not allowed - WFS/ZIMPOL splitter: GREY or DIC-HA - No coronagraph (allowing some saturation) or V_CLC_M_WF - Some saturation allowed - Detector/modulator: FastPol, SlowPol	S+V
	- Other coronagraphs - NB and BB filter combination	V
ZIMPOL_I	- Same as P1/P2 but with readout mode Std-Imaging. - Pupil-stabilized - SAM: V_SAM_7H (Pupil-stabilized)	S+V
	- Other coronagraphs	V
	- NB and BB filter combination	

2. TECHNICAL DESCRIPTION

The SPHERE subsystems CPI, IFS, IRDIS and ZIMPOL are described below.

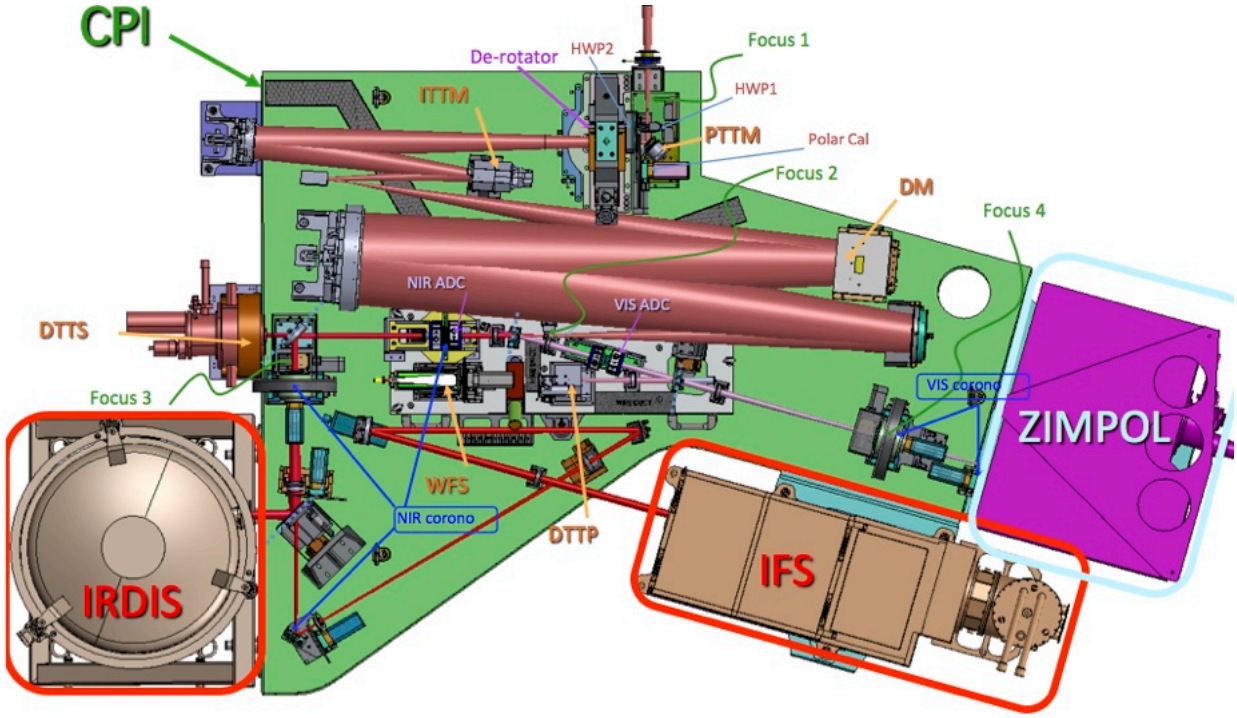

Figure 4: CPI, the common path optical beam on the main optical bench (green) feeding the 3 other sub-systems ZIMPOL (magenta), IRDIS (gray) and IFS (brown).

Common Path Infrastructure (CPI)

CPI includes the main optical bench, connects the other sub-systems to the light path, and guarantees a static alignment of SPHERE to the VLT focus (Figure 4**).** It feeds the cryostats and motors with power, includes servo-controlled pods, damping vibrations on the Nasmyth platform. An enclosure protects the SPHERE optics from dust and reduces temperature gradients. From the entrance focal plane up to the second focus (FP2; Focus 2) a reflective design propagates the complete spectral range from 450 to 2320 nm through the instrument. It includes the beam derotator, active optics, with pupil and image tilt mirrors, and the high order deformable mirror (DM), which is the heart of the system providing a stable AO-corrected image.

CPI also includes visible and infrared half-wave plates for polarization switching/modulation. After FP2, light is split between visible and NIR. The NIR beam path includes refractive optics: the NIR ADC, coronagraphic components, neutral densities filters and an exchangeable splitter between IRDIS and IFS.

In the optical, atmospheric dispersion correction is applied by the VIS ADC, and then the beam is split between ZIMPOL and AO (WFS). If ZIMPOL is not used, all the light goes to the WFS. If ZIMPOL is used, one can chose between the grey beam splitter (sending 80% of the light to ZIMPOL and the remaining 20% to the WFS) and a dichroic beam splitter (DIC_HA) sending the spectral range around the R band to ZIMPOL and the rest to the WFS. Before ZIMPOL, the beam goes through a coronagraphic focal plane (FP4; Focus 4) and a pupil plane hosting the corresponding Lyot stops.

The adaptive optics module is called SAXO. It is designed to correct for the turbulence perturbation at high frequency (1.2 kHz). The turbulence is measured by a 40x40 lenslet Shack-Hartmann sensor

that is equipped with a red-sensitive sub-electron noise EMCCD. Its servo controls the pupil position, and fine-tunes the centering on the coronagraph by means of a dedicated differential tip-tilt sensor (DTTS).

The coronagraphs are set-up by a mask in the focal plane (FP3 for NIR and FP4 for the visible), a Lyot stop in the downstream pupil, and an apodizer in the upstream pupil (before the focal mask). The wheels for the coronagraphs include also field stops and the IRDIS long slit masks. Several set-up combinations are defined for a range of observing conditions and science cases (seeing, inner working angle, wavelength, etc.); they are listed in the Appendix.

IFS

The SPHERE integral field spectrograph (IFS) is a lenslet-based integral field unit (called BIGRE, Antichi et al. 2009), providing a 1.73" x 1.73" FOV that is Nyquist sampled at 0.95 µm (Table 1). The IFS includes a flat calibration source and filters for accurate detector calibrations. The IFS instrument layout is displayed in Figure 4. The raw data 21000 spectra are aligned with the detector columns over a hexagonal grid rotated by ~10.7° with respect to the dispersion. Each spectrum from a spaxel is projected on a rectangular area of 5.1x41 pixels on the detector.
During data reduction, the image is translated into a (x,y,λ) data cube, which has for both available spectral resolutions a constant dimension of (291,291,38). Each image is resampled by the pipeline over a square regular grid at $(7.4\ \text{mas})^2$ / spaxel. Data outside this region are meaningless (see Figure 6).

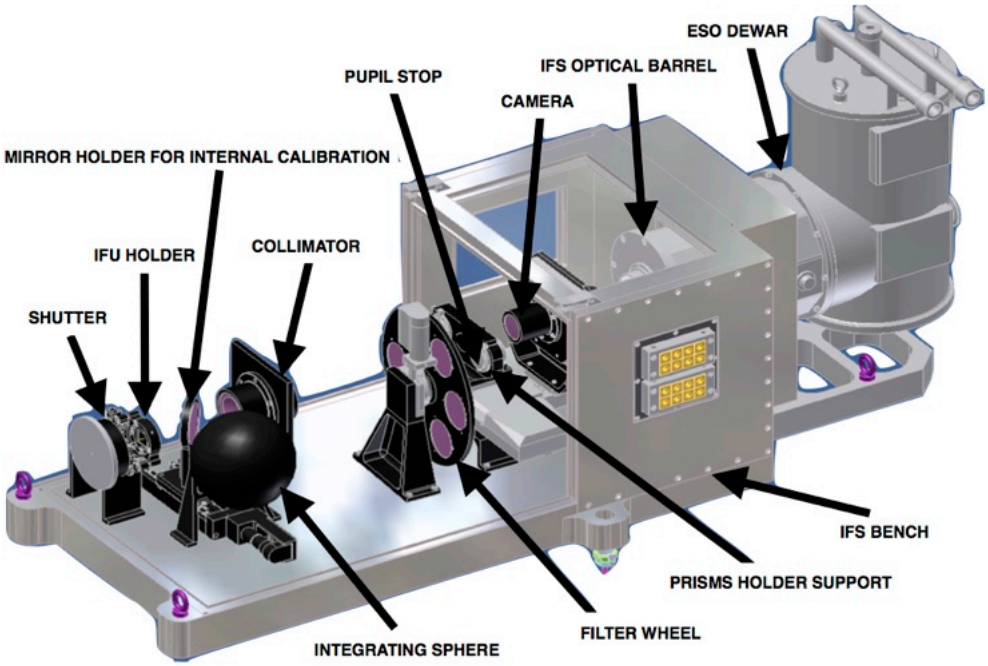

Figure 5: Inside the IFS. Note that the IFS optical bench is not cold, and that it has its own Lyot stop and internal calibration sources.

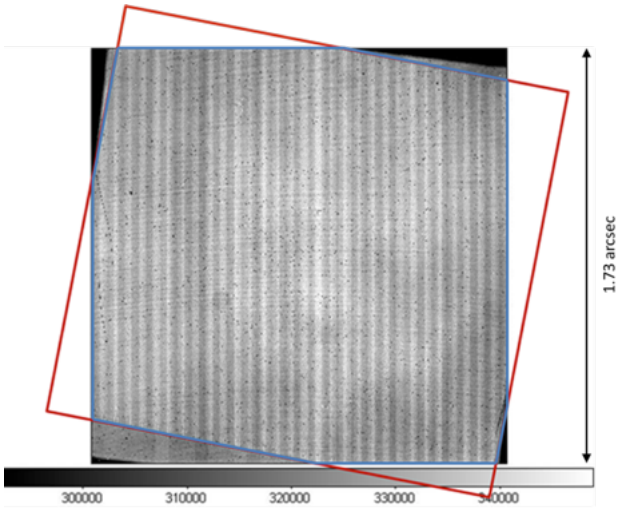

Figure 6: IFS flat-field and projection of the sky on the BIGRE detector (red) and ~1.73" x 1.73" FOV (blue).

IRDIS

The FOV is 11"x12.5" and the pixel scale is 12.25mas matching Nyquist sampling at 0.95 µm. Two parallel beams are projected onto the same 2kx2k detector and each occupies about half of the array. The IRDIS instrument layout is displayed in Figure 7. DBI provides images in two neighbouring filters, simultaneously. Various filter pairs are available for different spectral features. DPI uses crossed polarizers providing images in the two polarization directions at the same time. For LSS, the coronagraph mask is replaced by a coronagraphic slit.

Three wheels are provided within the cryogenic environment:

a. **The Lyot stop wheel, with Lyot stops for the coronagraphs of the CPI, LRS prism, and MRS grism.**
b. **The common filter wheel, with blocking filters, broadband and narrowband filters.**
c. **The dual filter wheel, with DBI and DPI filter pairs, polarizers, and a pupil-imaging lens.**

The complete list of available filters is summarized in the Appendix. Dual imaging separation is done using a beam-splitter combined with a mirror, producing two parallel beams. IRDIS achieves less than 10 nm differential aberrations between the two channels and, as a consequence, allows high contrast differential imaging.

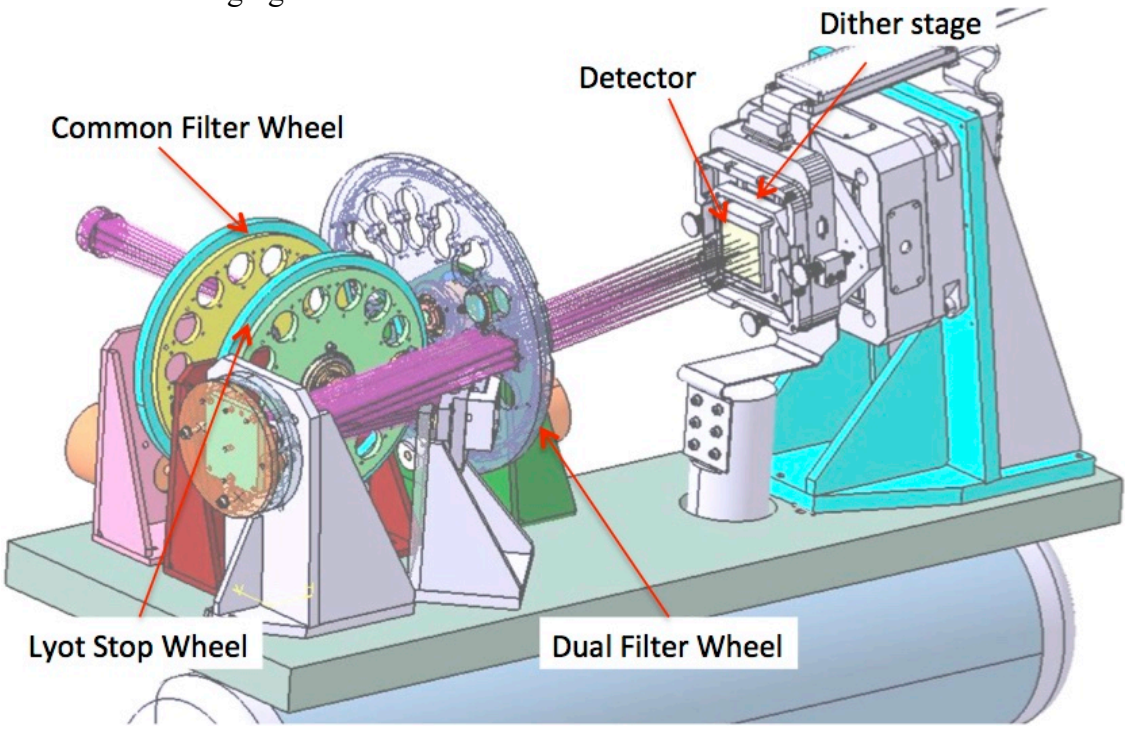

Figure 7: Inside view of the IRDIS cryostat. The CPI beam comes from the left, goes through the common filter and Lyot stop wheels, is split in two, then goes through the dual filter wheel before landing on the infrared detector.

The IRDIS detector is mounted on a detector motion stage (DMS). The DMS enables detector dithering in XY-directions at sub-micron accuracy. Detector dithering is available mainly to improve the flat-field accuracy and to handle cosmetic defects. The recommended pattern is 4×4 pixels (but can be extended up to 10×10).

ZIMPOL

ZIMPOL is designed as high contrast imaging polarimeter with very high polarimetric sensitivity for the visual range. It also provides at the same time imaging capabilities. Another VLT instrument, FORS2, provides a polarimetric mode for the visual range which is however complementary to ZIMPOL. FORS2 is a seeing limited Cassegrain imaging and spectrograph polarimeter for accurate absolute polarization measurements (0.1% in the field center). FORS2 has a very high throughput and is therefore suited for faint objects. ZIMPOL is a diffraction limited imaging polarimeter with a very small field of view centered on a bright target. Because ZIMPOL is a Nasmyth instrument, it provides only a limited absolute polarimetric accuracy (~0.5%). The basic observing strategy for ZIMPOL is a relative polarization measurement of the immediate surroundings of a central star, which is used as a (zero)-polarization reference for the correction of the instrument polarization.

Atmospheric seeing variations are a key problem when aiming to achieve high image quality. Differential measurements such as DPI with fast (kHz) polarization modulation can solve this problem. DPI is performed quasi-simultaneously by fast modulation revealing, e.g. faint structures around a bright point source.

The ZIMPOL instrument layout is displayed in Figure 8 and its main capabilities are summarized in Table 3. ZIMPOL includes a new concept for imaging polarimetry, which is based on fast polarimetric modulation and on-chip de-modulation by two CCDs (Figure 8). Thanks to a polarimetric beam-splitter, one polarization is sent to CCD1 and the other perpendicular polarization to CCD2.

Furthermore, the polarization modulation is synchronized with an innovative reading scheme of the detectors. By this technique, the polarization of the incoming light is converted by a polarization modulator and the following polarization beam splitter into an intensity modulation with an amplitude proportional to the polarization signal. The de-modulating CCD has every second row covered by a stripe mask and these covered rows can be used as a buffer storage area. With charge shifting on this masked CCD each "open" pixel can measure the intensity of the two alternating states. Photo-charges created during one half of the modulation cycle are shifted for the second half of the cycle to the next masked row and again back for the subsequent illumination during the next first half of the modulation cycle. In this way two frames are build up in alternating pixel rows, corresponding to opposite polarization states. After many modulations the CCDs can be readout and the raw polarization signal is then the difference between "even" and "odd" rows.

A single arm of ZIMPOL provides a full polarimetric measurement. Because a polarizing beamsplitter is used for the polarization analysis, half of the light goes to the other arm, which can perform polarimetry for the same or another filter.

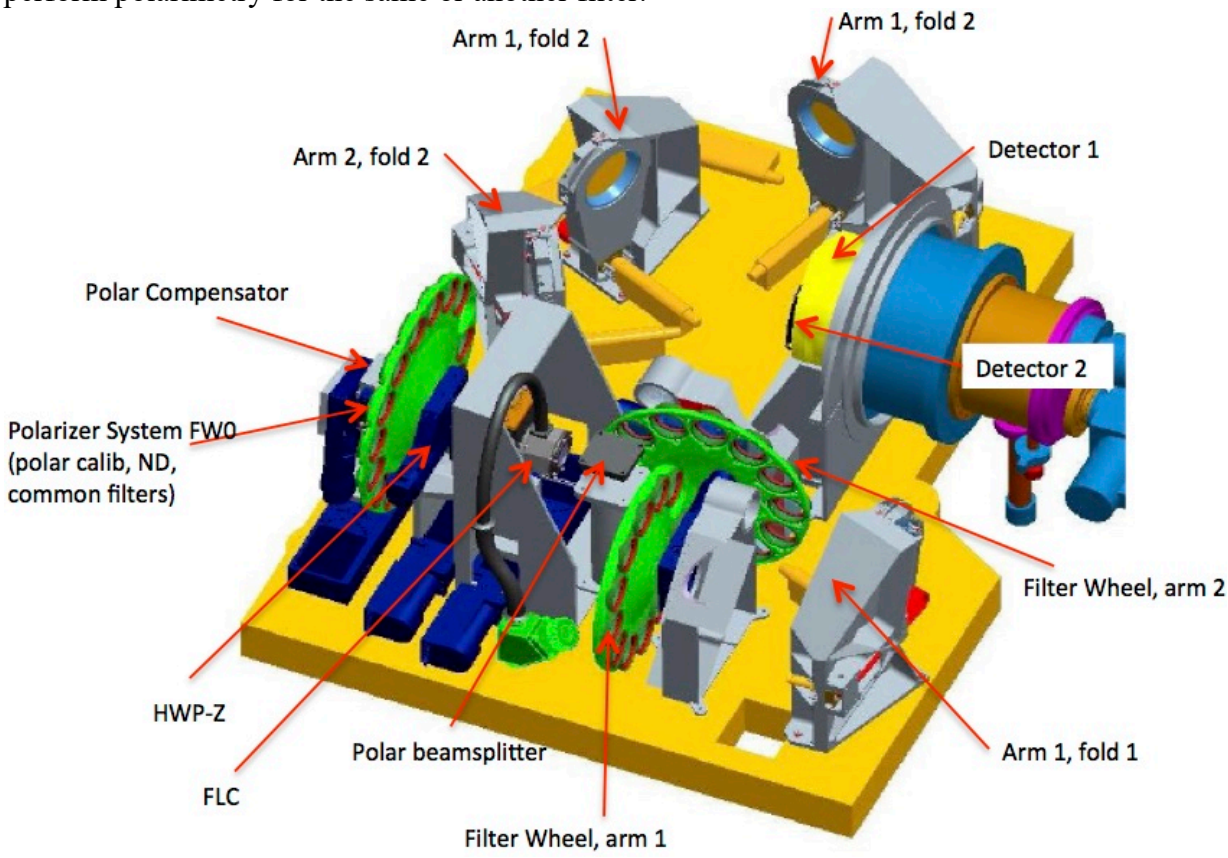

Figure 8: ZIMPOL schematic view showing the main elements of this visible polarimeter, from polarization compensator, common filter wheel, Ferroelectric Liquid Crystal (FLC) modulator to the splitter, filter wheels 1 and 2, and the two detectors.

Advantages of differential polarimetric technique are:

Both images are created *quasi-simultaneously* (the modulation is faster than the seeing variations), and both images are recorded with the *same pixels* reducing significantly flat-fielding issues.
Differential effects due to the storage of two images in different buffer pixels are compensated with *a demodulation phase-switch* between subsequent images.
There are only very small *differential aberrations* between the two images with opposite polarization.
The differential signal does not suffer from *chromatic effects* due to diffraction or speckle chromatism.

The efficiency of the modulation – demodulation process depends on the modulation frequency. The instrument offers a fast modulation mode with a frequency of about 1 kHz and a polarization efficiency of 80% and a slow modulation mode with a frequency of about 30 Hz and an efficiency of 90%. A simple calibration is foreseen to correct for the polarization efficiency taking into account a slight wavelength dependence and possible small temporal variations in the polarization measurement.

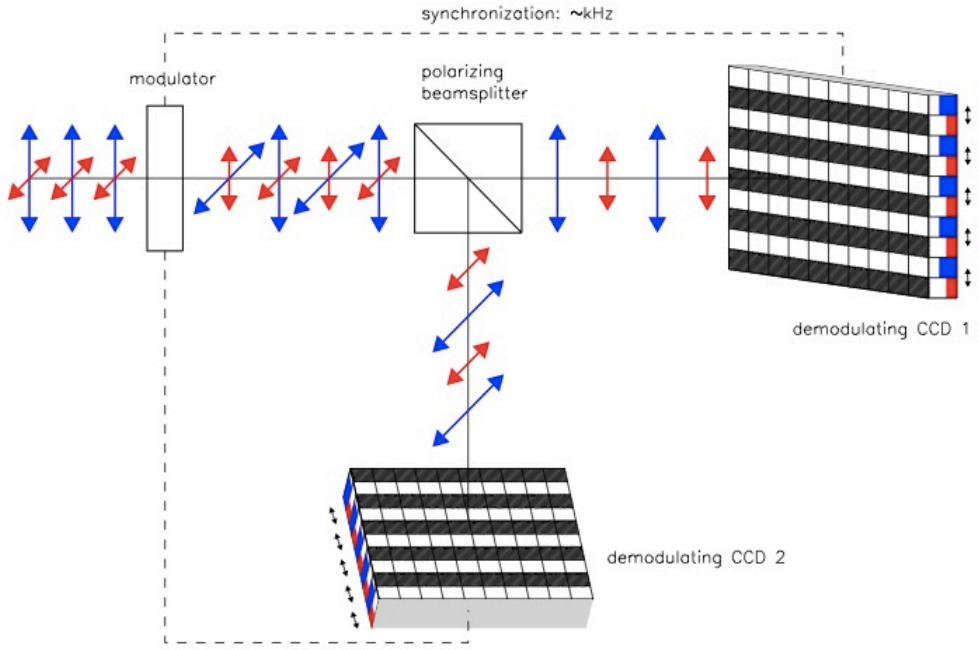

Figure 9: In ZIMPOL the polarized signal is modulated on CCD1 and CCD2. The detectors are read after a charge shifting sequence that is synchronized to the polarization swap.

2.1.1 Hardware

The ZIMPOL sub-system receives the beam from CPI after the visible coronagraph pupil Lyot stop plane. The instrument offers an extended list of broadband (BB) and narrowband (NB) filters that are described in the Appendix. The first filter wheel (FW0) is common to both arms and includes both filters and polarimetric components used to calibrate the intrinsic polarization of ZIMPOL. As a consequence, the filters located in this wheel cannot be calibrated polarimetrically and can therefore be used only for imaging observing mode and not for polarimetric imaging.

Depending on the observing mode, a polarization compensator that can be controlled in orientation and in amplitude, and internal Half-Wave Plates (HWP) are set within the observing template. A Ferro-electric Liquid Cristal polarization modulator (FLC) is inserted in the beam for polarimetric imaging to modulate the polarization direction as selected by the polarization beam-splitter. This splitter then feeds two optical beams of ZIMPOL. Each beam goes through filter wheels FW1 and FW2, the tip-tilt mirror that allows offsetting the FOV, and finally arrives on the detector. Both CCDs are located side by side in the same cryostat. The two filter wheels enable polarimetric observations in two bands. The common filter wheel FW0 contains polarimetric calibration components and additional filters for imaging.

2.1.2 Instrumental polarization

SPHERE includes many optical components that impact the instrumental polarisation. The optical path through the CPI and ZIMPOL is schematized in Figure 10. The polarization signal is measured by ZIMPOL at the position of the modulator and the beam-splitter. The linear polarization intensity is recorded either parallel I_0 or perpendicular I_{90} to the optical bench. Other polarization position angles can be selected by synchronously rotating half-wave plate HWP2 (mounted at the entrance of the CPI) and half-wave plate HWPZ (inside ZIMPOL).
The instrumental polarization is minimized by design. HWP1 and M4 (SPHERE fold mirror) enable reduction of the telescope polarization induced by M3. There is also a tilted, rotatable compensator plate to reduce the instrumental polarization introduced by the derotator.
For a given observation, both orthogonal polarization states are exchanged applying a frequent 45° rotation of HWP2. Thank to this design the introduced instrumental polarization is < 1%. In many science cases, the central bright star can be used as zero-polarization reference allowing for a very accurate correction of the instrument polarization for measurements of circumstellar sources. Cross-talk effects affect the measured fractional polarization signal p (or Q/I and U/I) by $\Delta p/p < 0.05$ providing very good polarization properties for a Nasmyth instrument.
A model of the instrumental polarization of ZIMPOL is currently built for cases where the central star cannot be used as polarization reference and other demanding applications. This should allow even a better correction for the instrumental polarization effects in the data reduction.

2.1.3 Detectors

Schmid et al. (2012) describe the observing method of ZIMPOL, in which a large number of charge states are accumulated and shifted across different detector pixels. The handling of the detector properties and calibration is of particular importance. A *2-phase demodulation scheme is used:* Electrons accumulated on the detector are shifted many times up and down and from one pixel to the next, before the exposure is finally read. Therefore, asymmetries in the charge transfer efficiency in a fraction (<1%) of detector pixels (charge traps) affect the resulting data. A phase switch between two subsequent DITs calibrates this out for the differential polarization signal I_0-I_{90}. Therefore, all science exposures and calibration frames for ZIMPOL polarimetric observations are taken with an even number of DITs.

It is important to note that the charge traps remain in the intensity frame I_0+I_{90} of polarimetric observations. Their strength is proportional to the number of polarization cycles and affects a substantial fraction (> 0.1%) of pixels for longer integrations (> 10 s) in fast polarimetry or (>300 s) in slow polarimetry. The impact of this special feature of the ZIMPOL polarimetric mode can be strongly reduced by an appropriate observing strategy, e.g. with dithering, selecting slow polarimetry instead of fast polarimetry mode, or by taking separate frames in ZIMPOL imaging mode where this effect is not present.

Detector bias: The detector readout process includes additional readouts of pre- and over-scan pixels. This ensures a better bias subtraction for all frames. These additional readouts are visible in the raw

data and appear at the border and in the middle of the array. In the standard data reduction cascade, average bias values for the overscan pixels are evaluated and subtracted for the two different readout areas of the ZIMPOL detectors. This provides a very good bias correction for imaging and slow polarimetry mode. For fast polarimetry mode two columns originating from the readout process are present which are not corrected by the overscan pixel bias subtraction method. This fixed pattern noise can be removed in a classical way by the subtraction bias frames.

Frame transfer smearing: The ZIMPOL data are taken with frame transfer CCDs. They can simultaneously take images with one half of the detector and readout the other half of the detector where the frame from the previous exposure is stored. At the end of an exposure which must last longer than the readout process (about 1.2s for fast polarimetry and imaging and 10s for slow polarimetry) the newly created frame in the image area is transferred rapidly to the readout area and a new illumination begins.

The detector illumination during the frame transfer introduces a smearing of the image in the direction of the detector columns. The smearing is proportional to the ratio of the frame transfer time, which is constant, and the DIT. For example, a 6s exposure of a point source with 100 000 counts (integrated over 5x5 pixels) and a frame transfer of about 60 ms, will produce a trace parallel to the column directions (~1000 pixels) where the illumination is enhanced by about 1 count.
The smearing effect is thus only important for short DITs, in particular, for non-coronagraphic, high contrast observations of saturated sources.

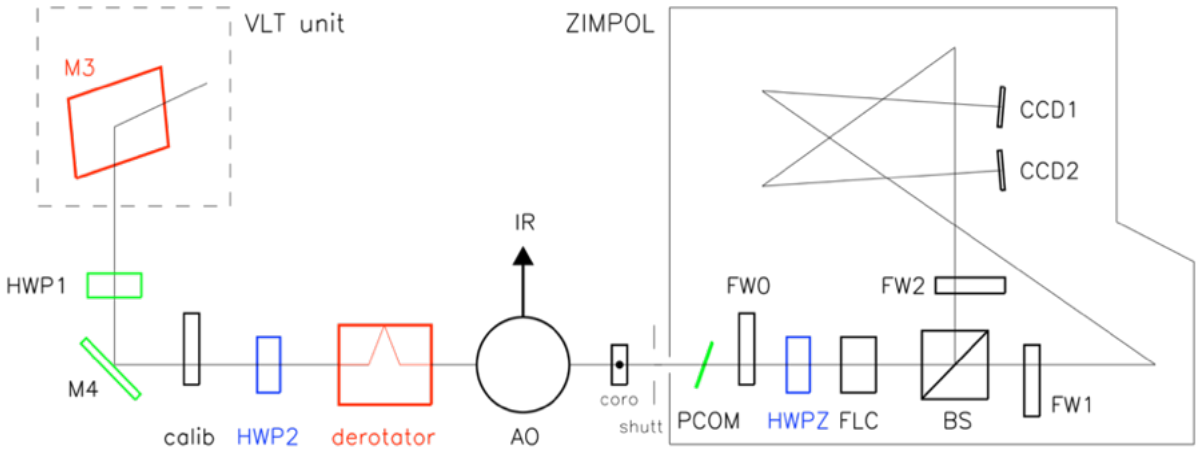

Figure 10: ZIMPOL optical path. Components, which introduce (red) or compensate (green) instrumental polarization, and those, which rotate the Stokes vector into the derotator system (blue), or instrument system (black) are indicated.

2.1.4 Imaging

The ZIMPOL imaging mode provides a higher image quality and is about 10% more efficient than polarimetric observing modes. Moreover, it does not suffer from the charge trap problem created by the charge shifting used for polarimetry.

2.1.5 Field of view

The ZIMPOL instantaneous FoV is 3.5 × 3.5 arcsec^2. This FoV is roughly centered on the coronagraph position and is identical for both CCDs. On both ZIMPOL optical arms, tip-tilt mirrors can be used to offset the field by small amplitudes. This enables dithering so that light falls onto different pixels. This scheme is commonly used to reduce the impact of bad pixels. The ability to use tip-tilt mirrors for mosaicking up to a radius of 4'' is not yet validated and not thus offered.

Instrument combinations

Dichroics allow IFS and IRDIS to take data in parallel. One dichroic setting (used in the IRDIFS_EXT mode) allows IFS observations in the Y-H range, and IRDIS observations in K at somewhat reduced performance (particularly coronagraphic).
Another setting (used in the IRDIFS mode) allows IFS observations in Y-J range, and IRDIS observations in the H band with optimum performance.
For IRDIS-alone observations, a mirror is used ensuring optimal K band performance and access to the complete 0.95 – 2.32µm spectral range.
ZIMPOL can only be used alone.

3. ADAPTIVE OPTICS PERFORMANCE

The performances given in this section are conservative, and still being consolidated. The following is thus a snapshot of the current performance level as measured during the acceptance tests in Europe, the integration in Paranal, and four commissioning runs on sky (between May and October 2014).

SAXO preliminary representative performance

The SPHERE Adaptive Optics module SAXO has been verified to perform nominally, and providing H-band Strehl ratio in excess of 90% for median seeing conditions (0.8”-1.2”) and bright NGS (R < 9 mag). See Figure 11 and Figure 12 for details.

The AO is not limited by the NGS flux up to R~9. In between R=9 and 11, the correction remains very good but the lack of photons induces residuals that translates into a brighter residual halo in coronagraphic images. For fainter objects, AO correction can still be applied but at a slower rate, with degraded image quality. Since P100 targets with R>11 are allowed in Service Mode.

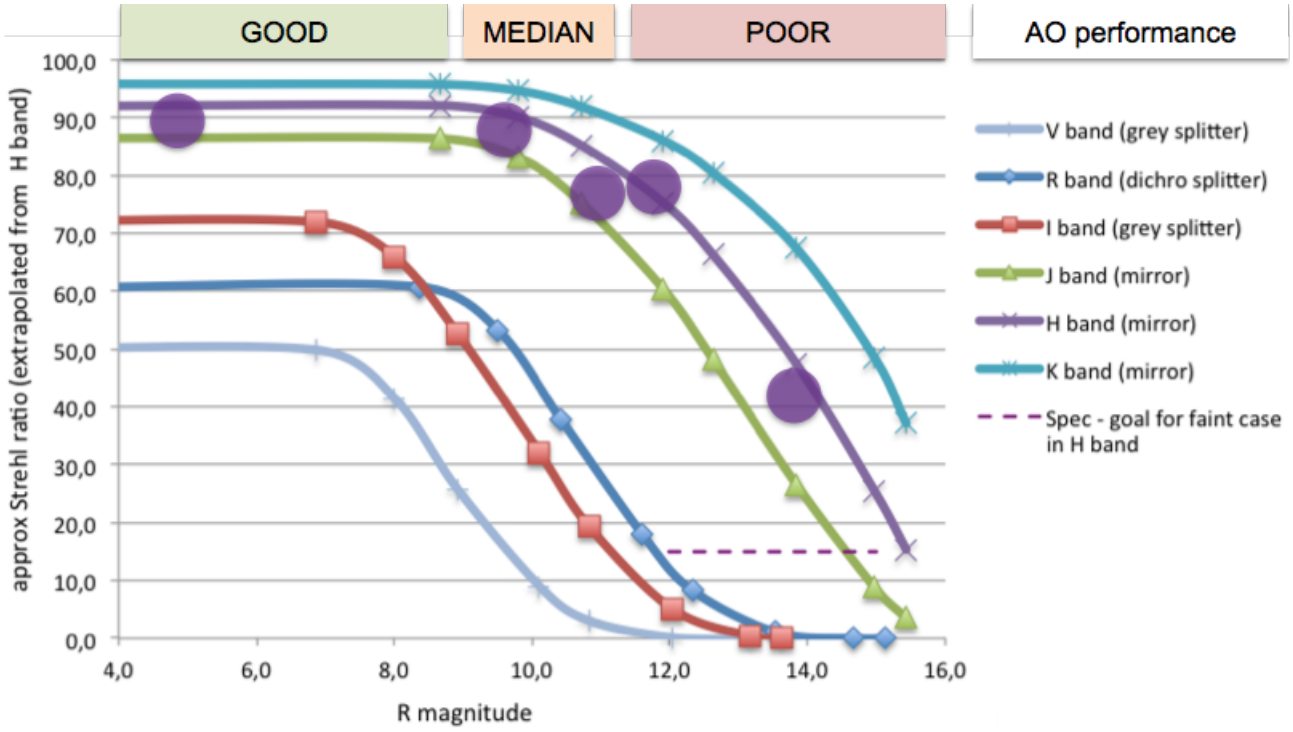

Figure 11: Theoretical and measured (purple circles) SPHERE-SAXO Strehl ratio as a function of R magnitude for good seeing conditions and different wavelength ranges from V to K (see Figure 33 and Figure 34 for more details).

Fusco et al. 2016 (SPIE 9909) provides more on-sky performance measurements (Strehl ratio) which confirm the plot in Figure 11. For current faint-star observing recommendations, use the Gaia G magnitude rather than R whenever available (see the following subsections and Section 5.1).

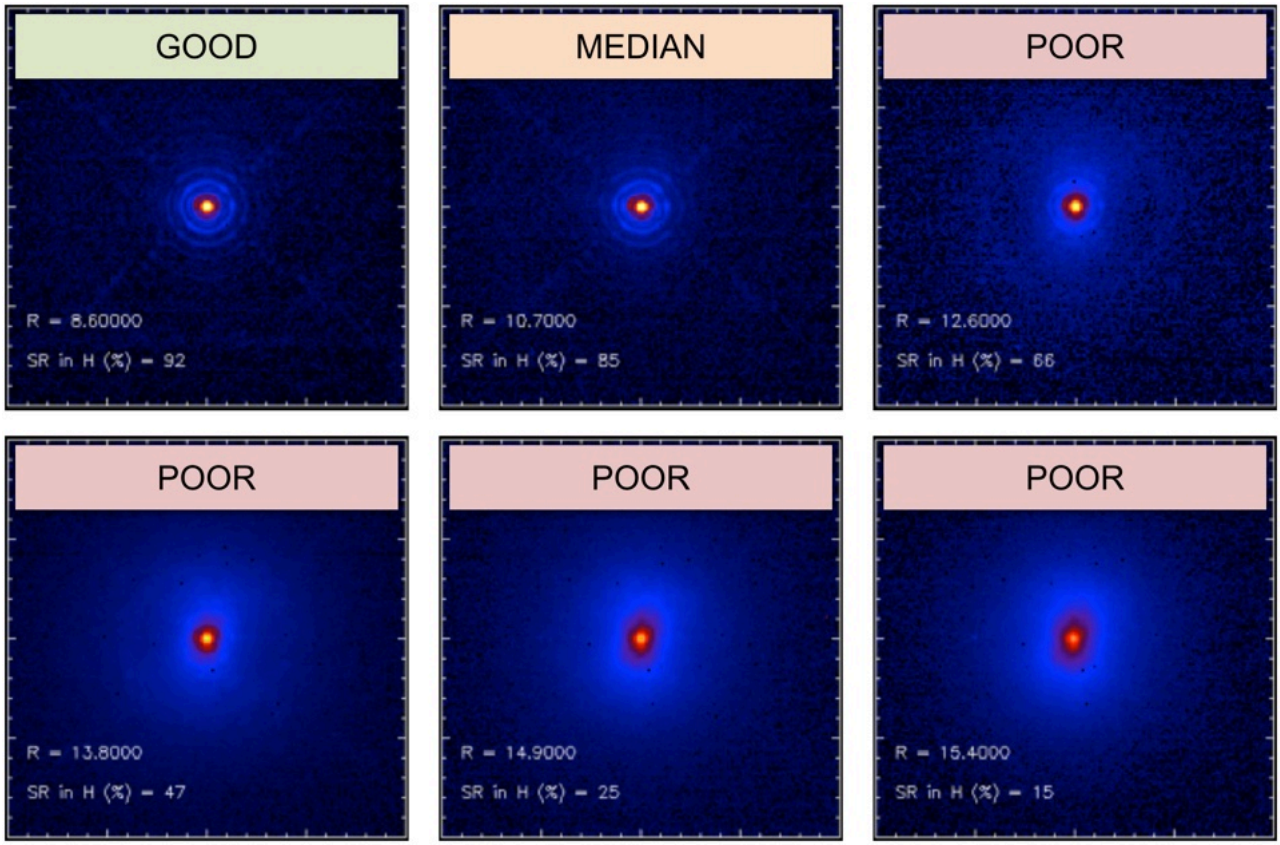

Figure 12: SPHERE PSF morphology and Strehl ratio as a function of R magnitude (see Figure 33 and Figure 34 for more details).

Faint star performance

We reviewed the SPHERE's performance on faint stars, using data collected between 2016 and 2022. Here we refer to G-band magnitudes from GAIA, as these have become available, and the WFS response (spectral filter in OPEN position is used for faint stars) is actually closer to G-band than the R-band. For stars fainter than G=12.5 mag, the FWHM of the PSF quickly becomes much larger than the diffraction limit (See Figure 13). Similarly, the strehl ratio is strongly reduced (see Figure 14). See Jones et al. (2020, A&A, 667, 114) for more details. **Therefore, we provide no performance assurance beyond G=12.5**. However, one can attempt AO observations (with special waivers) for stars as faint as G=15.5, as strehls over 15% can still be achieved in excellent conditions. Below, we provide a rough estimate of the FWHM of the PSF in two the turbulence categories (see Section 5.1 Atmospheric Constraints), 10% (seeing < 0.6", coherence time > 5.2 ms) and 30% (seeing < 0.8", coherence time > 4.1 ms). Between G = 12.5 to 15.5, we expect:

T-cat 10% FWHM = [1 + (G - 12.5) . 4/3] . DL
T-cat 30% FWHM = [1 + (G - 12.5) . 8/3] . DL
Where DL = Diffraction limit (~ 50 mas in H-band).

Some reference FWHM values in this "seeing enhanced" regime are given in Table 5. Based on these estimates, **we strongly recommend Turbulence Category 10% for targets with G > 12.5**, if image resolution is important. Also, we recommend Turbulence Category 30% or better for targets with G > 11.

Table 5: Expected FWHM in poor performance regime for T-categories 10% and 30%. DL stands for diffraction limit.

T-cat	Gmag	FWHM/DL	H-band FWHM mas
10%	15.5	5	250
10%	14.75	4	200
10%	14.0	3	150
10%	12.9	2	100
30%	14.0	5	250
30%	13.6	4	200
30%	13.3	3	150
30%	12.6	2	100

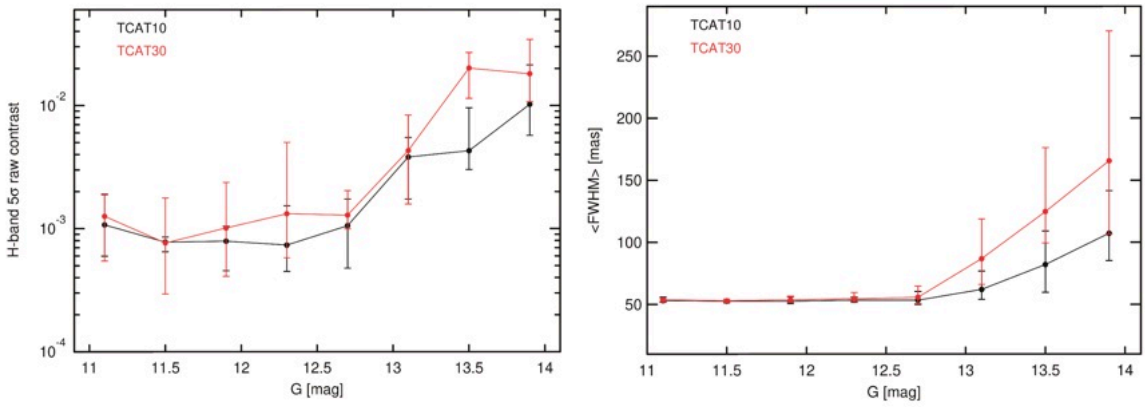

Figure 13: (Left): 5-σ raw contrast at 300 mas as a function of the stellar G-band magnitude. The black and red lines correspond to the atmospheric turbulence categories TCAT10 and TCAT30, respectively. (Right): Same as left figure, but for the FWHM. Figure from Jones et al. (2022).

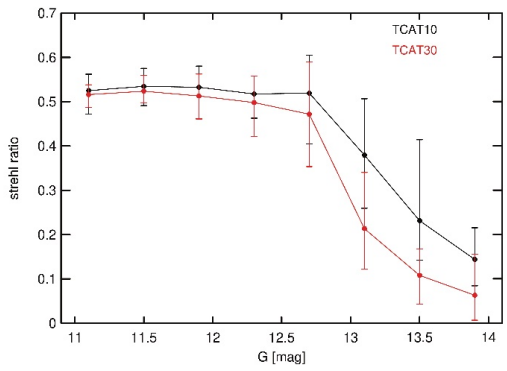

Figure 14: Strehl ratio as a function of the stellar G-band magnitude, using the SR-FWHM correlation derived in Jones et al. (2022). The solid black and red dots (lines) correspond to the atmospheric turbulence categories TCAT10 and TCAT30 , respectively.

Performance improvement at G ~ 11 mag

On July 2024, and following the results obtained in Jones et al. (2022), we updated the AO setup table, to extend the 600 Hz frequency mode to stars as faint as G = 11.5 (previous threshold was 10.5, meaning that 300 Hz has been used for G~11.5 thus far). We performed several tests in different atmospheric conditions, by observing the different stars with G-mag between 10.5 and 11.5, by switching between the 300 Hz and the 600 Hz mode. A few examples of these tests are presented in Figure 13. As can be seen, there is a substantial improvement in the contrast attained when using the 600 Hz mode, when compared to the 300 Hz mode. More details will be presented soon in Jones (2024, in preparation).

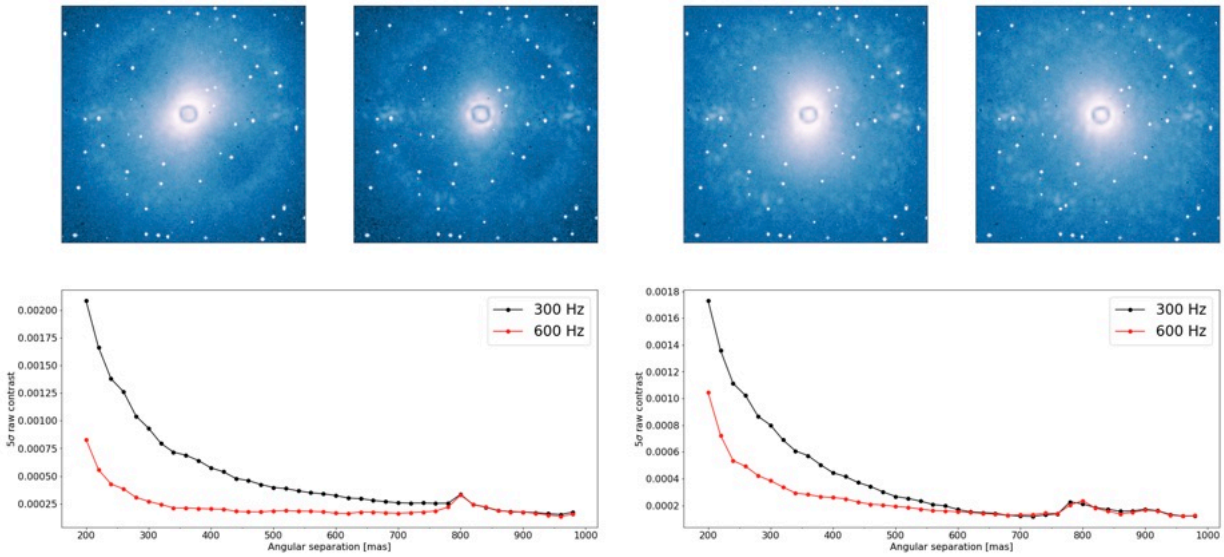

Figure 15: (Left) IRDIS coronagraphic raw images of CD-32 1104 (G = 10.7) observed under average atmospheric conditions seeing~ 1" and τ0 ~ 4.5 ms), in the 300 Hz and 600 Hz frequency modes (left and right, respectively). The corresponding raw contrast curves are shown below. (Right): Same as left, but for UCAC2 18885095 (G = 11.3), observed under good atmospheric conditions (seeing ~ 0.65" and τ0 ~ 5.0 ms).

Coronagraphs not recommended for faint targets

Targets with H > 12 are likely too faint to be robustly detected in the DTTS and drift control of the star in the IR will be poor. Thus, coronagraph use is discouraged for these targets. Also, in an observatory project by Daniela Iglesias, it was demonstrated that for stars with R > 12, coronagraph use yields little gain. In the experiment, observations of a faint star (2MASS J10412146-2830148, H = 10.6, R = 11.8) were obtained with SPHERE-IRDIS to compare the contrast achieved at small separations with and without the use of the coronagraph. The observations were taken during the twilight of the night of 2017-05-31 with clear sky conditions and an average DIMM seeing of ~0.6. Two sets of interleaved observations, one set with and one set without the coronagraph were obtained over roughly an hour of elapsed time. Specifically, an exposure of 32 seconds was taken with the coronagraph, and then one 32 second exposure was taken without the coronagraph, and so

on until one hour had elapsed. Thus, both sets of observations are taken under very similar sky conditions. In addition, OBJECT CENTER images of 32s were taken every ~5 minutes to be used for centering in the reduction process and a couple of 1s images were taken for flux calibration. The images were taken in dual-band mode using the D_H23 filter. The contrast achieved after reductions applying both angular and spectral differencing simultaneously is shown in Figure 16. Both observations achieve a contrast of roughly 7 mags at 0.2" separation and 9 mags beyond 1".

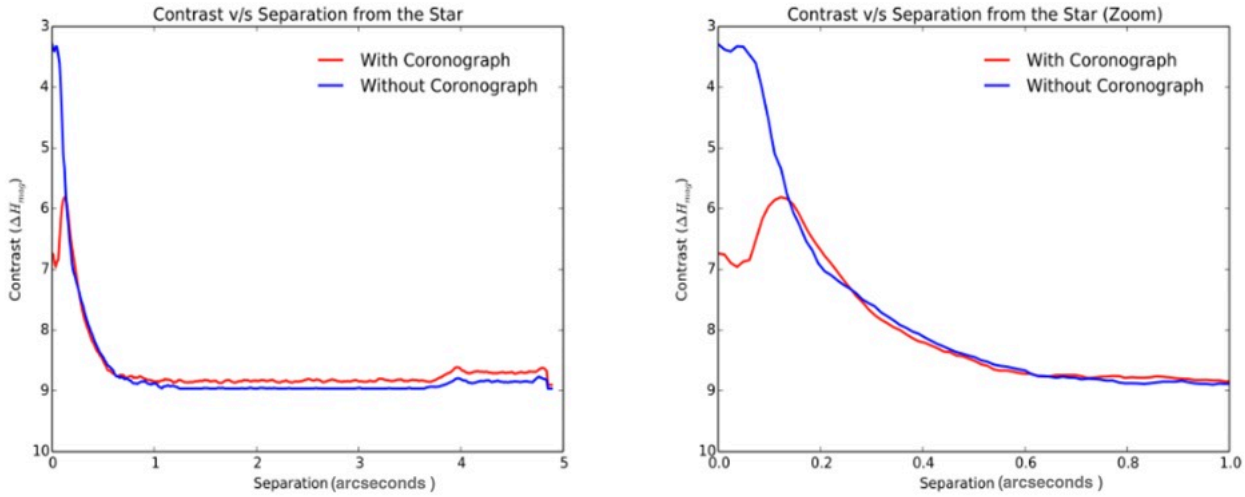

Figure 16: Contrast obtained with and without the use of the coronograph. Contrast is in H band magnitudes. Right: zoom for separations less than 1".

IRDIS preliminary representative performance

3.1.1 IRDIS DBI

The 1σ-contrast achieved in coronagraphic imaging (IRDIFS_DBI) with filter combination DB_H23 (Figure 17) is shown as a function of angular separation (contrast curves) in Figure 18 for various differential imaging strategy combinations (SDI alone or combined with ADI). Note that in most coronagraphic images of stars obtained with IRDIS and IFS, a point source is seen at the center of the coronagraphic mask (see Figure 17), **This point source does not show the location of the star but shows the Fresnel diffraction pattern originating from the coronagraph, known as the bright spot of Arago.** For accurate measurements of the star center, one must use the CENTER "C" observations, which create the four waffle spots symmetrically around the stellar position.

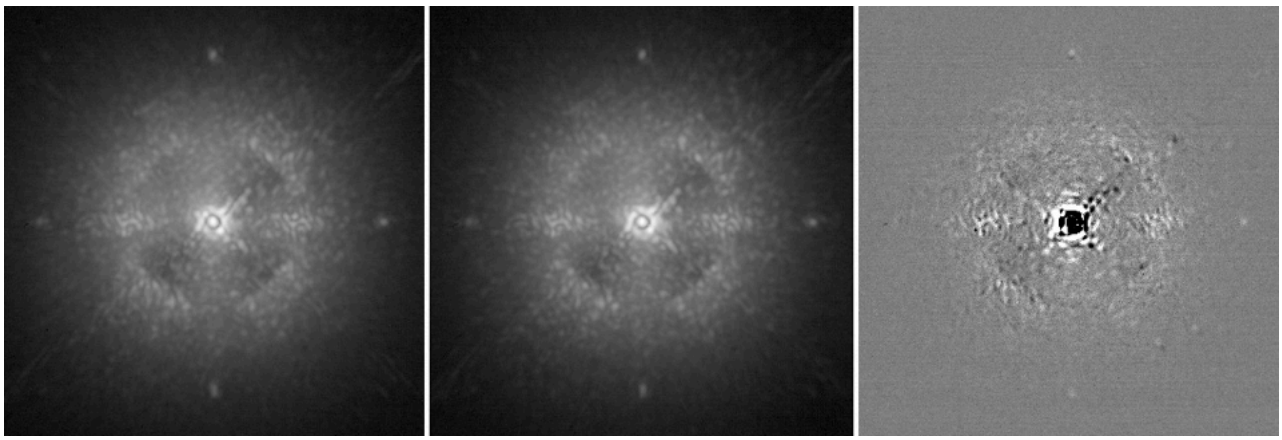

Figure 17: Coronagraphic images obtained in IRDIS H2 (left) and H3 (center) DBI filters, and the result of spectral differential imaging H2-H3 (right).

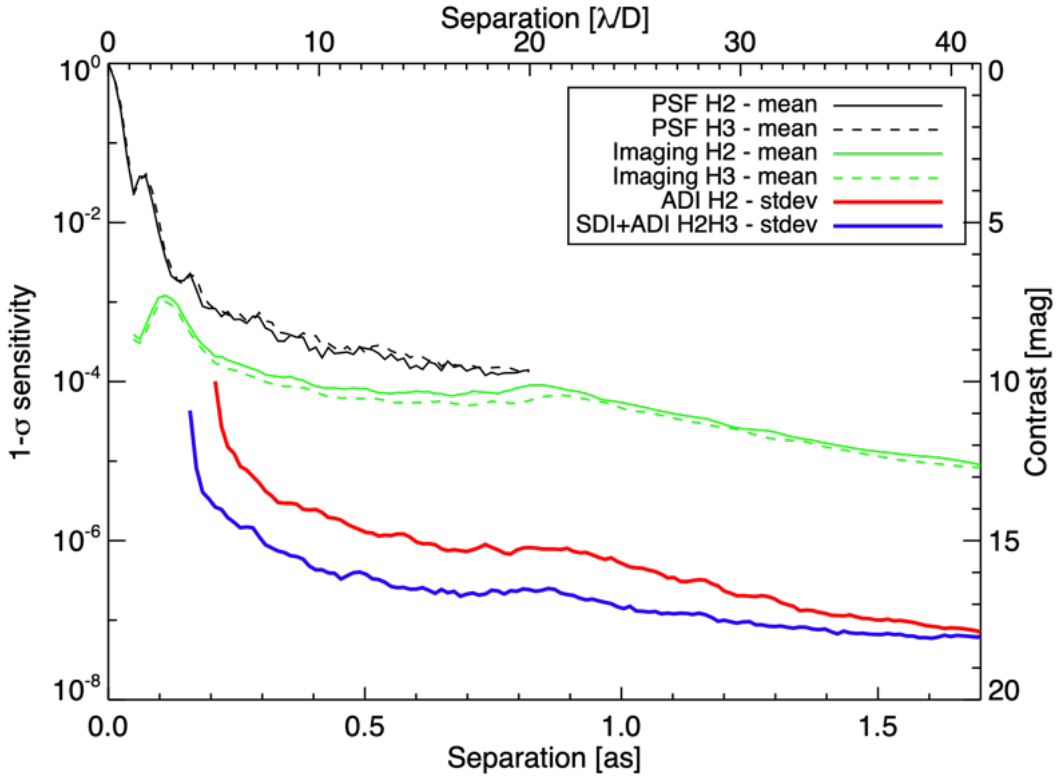

Figure 18: IRDIS DBI H2H3 contrast curves obtained on-sky for a bright target (H=0.2), in average conditions (seeing ~1.0"), with an ADI field rotation of 30 degrees. The plot shows the PSF profiles (black) and coronagraphic profiles (green) in the H2 and H3 filters, the 1σ contrast curve for ADI on the H2 data (red), and the 1σ contrast curve for SDI+ADI on the H2 and H3 data. For the ADI and SDI+ADI analysis, the algorithm throughput is taken into account and compensated, assuming a T8 spectral-type for the planet in SDI.

3.1.2 IRDIS LSS

The ESO's VLT/SPHERE instrument includes a unique long-slit spectroscopy (LSS) mode coupled with Lyot coronagraphy in its infrared dual-band imager and spectrograph (IRDIS) for spectral characterization of young, giant exoplanets detected by direct imaging. LSS can be used in two modes, in the low-resolution (LRS) and medium-resolution (MRS) mode. Their specifications are provided in the following table:

	Resolving power	*Spectral range*
LRS	50	0.95 - 2.32 µm
MRS	350	0.95 - 1.65 µm

Representative raw, and processed spectra, and contrast performance for the LSS mode of IRDIS are shown in Figure 19 and Figure 20. For better performance at small separations (0.2-0.5") for bright companions, consider using the new apodizer for LSS called the SLLC or the stop-less Lyot coronagraph, offered from P101 (see Section 7).

Important: the position of true north is –1.75 degrees in IRDIS/LSS. When preparing an IRDIS/LSS OB in Phase 2, add +1.75 degrees to the desired on-sky slit position angle PA (CPRT.POSANG = PA + 1.75 degrees in IRDIS/LSS templates). For imaging astrometric calibration, see Section 8.

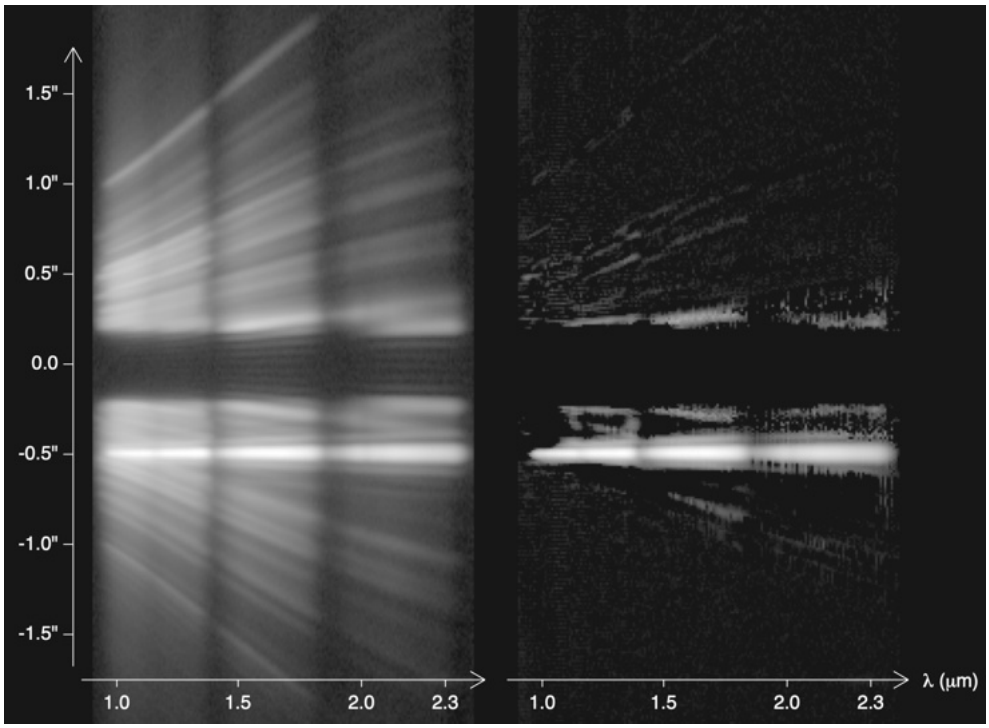

Figure 19: IRDIS LRS data obtained on PZ Tel (H = 6.5 mag). The left image is the spectrum after preprocessing and cleaning using the data reduction and handling pipeline (DRH). It corresponds to a 20 minutes exposure (DITxNDITxNEXP=20x10x6) in very good conditions (seeing of 0.5”-0.6”). The spectrum of the companion PZ Tel B is visible as a straight line amidst the speckles at an angular separation of ~0.5”. The obscured part between ±0.2” corresponds to the position of the opaque coronagraphic mask. The contrast of the companion is ~5.4 mag in H-band (Biller et al. 2010, ApJ, 720, 82). The right image is the data after stellar halo and speckles subtraction using the spectral difference approach described in Vigan et al. 2008 (A&A, 489, 1345). The spectra are displayed with the same logarithmic color scale.

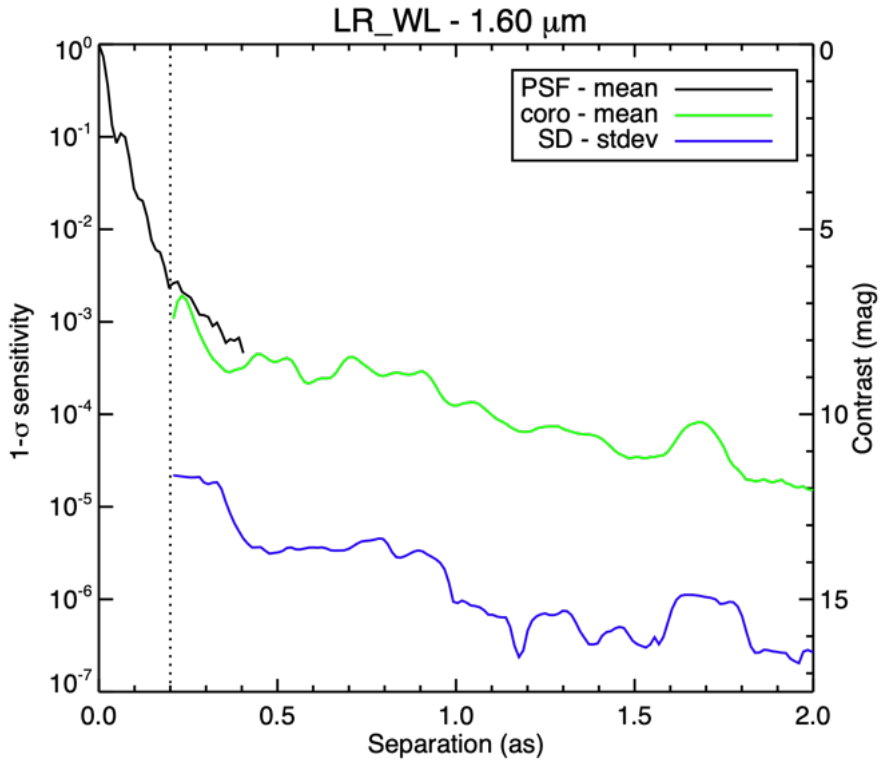

Figure 20: IRDIS LRS 1σ sensitivity curve at 1.6 µm obtained on PZ Tel (H = 6.5 mag). The plot shows the PSF profile (black), the coronagraphic profile (green) and the noise level after subtraction of the stellar halo and speckles using spectral difference (SD). The dotted vertical line represents the edge of the coronagraphic mask. At a separation of 0.5", the raw contrast in LRS data is 2-5x10^{-4}, and the speckles can be estimated and subtracted down to a level of a few 10^{-6}. However, this noise level curve does not completely represent the capabilities of IRDIS LRS mode, because one has to consider that the final characterization performance is defined by the overall quality of the spectral subtraction, and not only by the noise level in a single spectral channel, which is always optimistic. A safety margin of a factor 3 to 5 with respect to these limits has to be taken into account when foreseeing LRS observations.

3.1.3 IFS preliminary representative performance

The IFS contrast floor after speckle subtraction using principal component analysis on Iota Sgr is shown in Figure 21.

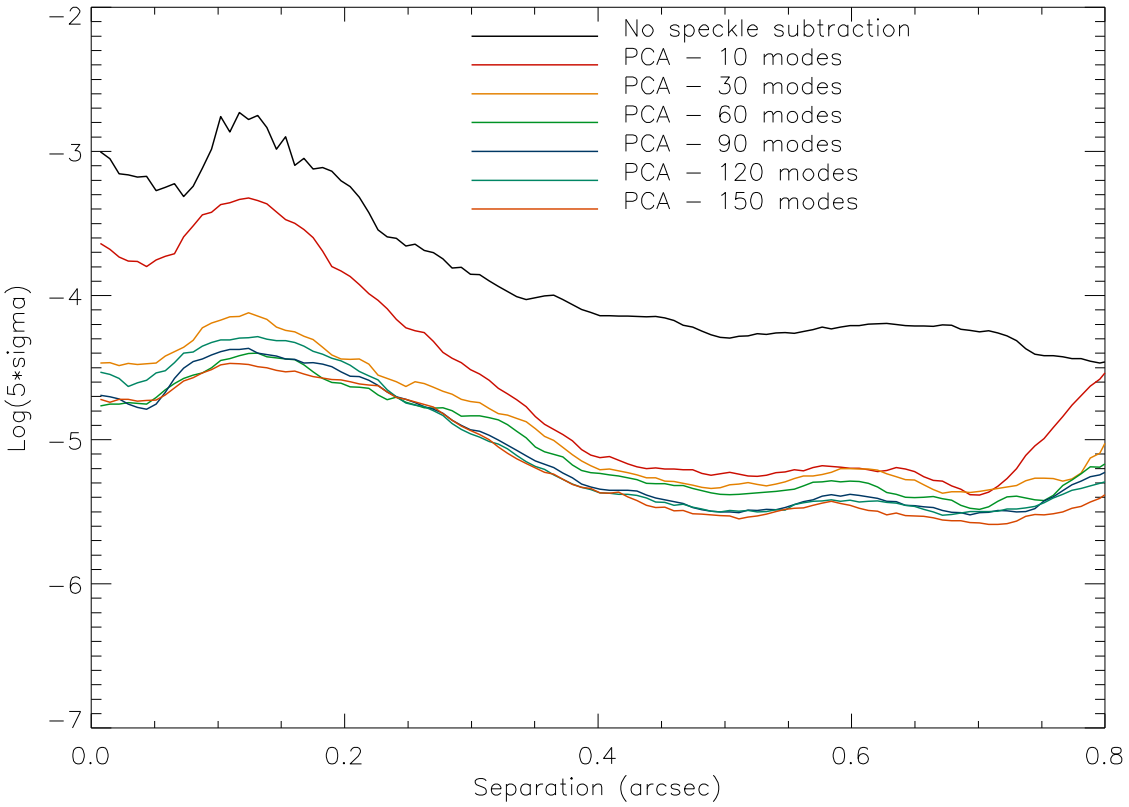

Figure 21: IFS 5σ sensitivity on Iota Sgr as function of angular separation, for different principal components retained in the speckle subtraction using both spectral and temporal diversity (ADI).

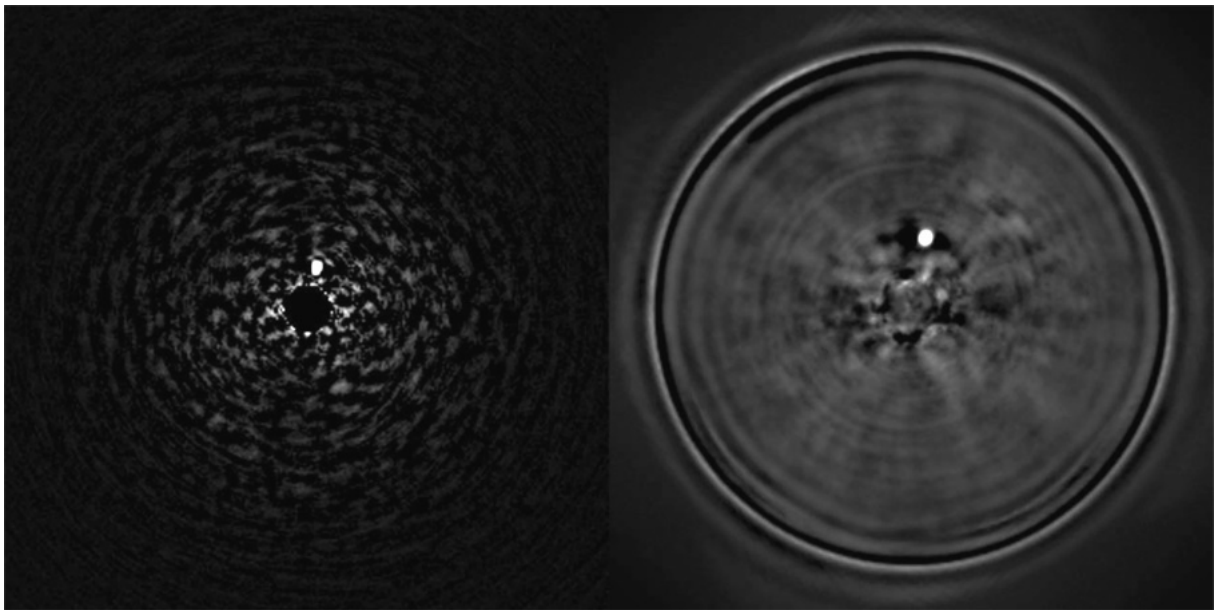

Figure 22: Detection in parallel by IRDIS (left) and IFS (right) of a faint companion at 0.24" around the bright star HR7581 (see ESO Press Release 1417, http://www.eso.org/public/news/eso1417/).

3.1.4 ZIMPOL preliminary representative performance

ZIMPOL performance as during commissioning is shown in Figure 23 and Figure 24.

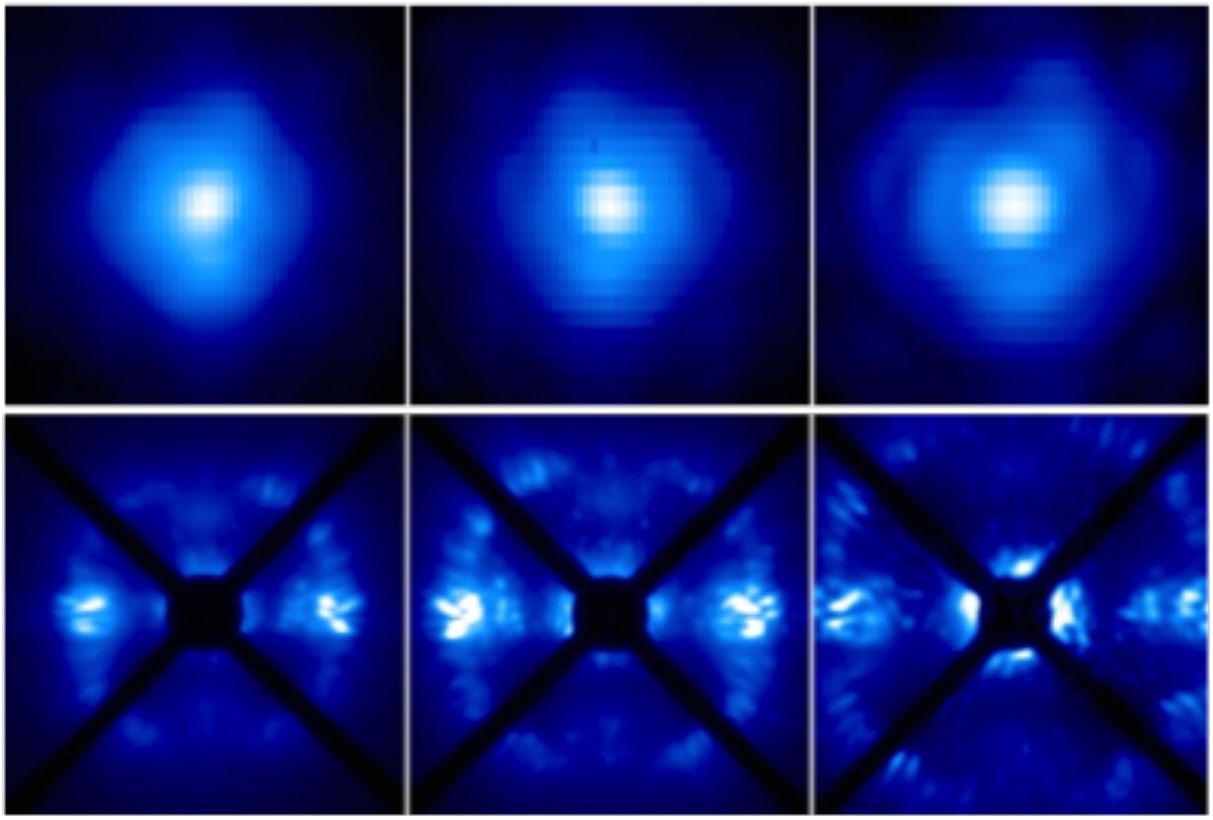

Figure 23: PSF (top) and coronagraphic (bottom) images of ZIMPOL in V, N_R, N_I filters.

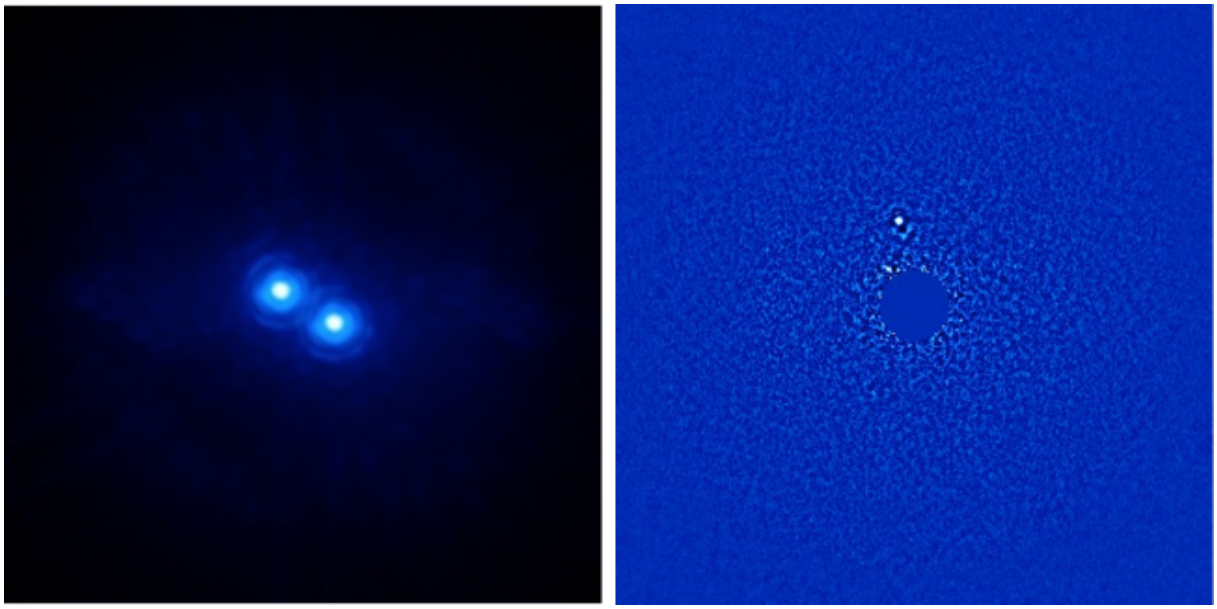

Figure 24: Left: High angular resolution imaging of a binary (150 mas separation) as seen by ZIMPOL in I band. Right: Pupil-stabilized ZIMPOL imaging providing ADI contrast close to 12 mag at 0.2" (previously unknown companion).

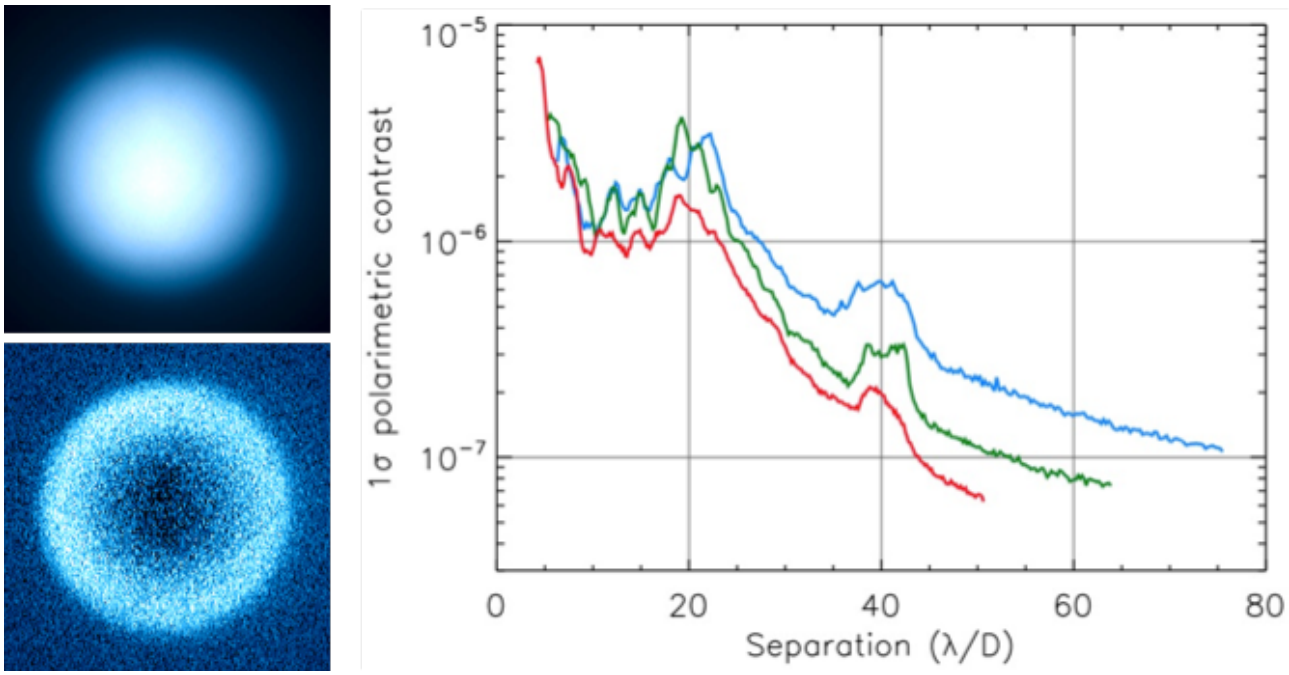

Figure 25: Top left: intensity image of Titan. Bottom Light: polarized intensity. Right: polarimetric contrast (right) on a bright target for the V (blue), N_R (green), N_I (red) filters.

3.1.5 SAM preliminary performance

The performance with SAM relies on the adaptive optics correction and parameters (tau0 and residual piston between the apertures, partially taken care of by the closure phase signal). It also depends on a good knowledge of the optical transfer function of the whole system (atmosphere, telescope, AO instrument). This can be provided by the use of a calibrator star in the vicinity of the science target, ideally within a degree or so. Since the science target and the calibrator(s) have to be observed sequentially, the calibration of the OTF is imperfect (as the atmosphere and the telescope active optics correction evolve). The smaller the duty cycle between science and calibrator, the better. Users can build their observing sequence using concatenation of OBs. The "GoTo" acquisition template will help to switch between stars in a timely manner. It is recommended to use calibrators of the same brightness (well within 2 magnitudes at R for the WFS and at the wavelengths of interest) and spectral type than the science target in order to have comparable OTF, yielding better performances.

Two other similar templates have been introduced since P103, "Starhop" and "Hopback". These two templates should be used for small hops (< 2 degrees) between science and calibrator stars and back, while the GoTo template should be used for larger jumps. For small hops the guide star often does not need to be changed, so that these is only one minute between stopping integration on one star and starting integration on the next star.

Test SAM observations were taken on July 2nd 2015 using all 3 masks and a variety of modes. Most data were taken on the Herbig AeBe star HD142527 which harbors a bright transitional disk and features a low-mass stellar companion at a separation of ~0.07". The early analysis of this data was discussed in a SPIE poster/proceeding: Cheetham, Girard et al. 2016 (SPIE 9907). The astrometric and spectroscopic analysis will be part of a later refeered publication (Cheetham et al., in preparation).

Figure 26 displays 4 SAM_7H PSF from the visible to the Ks band obtained from the same run. The level of wavefront correction and stability of the SPHERE Extreme AO system is enough to allow long exposures at visible wavelengths (at least with decent seeing conditions and using a bright reference star).

Preliminary contrast curves for ZIMPOL (R+I), IFS (Y to J), IRDIS (H and Ks) are displayed in Figure 28. Figure 27 illustrates the image and its Fourier transform, and Figure 29 presents the astrometry of the companion. In the image space, the large rings correspond to the diffraction pattern of a 1-meter aperture (each hole).

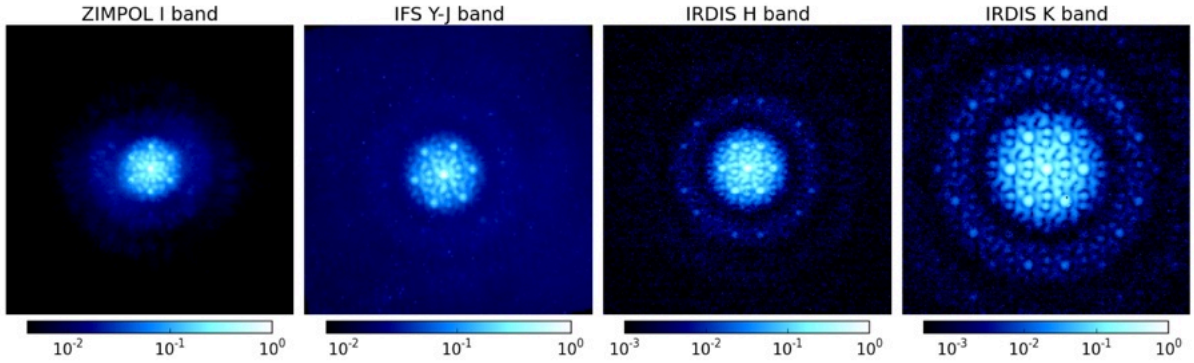

. Figure 26: SAM_7H on-sky point spread functions for 4 observing wavelengths with 3 cameras: a ZIMPOL I band exposure, a IFS wavelength slice between Y and J bands, an IRDIS H band image and an IRDIS Ks band image.

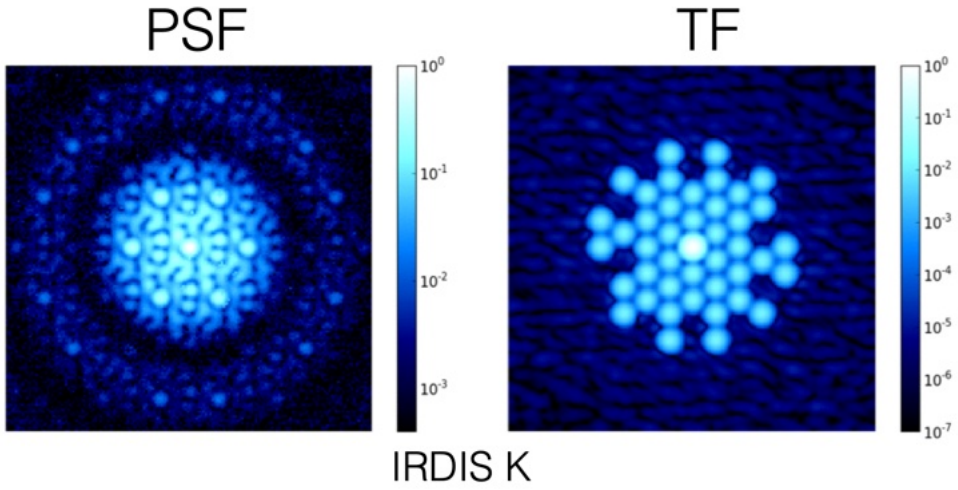

Figure 27: An image (left) produced by the aperture mask. For the 7 hole mask, the PSF is a combination of 21 sets of interference fringes. The phase and amplitude of each baseline contains information about the structure of the object being observed. The Fourier Transform of the previous image (right) allows to work in the Fourier space. Each set of interference fringes has a different frequency and direction, and so they are well separated in Fourier space and the phase and amplitude of each can be measured directly.

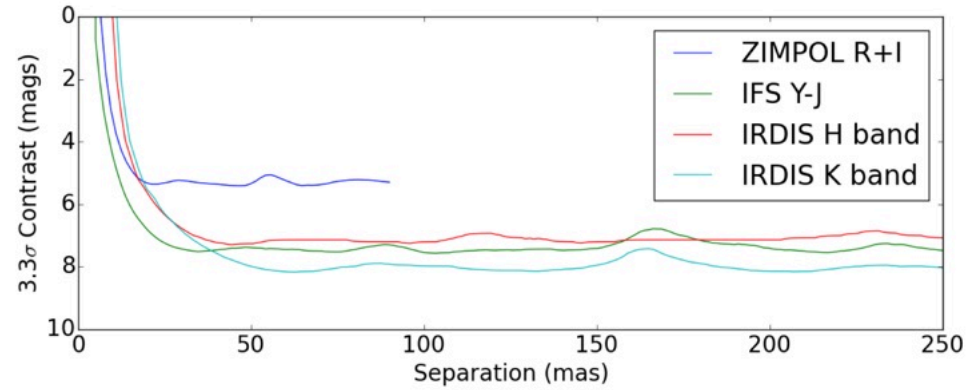

Figure 28: SAM_7H contrast limits for the detection of companions in various bands from the test data (July 2015). Each dataset consisted of approximately 1hr in execution time, including time for observations of calibrator stars. This was obtained on the F6 star HD142527 with R=8.3, J=6.5, H=5.7, K=4.98 with a seeing ~0.6-0.8". HIP113246 and HD169319 were used as calibrator stars (Cheetham et al., in prep.).

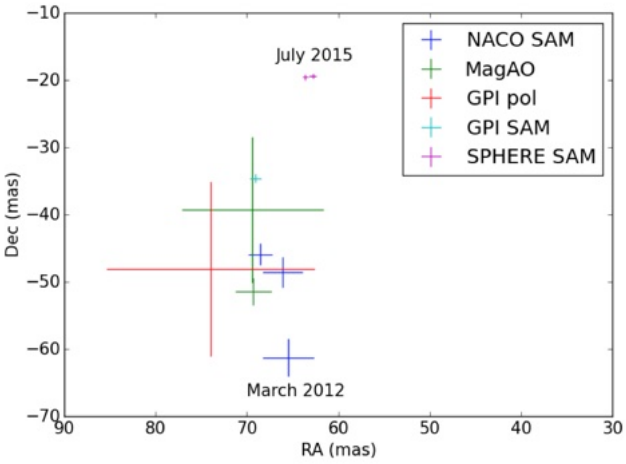

Figure 29: SAM_7H astrometry of the low-mass star companion HD142527B with respect to its host: the position uncertainty (~0.6 mas at 70 mas separation) is smaller than the one obtained by other instruments and at different epochs (Cheetham et al., in prep.).

4. EXPOSURE TIME CALCULATORS

The SPHERE ETCs can be found at: http://www.eso.org/observing/etc
It returns a realistic estimation of the detection limit. This limit is expressed as the achievable image contrast as a function of separation from the central star. It covers the various observing modes, filters and coronagraph set-ups. **When applying for telescope time, please remember to add the observational overheads as detailed in Section 11.**

Currently the SPHERE ETCs comply with the Phase 1 goals mostly, especially in terms of exploring the noise & SNR regimes as well as the contrast (versus angular distance) performances to identify the right mode(s) for the right project and the approximate time needed. The SPHERE ETCs were updated for P100 to make better DIT predictions, across the suite of instrument modes and filters. However, because of the strong sensitivity of the peak fluxes to adaptive optics performance and seeing, the recommended DITs sometimes still result in saturation. Thus we ask users, if possible, to allow us to adjust the DITs prior to observations if needed.

The formulas for the DIT predictions can be found here:
https://www.eso.org/sci/facilities/paranal/instruments/sphere/betaETC.html
On this page you will find Excel DIT calculators for both IRDIS/IFS and ZIMPOL. You can address any questions to sphere@eso.org

Some modes do not have direct ETC support, but the exposure times can be estimated from the ETC for other modes. For SAM, the central peak flux is roughly 45 times less than the corresponding peak flux in full aperture. For IRDIS DPI, one should use the ETC for IRDIS classical imaging (CI) and double the DIT recommendations. This is because the polarizers in the DPI mode cause half the photons to be lost.

5. QUALITY ASSESSMENT

5.1 Atmospheric Constraints

Stable adaptive optics performance is only expected for optical seeing < 1.4" and coherence time above 1ms. Of lesser importance, the wind velocity may also affect observations as described in the next section.

The service mode quality assessment for SPHERE depends on many parameters that affect the achieved contrast at a given angular separation:

- intrinsic calibration of the AO system and the non-common path aberrations
- external conditions (seeing, coherence time, wind speed, etc.)
- many OB-depend parameters: star brightness, wavelength range and filter bandwidth, length/field rotation, differential technique(s), post-processing, etc.

Recent analysis has shown that the coherence time (τ_0) is the best predictor of the AO performance (Milli et al. 2017). Therefore, from P105 onwards, we have defined six turbulence (T) categories based on a combination of seeing and coherence time as detailed in Figure 30. For more information go to this web page: https://www.eso.org/sci/observing/phase2/ObsConditions.SPHERE.html.

Unlike other VLT instruments, we use the seeing and coherence time at zenith, and not along the line of sight, to decide if an observation is executable and to grade it.

Turbulence Category	Maximum Seeing	Minimum Coherence Time
10%	0.60"	5.2 ms
20%	0.70"	4.4 ms
30%	0.80"	4.1 ms
50%	1.00"	3.2 ms
70%	1.15"	2.2 ms
85%	1.40"	1.6 ms

Figure 30. Definition of the 6 categories of atmospheric conditions. These conditions are defined at zenith, as measured by the MASS-DIMM.

The probability for such conditions to occur is detailed in Figure 31 and also available as an output of the SPHERE ETC.

Depending on the magnitude of the target, the defined T categories will translate to a given AO correction, in the range excellent, good, median and poor. For example, the 10% category for R < 11 and the 20% category for R < 8 will lead to an excellent correction. The 50% category for R > 11 will lead to a poor correction. For faint targets, use the Gaia G-magnitude recommendations below.

If you want to observe faint stars, use the T-category limits listed below as reference when writing your proposal (see Jones et al. 2022). If you are proposing for a non-optimal T-category, a waiver will be needed. The AO PSF worsens drastically at the T-category and Gmag limits given below.

AO PSF core doubles when (no waiver needed):
- TCAT >= 30% & Gmag >= 12.6
- TCAT >= 20% & Gmag >= 12.8
- TCAT >= 10% & Gmag >= 13

Beyond these limits, you just get a poor performance warning when preparing your OBs on p2.

PSF FWHM worsens to ~ seeing/2 at these limits (waiver needed):
- TCAT >= 30% & Gmag >= 13.3
- TCAT >= 20% & Gmag >= 13.6
- TCAT >= 10% & Gmag >= 14.0

Beyond these limits, you will need a waiver.

The ETC details the expected contrast provided for each T-category and Figure 31 shows their respective occurrence probabilities.

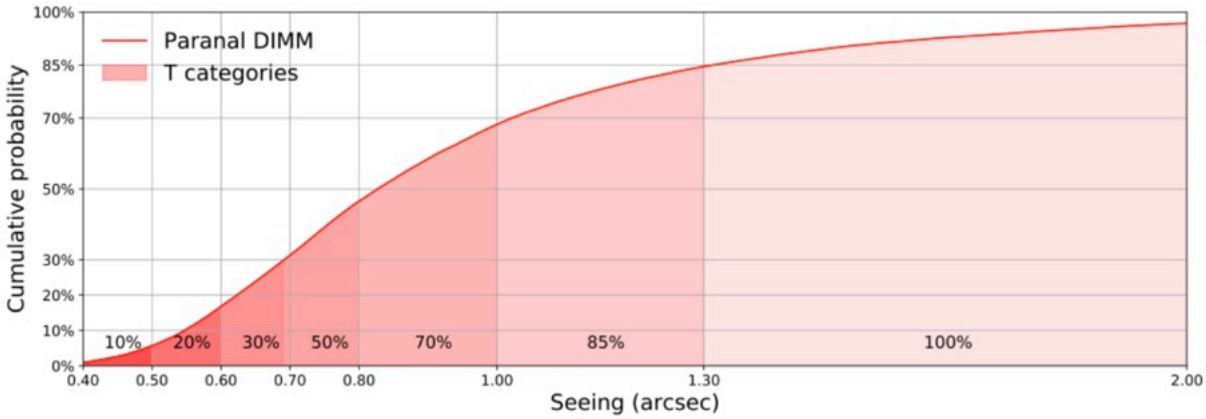

Figure 31 Probability of occurrence of each of the T-categories.

To grade an OB, we use the MASS-DIMM coherence time and the new DIMM seeing. Table 6 explains the OB classification scheme for SM operations.

Table 6. QC scheme in Service Mode operations.

OB Grade	**Constraints met**
A	*90% of the time*
B	*50% of the time*
C (to be repeated)	*Less than 50% of the time*

5.2 Low-wind effect (LWE)

The low-wind effect appears when the outdoor wind speed (at 10 or 30 m) drops below ~ 3 m/s. Since November 19, 2017, black coatings were applied to the UT3 telescope spiders to mitigate their temperature difference with the ambient air, this difference being the most likely cause of the LWE (Milli et al. 2018). Currently, the problem appears about 3.5% of the time, usually under good seeing conditions. Before the coatings, the problem appeared about 15 to 20% of the time.

The closer the wind is to 0 m/s, the stronger the effect. It is also referred as the "mickey-mouse" because it affects the PSF which can become double, triple (like "mickey-mouse" ears) or even quadruple. The effect is totally unnoticed by the AO system (Shack-Hartmann wavefront sensors are insensitive to differential piston). However, in the image plane, the PSF can be heavily affected by low-order aberrations which change on seconds to minutes time scales.

We record the LWE when it occurs and apply the scheme reported in Table 7. If it is strong and affects > 50% of the frames, we will classify the OB as "C" (must repeat). Otherwise, if shallow and < 50% of the time, we classify the OB as "B" (if all other constraints are met) and eventually add some frames. Behind the coronagraph, the effect is such that the telescope spiders aren't well suppressed and some time-varying bright speckles appear around the mask. On the F(flux) frames without the mask, **the PSF can appear double or with "mickey-type ears" or even quadruple (when very strong)** as shown on Figure 32.

Table 7: Low-Wind-Effect

5.1.1 LWE Strength	**Action for support astronomers/operators, influence on the quality assessment**
Very strong	We quit operations on SPHERE and wait (i.e VM mode). Eventually we try to point in the very direction of the wind. Data cannot be used.
Strong to mild	We wait and see if the wind increases. We evaluate if it is worth finishing the OB. In mild cases, we might add some frames to make up for it.
Mild/Nominal	We keep observing with SPHERE.

Figure 32: Low-wind-effect qualitative assessment

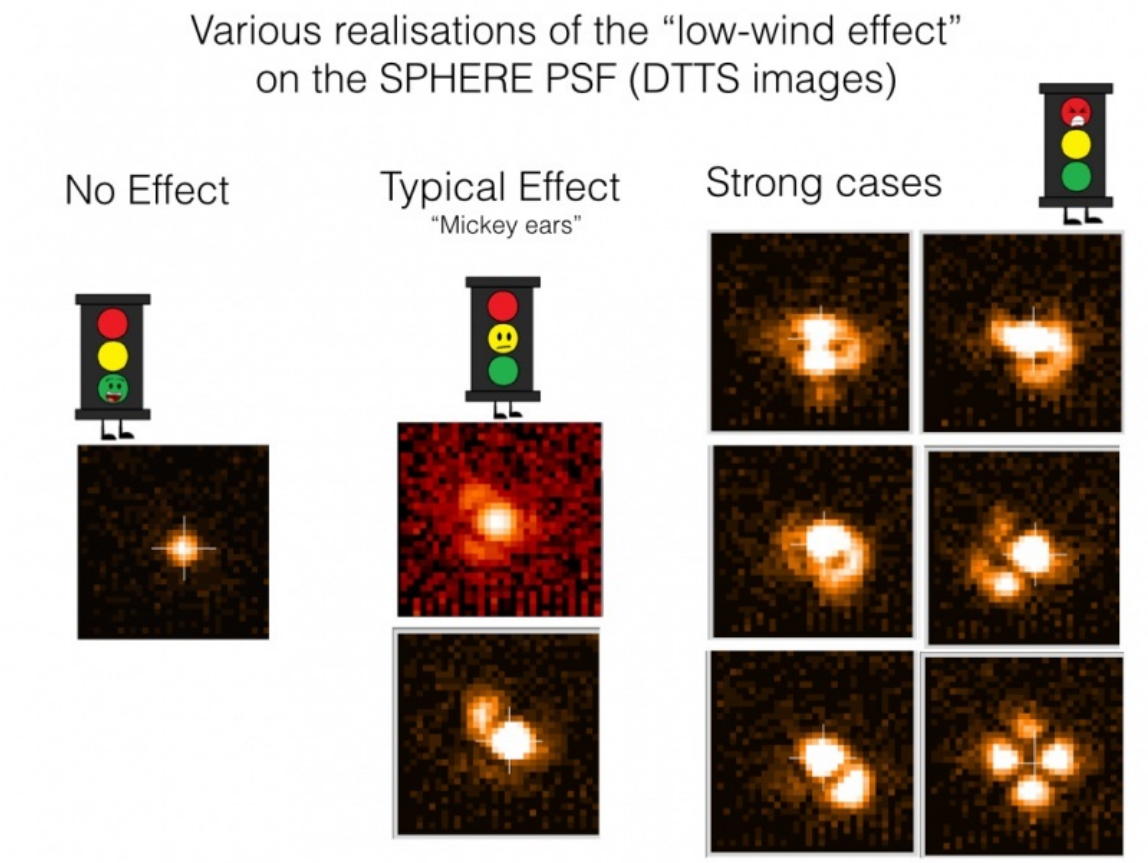

5.3 Using SPARTA files to review image quality

SPARTA files with information on the observing conditions sampled in minute time-scales are saved in the SPHERE archive page (http://archive.eso.org/wdb/wdb/eso/sphere/form). To access these files, select "SPHERE/VLT" under ***Imaging***, and enter "OBJECT, AO" for *user defined type*, under *Type* in the ***Data Product Info*** section. From these files one can obtain the SPARTA estimates of the wind and seeing during specific observations. One can also obtain images of the PSF without the coronagraph in the H-band, recorded on the DTTS, a 0.32"x0.32" FoV detector. If the primary target was brighter than ~9-10 mag in the H-band, it should be detected on the DTTS. Hence one can check the PSF-quality, and in particular, whether the low-wind effect was present during a specific observation.

6. SPHERE OBSERVING PROPOSALS

ESO issues calls for proposals. All relevant information on how to complete the so-called Phase 1 proposal submission is available at:

www.eso.org/sci/observing/phase1/proposals.html

Below, we describe SPHERE observing modes and summarize them for IRDIS and IFS observations in Table 8 and for ZIMPOL in Table 9. A recommended choice of observing parameters is shown for some science cases. The feasibility of the project, the expected performance, and required telescope time should to be worked out by the proposer with the help of the ETC, adding the observational overheads listed in Section 11.

Observing modes

NIR observations of young planetary mass companions around bright stars can be performed using IRDIS and IFS simultaneously. This mode is called IRDIFS. This is the nominal infrared mode of SPHERE, recommended for surveys, with the IFS covering the Y-J wavelength range, and IRDIS offering dual-band filters in and out of the methane spectral features in the H band (around 1.65 µm). The broad-band H filter is also offered in this mode from observing period 97. IRDIFS offers a limited range of coronagraphs, and allows the user to choose between pupil and field tracking (pupil tracking is recommended for highest contrast performance).
IRDIFS_EXT is similar to IRDIFS but extends IFS coverage to the Y-H range, while enabling (sub-optimal) dual narrow-band observations in the K band with IRDIS. The broad-band K filter is also offered in this mode from period 97. Thanks to a wider spectral range, IRDIFS_EXT improves the IFS detection capability at small inner working angles (inside ~0.2”). This mode is recommended if additional spectral range is needed (e.g. characterization of known candidate companions).

IRDIS may also be used alone, where it offers a larger range of narrowband and broadband filter choices between 0.95 to 2.32 µm, coronagraphic, polarimetric and long-slit spectroscopic capabilities:

- IRDIS_DBI (dual-band imaging) offers filter pairs in the complete spectral range. This will in particular provide essential spectral information for companions out of the IFS FoV.
- IRDIS_CI (classical imaging) provides a larger choice of observing parameters such as broadband filters (wider and more sensitive than DBI for faint stars) and narrowband filters. The narrowband filters often suffer from more ghosts. The locations of these ghost images can be found on this SPHERE web page **link**.
- IRDIS_DPI (dual-polarization imaging, offered from P96).
- IRDIS_LSS (long slit spectroscopy) merges long slit spectroscopy with coronagraphy (the slit is equipped with a blocking mask at its center, see Appendix for details). The IRDIS_LSS mode spectral range starts from Y, either up to H band at resolving power R~350 (with 0.09” wide slit), or up to the K band at R~50 (with 0.12” wide slit). The latter is useful for confirmation of a companion that is solely detected by IFS, or to take advantage of IRDIS’s larger field of view. However, since speckles scale with wavelength, they move out of the field of view at long wavelengths, such that speckle subtraction is compromised for field of view larger than 5”×5”.
-

For other science cases, such as extended sources, DPI or classical imaging is possible in all filters, with or without coronagraph, in pupil or field tracking. Please note that most differential techniques can cause significant self-subtraction for extended sources (Angular Differential Imaging, ADI), for

sources without spectral features (Spectral Differential Imaging, SDI), or unpolarized sources (Polarimetric Differential Imaging, PDI).

Table 8: IRDIS and IFS observing modes.

Mode	**Sub-mode**	**Description**			**Main Science case**
		Module/ Spectral range	**Derotator**	**Setup/ options**	
IRDIFS	**IRDIFS**	Simultaneous: IFS (Y-J) + IRDIS/DBI (narrow-band) or broad-band H.	Pupil or field stab.	None/ selected coronagraphs, SAM_7H	Exoplanet detection and characterization
	IRDIFS_EXT	Simultaneous: IFS (Y-H) + IRDIS/DBI (narrow-band) or broad-band K.	Pupil or field stab.	None/ selected coronagraphs, SAM_7H	Specific charact. using IFS up to H band
IRDIS alone	**DBI**	Dual Band Imaging, any dual-band filter pair: Y to Ks	Pupil or field stab.	None/ selected coronagraphs, SAM_7H	Charact. of companions in outer field, or confirmation of IFS detection
	DPI	Dual Polarization Imaging, any BB/NB filter: Y to Ks (BB recommended, especially J)	Pupil or field stab.	None/ selected coronagraphs (CPI HWP in) SAM_7H	Polarized circumstellar disks
	LSS	Long slit spectroscopy	Field stab.	Low or medium resolution	Characterization of companions
	CI	Classical imaging, any BB/NB filter: Y to Ks	Pupil or field stab.	None/ selected coronagraphs SAM_7H	High contrast and high sensitivity (broadband) imaging

Imaging and polarimetry are available in the optical with ZIMPOL. In imaging mode “I”, polarimetric devices are not used. Both detectors can either observe in the same or in different filters (e.g. H**α** on/off for differential imaging). For polarimetric imaging, each arm provides a full polarimetric measurement.

Table 9: ZIMPOL observing modes.

Mode	Description		Science case
	Derotator	Set-up/options	
P1	Fixed	CPI HWPs in, FLC in *Options*: focal plane coronagraphic mask or clear field mask, FW1 and FW2 filters, WFS/ZIMPOL beamsplitter	Highest (absolute) precision polarimetry mode
P2	Field stab.	CPI HWPs in, ZIMPOL HWPZ and FLC in *Options*: focal plane coronagraphic mask or clear field mask, FW1 and FW2 filters, WFS/ZIMPOL beamsplitter	High precision polarimetry suited for fainter targets
I	Pupil or field stab.	All polarimetric components out *Options*: focal plane coronagraphic mask or clear field mask, FW0, FW1 and FW2 filters, FW0 ND-filters, WFS/ZIMPOL beamsplitter SAM_7H	High angular resolution imaging and Aperture Masking

The detector has 3 different readout modes (see Appendix for details). The fast polarimetry mode is used for high precision polarimetry of bright targets (with R ~ 3–7 mag). The slow polarimetry mode (with lower RON, better efficiency, but also reduced dynamic and longer minimum DIT) is more sensitive to probe the fainter environments (in the outer PSF and/or in narrowband filters). The standard imaging mode is used for non-polarimetric imaging.

Rapid Response Modes

For observing transient events around bright objects (R < 11 mag), starting in period 100, we offer the rapid response mode (RRM) for the SPHERE instrument. The new acquisition templates offered for these modes (all practically identical to their non-RRM counterparts) are presented in templates section at the end of this manual. Only the IRDIS DPI and LSS modes will not be available for RRM. More information on the RRM can be found at: https://www.eso.org/sci/observing/phase2/SMSpecial/RRMObservation.html

Coronagraphs and filters

The choice of the coronagraph depends on the observing wavelength and inner working angle (see Appendix A6). Filter sets are detailed for IRDIS in Section 10.3 and for ZIMPOL in Section 10.8. For ZIMPOL please note the AO limiting magnitudes with the grey beam splitter are ~1.74 mag brighter in R than with the dichroic (see Table 3). Also note that the use of some filters and neutral densities (located in FW0) will result in additional instrumental polarization which cannot be calibrated using the polarization compensator. Therefore the use of filters and neutral densities in the FW0 filter wheel is not recommended for ZIMPOL polarimetric imaging modes.

Coronagraphs set-ups and centering, which are performed in the acquisition template, take ~5 minutes. Hence the observer is advised to limit the number of set-up changes of the coronagraph.

Sparse Aperture Masks

Three aperture masks are installed in SPHERE. All are of the same basic 7-hole design, but are located within the different sub-instruments such that SAM can be used with IRDIS (ST_SAM in the Lyot wheel), IFS (ST_SAM) and ZIMPOL (V_SAM). The general layout of the mask is shown in Figure

3. The rotation and size of each mask varies between the sub-instruments. The approximate coordinates of each mask hole for each instrument is listed in Table 10 (see Cheetham et al. 2016), expressed with reference to the VLT primary mirror size and projected onto the detector coordinates. However, we caution that these were measured from a single epoch in July 2015 and are provided as a guide only; the hole positions should be updated for each new set of observations.
The design of these masks requires balancing several competing factors. The 7-hole design employed in SPHERE is optimized for detecting point sources around faint targets. However, this does not preclude its use for other purposes.

IFS		IRDIS		ZIMPOL	
X (m)	Y (m)	X (m)	Y (m)	X (m)	Y (m)
-2.07	2.71	-1.46	2.87	3.06	1.50
0.98	3.27	1.46	2.87	3.02	-1.60
-3.11	-0.20	-2.92	0.34	0.41	3.09
-1.43	-0.81	-1.46	-0.51	-0.51	1.56
-2.79	-1.96	-2.92	-1.35	-1.38	3.12
3.30	-0.85	2.92	-1.35	-1.48	-3.07
0.58	-3.17	0.00	-3.04	-3.22	0.05

Table 10: SPHERE aperture mask hole positions in July 2015.

AO limiting magnitudes

The most important feasibility check for SPHERE observations concerns the AO performance, measured by the Strehl ratio (SR). The SR directly impacts raw contrast level C through the rule of thumb $C \propto (1\text{-}SR)/N^2$ (Serabyn et al. 2007, ApJ 658, 1386) with N^2, the number of AO correcting elements (~1300 in SAXO).

In Figure 33, we show the Strehl ratios obtained for four AO correction regimes: excellent, good, median, and poor for faint stars. In Figure 34, we show when these corrections regimes are obtained in terms of T-categories and R magnitudes of the target star. For current turbulence-category definitions and faint-star observing recommendations, see Sections 5.1 and 3.

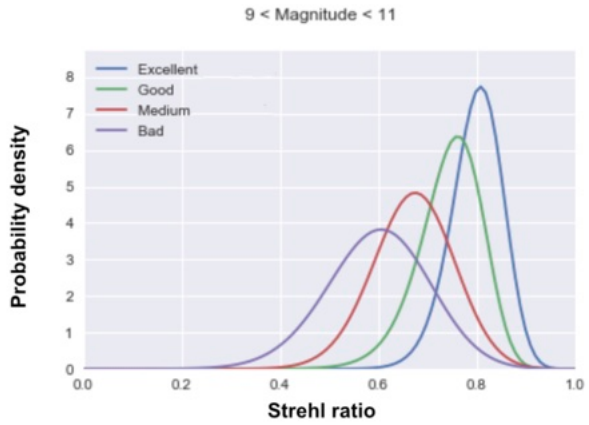

Figure 33: AO correction categories and their performance for faint stars.

AO flux\turb categories	5%	10%	25%	40%	60%	80%	100%
>100e-/subpup/frame (Rmag 0-8)	excellent	excellent	good	good	median	median	not offered
between 30 and 100 (Rmag 8-11)	excellent	good	good	median	poor	poor	
below 30 (Rmag >11)	good	median	median	poor	poor	poor	

Figure 34: The AO performance expected in each of the T categories for ranges of Stellar R magnitudes. Historical turbulence categories; for current definitions, see Section 5.1.

The contrast depends weakly on the seeing for seeing up to about 1.2" and degrades rapidly for seeing > 1.2", and NGS R mag > 11.

Telescope time

For proposal submission, the astronomer should estimate the total telescope time required for the observing program. The ETC should be used to compute the integration times (see Section 4). When applying for telescope time, please remember to add the overheads described in Section 11. In service mode, observations are executed with observing blocks of at most 1-hour duration. An observing program must therefore take this constraint into account at Phase 1. A waiver for longer OBs can be requested in Phase 2.

For the vast majority of projects, the night-time OBs will contain only one science template and the mandatory target acquisition template. The usual calibration measurements such as darks, flat-field and wavelength calibrations, are taken during the day-time as part of the calibration plan (Section 8). If for some observations, particular calibrations are needed immediately after the science exposure, these can be obtained by attaching specific calibration templates at the end of the OB or by concatenating a standard-star OB to the science OB.

For Phase 2, the new ESO Phase 2 Preparation Tool (P2, which has replaced P2PP since P101) will be able to provide accurate estimates of the execution time, including overheads. It is available at: https://www.eso.org/p2demo/

7. PREPARING THE OBSERVATIONS

Phase 2

After proposal submission (Phase 1, Section 4), when telescope time has been granted, the observations need to be prepared during phase 2. Please consult the general guidelines on phase 2, service and visitor mode, which are available at:

- Phase 2 preparation: http://www.eso.org/sci/observing/phase2.html
- Service mode: http://www.eso.org/sci/observing/phase2/SMGuidelines.html
- Visitor mode: http://www.eso.org/paranal/sciops/VA_GeneralInfo.html

The observing blocks (OBs) are created with the aid of the new P2 tool (since P101) during Phase 2. OBs include: one acquisition template, followed by one or more templates for science observations and/or night-time calibrations. Finding charts and readme files need to be created according to the instructions available at:
http://www.eso.org/sci/observing/phase2/SMGuidelines/FindingCharts.SPHERE
and,
http://www.eso.org/sci/observing/phase2/SMGuidelines/ReadmeFile.SPHERE

Observing constraints

The SPHERE observing constraints which can be included in Observing Blocks when preparing the observations are:

- Turbulence categories: Six categories of atmospheric conditions based on a combination of seeing and coherence time.
- Transparency: SPHERE's adaptive optics system SAXO has been shown to be very tolerant to THIN conditions, **so user should only request photometric (PHO) or clear (CLR) conditions only for programs requiring absolute flux measurements.**
- Moon illumination and Moon distance: SPHERE's small field of view and pixel scale is such that observations are not sensitive to the moon illumination. The angular distance, however, is recommended to be > 30º because of the VLT active optics.
- Airmass: Considering the maximum compensable atmospheric dispersion by ADCs, pointing is restricted to z < 60º (airmass < 2).
- Sidereal time: Observing close to meridian is strongly recommended for ADI performance as it yields more field rotation and also PSF stability. To ensure this, the sidereal time constraints should be used. However, for declinations < -50º or > 0º the field rotates quite uniformly with hour angle (see Figure 35), and lax sidereal time constraints are strongly recommended. **These constraints should be very lax for star-hopping concatenation allowing HA or -4 to +4.**
- Declination constraints: targets with declinations between -27:40:00 and -21:35:00 cannot be observed during the meridian passage, as the telescope cannot be pointed closer than 3 degrees to the zenith. That means that only a very small field rotation can be attained for targets with declinations within that range, and thus they might not be suitable for ADI.
- Twilight constraint: In general, IRDIS/IFS OBs can be done in twilight, and thus this constraint is set by default to –30 (30 min before the end of evening twilight).

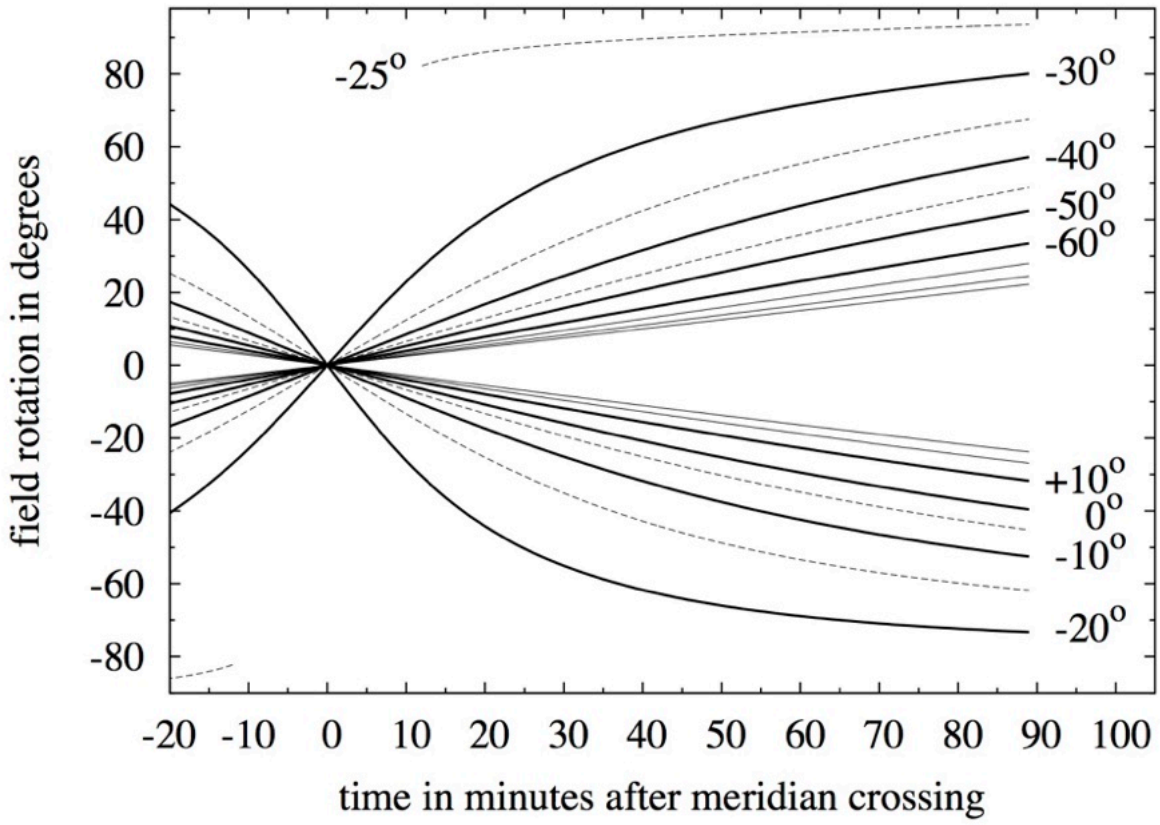

Figure 35: Rotation of field relative to orientation at meridian crossing for targets at different declinations (dotted and dashed lines), for pupil-stabilized observations.

ESO will consider an OB as successfully executed if all the conditions in the constraint set are fulfilled. OBs executed under conditions marginally outside constraints by no more than 10% of the specified value will not be scheduled for re-execution. Unlike other Adaptive Optics-assisted instruments on Paranal, the image quality of observation conducted in service-mode will be classified according to the seeing constraint only. Once more experience is gained with the instrument performance under a wide range of observing conditions, this situation will change, and Strehl or contrast will be introduced as a formal observing constraint for SPHERE.

SPHERE has been verified to provide optimal performance under stable temperature conditions. Moreover, critical components are sensitive to temperature and humidity. For these reasons, the observatory reserves the right to interrupt observations if conditions put the instrument or the quality of the data in jeopardy. For instance:

- Temperature should be between 5°–18°C. Temperatures outside of this range change the DM shape at rest and reduce the tolerance to high seeing values.
- Temperature variations < 1°C/h, and excursions over the night < 4°C. Strong temperature gradients will degrade the PSF stability.
- The internal humidity must stay below 50%, as it might potentially damage the deformable mirror.

Target acquisition templates

Each OB starts with an acquisition template. The selection of the appropriate acquisition template is detailed in Table 11. It depends on the subsequent observing mode. Target acquisition is done in a narrow 2"×2" field of the WFS sub-apertures, and so requires precise target coordinates and proper motion. Requiring a larger FoV by imaging using IRDIS introduces unnecessary overheads times. It is important to note that all observations in a given OB should share the same sub-mode. For SPHERE, it is typically not necessary to define a specific telescope guide star. Therefore, the telescope guide star selection can be set to "catalogue", in which case a suitable telescope guide star will automatically be selected from one of the catalogues present at the telescope. Parameters to be set by the observer will be discussed in Section 739.

Table 11: List of SPHERE acquisition templates.

Acquisition template	Observing mode
SPHERE_irdifs_acq	IRDIFS, IRDIFS_EXT
SPHERE_irdis_acq	IRDIS alone in DBI or CI.
SPHERE_irdis_dpi_acq	IRDIS alone in DPI mode.
SPHERE_irdis_lss_acq	IRDIS alone in LSS.
SPHERE_zimpol_i_acq	ZIMPOL: Imaging (I).
SPHERE_zimpol_p_acq	ZIMPOL: Polarimetric Imaging P1 (derotator fixed) or P2 (field-stabilized).
SPHERE_irdifs_acq_rrm	IRDIFS, IRDIFS_EXT for rapid response.
SPHERE_irdis_acq_rrm	IRDIS alone in DBI or CI for rapid response.
SPHERE_zimpol_i_acq_rrm	ZIMPOL: Imaging (I) for rapid response.
SPHERE_zimpol_p_acq_rrm	ZIMPOL: Polarimetric Imaging P1 (derotator fixed) or P2 (field-stabilized) for rapid response.
SPHERE_gen_acq_GoTo_acq	All modes Note: not stand alone, only for sub-sequent OBs in a concatenation.

The acquisition templates include:

- Telescope preset to the target coordinates and acquisition of telescope guide star.
- Automatic setting of AO parameters, servo loops and checks (except for SPHERE_gen_acq_GoTo).
- Start of tracking components: derotator, ADCs, and polarization components if relevant.
- Centering on the coronagraphic focal mask, if any. When the user-defined focal mask is different from the previous OB, the new mask is set in and a corresponding calibration can be performed to ensure the best centering and focus accuracy. Note that this coronagraphic device selection cannot be modified in subsequent observation templates: it remains the same in all the templates of the OB.

General user defined parameters for IRDIFS and IRDIS templates

IRDIFS and IRDIS observation templates share many common parameters defined by the observer. They include settings of:

- DIT, NDIT, NEXP for IFS and IRDIS. A DIT value of 0 indicates that the smallest possible DIT value (currently 0.83 seconds for IRDIS and 1.67 for IFS) is to be used.
- Number of dithering positions for IRDIS (4x4 recommended). No dithering is offered for IFS.
- Observation type list. Defines the sequence of Object (O), Sky (S), Flux (F) and Star Center (C) measurements (see below) to be obtained.
- Detector X and Y offset for flux measurements. Indicates the offset (in mas) which is performed to offset the source from the coronagraphic mask for the flux measurement. The recommended value (and also maximum value) is +500mas or -500mas.
- Sky RA and Dec offset list. A list of sky offsets (in arcseconds) for the sky background measurements. The number of sky measurements for each "Sky" in the observation type list is equal to the number of offsets defined in the Sky RA and Dec offset list, i.e. for an RA and Dec Sky offset list of "10 -20", "-20 40" will result in two sky background measurements per "S" in the observation type list. An offset greater than 10" but less than 60" is recommended. The offsets are cumulative, namely "10 10" followed by "-10 -10" returns to the star position.
- Deformable mirror waffle parameters. These parameters control the amplitude and the pattern of the four symmetric echoes of the PSF core in the Star Center measurement. Details are given in Appendix A 12 concerning the use of the waffle spots for accurate centring. In case of observing an object with a known companion, changing these parameters may be useful to ensure that the position of the echoes do not coincide with the location of the companion. From period 106, we recommend that amplitude be left as "AUTO", the default value so that it is calculated automatically based on the brightness of the star and the DIT.
- Choice of neutral density filters.
- Field orientation, for field-stabilized observations. Note that the angle of the true north TN is -1.75 degrees.

Besides the on-axis (coronagraphic or not) observation of the **object (observation type O)**, the observing template sequence should also include these observation types whenever using a coronagraph, or when observing extended objects for the third one:

- Star Center - C: in the pupil-stabilized mode, the field rotates. It is thus critical to obtain the exact position of the rotation center. This is also important for accurate measurement of the separation of any potential companion. This allows measuring this position by applying a waffle pattern to the deformable mirror, which creates four replicas of the PSF away from the coronagraphic mask (see Appendix A12). Localizing the four peaks allows computing the rotation center, at the middle of the square pattern. This measurement is performed with the science template and can be repeated several times during a long science sequence. For SAM, "C" frames are not relevant.
- Flux - F: a PSF core off-axis measurement can be inserted before and/or after deep coronagraphic observations in order to register the PSF core flux. Contrast curves are derived from this measurement. Off-axis measurements can be performed by moving the star and inserting a neutral density but without moving the coronagraphic focal mask and thus without perturbing the centering accuracy. For SAM, "F" frames are not relevant.
- Sky – S, optional: observes the sky background. Accurate knowledge of the background is not important for point-like objects. However, it might be important for faint extended emission.
- The DIT values for the C and S observations, are not user-defined parameters, but are identical to the DIT used for the O observation. The DIT value for the F observations has to be defined separately within the observing template, in combination with ND filters.

Important: if the observer concerned about saturating the detector because of uncertain target brightness, it is strongly recommended to isolate a Flux (F) and Star Center (C) in two independent templates to allow the night astronomer to check the saturation level of these frames before continuing with the rest of the observations (typically observations of type O). This way, the detector integration time can be more easily adjusted, in case of detrimental over- or under-illumination of these critical frames, without aborting the whole sequence of observations.

"GoTo" acquisition template

SPHERE_gen_acq_GoTo_acq

In P100, a new acquisition template called "GoTo" was introduced. It allows the user to switch from one target to another in a timely manner. It will perform a preset to the new target (i.e. a PSF calibrator) without performing any AO nor instrument setup. This template will be instrument independent and it will not be "stand alone", it will only be used after one of the normal acquisition templates has been executed at the beginning of a concatenation of OBs. The gain in overheads will be considerable, at least 5 minutes per sub-sequent OB in the concatenation (C container). The R magnitude of all targets within the concatenation must not differ from the magnitude in the 1st acquisition template by more than 1 mag and with all R < 13.

"Starhop and Hopback" templates

We strongly recommend the star-hopping RDI technique as an alternative to ADI for high contrast imaging within 1" separation from the host star, especially when small sky rotations are expected for ADI. The contrast performance details can be found in Wahhaj et al. 2021, along with a special data reduction pipeline for star-hopping IRDIFS data.

For starhopping, the ***SPHERE_gen_acq_starhop*** and ***SPHERE_gen_acq_hopback*** templates should be used (as opposed to the GoTo template) for hopping to a reference star, which is a few degrees away. The hop is expected to take just 1 minute, but with detector readout time, there will be a 2 minute gap in integration during the hop. As described below, the performance at small separations is unprecedented and the gain is attributed to the quick hops now possible.

The SPHERE_gen_acq_starhop performs a telescope offset to a nearby star (e.g. a PSF reference). The best performances are expected for hops to reference stars within a degree. As with the GoTo template, no further AO or instrument setups are performed here. The template has to be used after one of the normal acquisition templates. After the SPHERE_gen_acq_starhop is used, the hop vector and the guide star (or guide stars, if a second one had to be used) are saved for duration of the concatenation. Then, the SPHERE_gen_acq_hopback template can be called to hop back and forth between the science and the reference star, while guiding is started automatically on each hop using the previously stored parameters. No keyword parameters need to be supplied to the hopback template as it alternatively uses the hop vector with a positive and then a negative direction. However, the vector direction can be forced to be positive or negative. The star hopping templates can be used with all observing modes of SPHERE, given that an appropriate reference star is available.

We obtained a technical calibration data set on August 21, 2019 to help design a star-hopping RDI sequence as an alternative to the ADI technique. Please search under program ID 60.A-9801(S) for further calibration data sets, obtained during otherwise idle time. Since, close to the target star, sensitivities are contrast limited instead of photon limited, we can afford to spend 50% of the time on the reference star and the hop overhead. So we set the observing efficiency = 0.5 = S/(S+2 +

R+2 min), where S = science target time, R=reference time. Solving this equation, we get S=R+4 min or S = (R+4) x/(1-x), for efficiency = x. We also want to jump to the reference star quite often to capture a good number of similar PSF images (in comparison to the science PSF). So we chose R=4 min, and thus S=8 min or 10 min total on each science OB and 6 min total on each reference OB in the concatenation.

The seeing and coherence time during the star-hopping calibrations were 0.6-0.8" and 5-8 ms respectively. There were thin clouds. The target star was HD 5078 (G3/5V, H=6.3) and the reference star was HD 5077 (K3III, H=5.3), about 1.1" away. The airmass was about 1.2. The observations were in the IRDIFS_EXT mode (IRDIS in K12 bands). We used the K-band coronagraph here, but results using smaller coronagraphs to access smaller separations were published in Wahhaj et al. 2021. In summary, the coronagraph should be small enough to access the desired separations but no smaller, to achieve the best contrasts. We used a DIT of 16s in IRDIS to avoid being limited by read noise, and to obtain enough images to capture the PSF diversity.

The final contrast numbers were 12 mag at 0.12" and 13 mag at 0.3" separation. Moreover, the typical reduction in the RMS noise at 0.12" separation after PSF subtraction was a factor of 60 (4.4 mag improvement). The reduction in the RMS after adding all the difference images was a further factor of 5 (~ 1.75 mag improvement). The reduced images are shown in Figure 36.

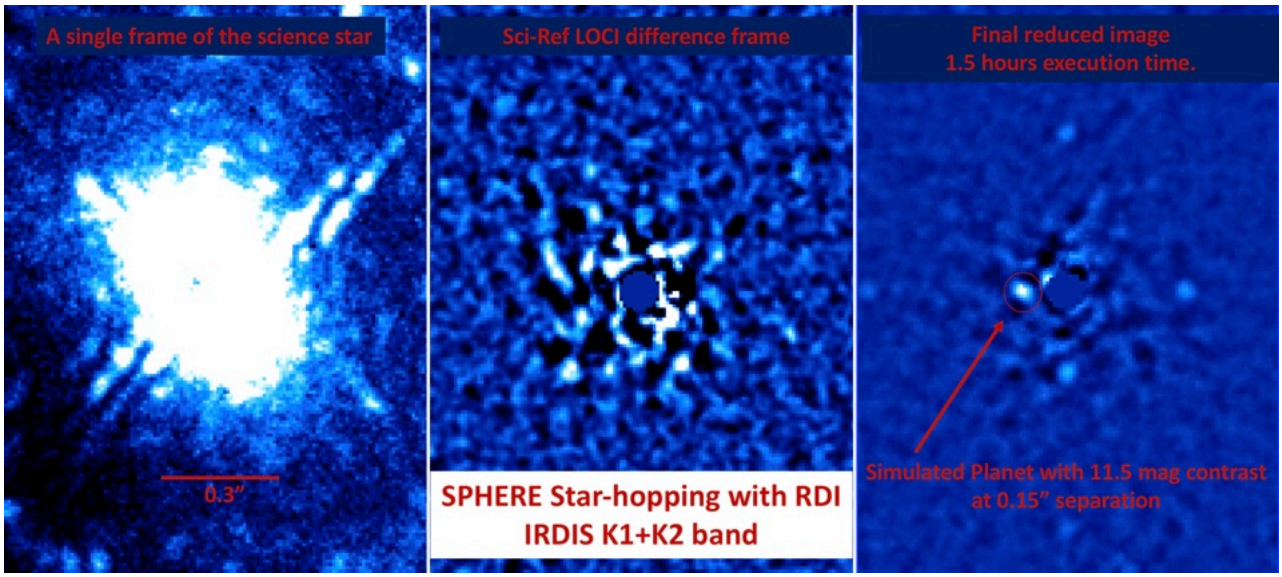

Figure 36: Reduced images from a star-hopping RDI data set. Left: a single DIT=16s image of the target star. Middle: The corresponding difference image after RDI. Right: The final RDI reduced image after derotation and coadding. A simulated planet, implanted with contrast 11.5 mags at 0.15" separation is recovered after reduction. No spectral differencing was done. The K1 and K2 channels were added together, and the simulated planet was given the same contrast in the two channels. All images show the same intensity range in square-root stretch. The images are 0.8"x0.8". See Wahhaj et al. 2021 for more details.

A star hopping concatenation would typically look like:

OB1
SPHERE_xxx_acq [aquire science star, do some instrument setup and AO setup]
SPHERE_xxx_obs [take data on science star]

OB2
SPHERE_gen_acq_starhop [offset to PSF calibrator star, store hop vector and guide star(s)]
SPHERE_xxx_obs [take data on calibrator]

OB3
SPHERE_gen_acq_hopback [hop back to **science** star]
SPHERE_xxx_obs [take data on **science** star]

OB4
SPHERE_gen_acq_hopback [hop back to **calibrator**]
SPHERE_xxx_obs [take data on **calibrator**]
…

It is recommended that CENTER and FLUX observations are not taken in any of the concatenations which include the hopback template, except the last one. This is because these templates incur overheads larger than a minute, while the purpose of the hopback template is efficient observations of science and reference star, switching between them as quickly as every 10 minutes. We recommend that cycles slower than S=13 min be avoided (thus keep S<13) for RDI.

To find ideal reference stars (within 1 mags and 2 degree of the science target), the following searchcal tool may be helpful: http://www.jmmc.fr/searchcal. However one can also use SIMBAD and search for reference stars of similar magnitude within 2 degrees. Guide stars can be provided but are not compulsory.

IRDIFS templates

7.1.1 Observation templates and user-defined parameters

IRDIFS observation templates are detailed in Table 12. Parameters defined by the observer will be presented in Section 9.

Table 12: IRDIFS observing templates.

IRDIFS observation templates	Observing modes
SPHERE_irdifs_obs	IRDIFS observations, with IFS observing in Y-J and IRDIS in H-band, DB_H23, or DB_H34
SPHERE_irdifs_ext_obs	IRDIFS_EXT observations, with IFS observing in Y-H and IRDIS in K-band or DB_K12

For efficiency reasons it is recommended that the total duration of IFS and IRDIS exposures are similar. The neutral densities inserted in CPI are common to IRDIS and IFS. For minor differential adjustment another ND0.5 (factor $10^{-0.5}$) is available inside IRDIS for the H band dual-band filters.

7.1.2 Calibrations

Calibrating IRDIFS data involves usual day-time internal calibrations (darks/background, flat, spectral calibration of the IFS, see Section 8 for details).

IRDIS Dual Band Imaging (DBI)

7.1.3 Observation templates and user-defined parameters

IRDIS observation templates	Observing modes
SPHERE_irdis_dbi_obs	IRDIFS DBI

For IRDIS-only observations in dual band imaging mode, there is a single template called SPHERE_IRDIS_dbi. Parameters defined by the observer are discussed in Section 9. The Appendix lists all the available filters. The filter pair DB_ND23 includes a ND0.5 neutral density but is otherwise identical to DB_H23.

7.1.4 Calibrations

Calibrating IRDIS-DBI data involves on-sky and internal (day-time) calibrations similar to the IRDIFS and IRDIFS_EXT modes (see Section 7.1.2). Other night-time and day-time calibrations provided as part of the SPHERE calibration plan are detailed in Section 8.

IRDIS alone Classical Imaging (CI)

7.1.5 Observation templates and user-defined parameters

IRDIS observation template	Observing mode
SPHERE_irdis_ci_obs	IRDIS CI

A complete list of user-defined parameters is presented in Section 9.

7.1.6 Purpose and properties

This mode is a general-purpose mode, which can be used in pupil, or field-stabilized regime. In this mode any filters from the common filter wheel can be used. The recommended derotator rotation law to be used for observation of extended objects should be the field stabilized to avoid image smearing. Coronagraphs can also be used with any filter in classical imaging mode (see Appendix for details).

7.1.7 Calibrations

The calibrations for IRDIS CI observations are the same as for DBI observations.

IRDIS Dual Polarization Imaging (DPI)

Dual polarimetry (via DPI) can achieve greater contrasts at small inner-working-angles, provided that the object of interest features polarized scattered light in the near IR (i.e debris and proto-planetary disks, etc.). If the latter condition is satisfied, DPI offers an enormous advantage over other high contrast differential techniques: images at orthogonal linear polarizations are taken simultaneously. If both beams have the same optical aberrations, DPI allows very efficient speckle suppression in the control radius of the AO/coronagraph.

This mode has been used in Science Verification time and by the GTO in “shared risks” because its characterization was incomplete. It was offered starting P96. Also from P101, dithering was enabled for the IRDIS/DPI mode.

7.1.8 Instrumental polarization

Thanks to the SVT and P95/P94 experience, we were able to better characterize the IRDIS DPI mode. We found out that the control law of the HWP for field tracking was not ideal and changed it in late

April 2015. Moreover, we optimized the HWP law for pupil tracking in January 2019. The effect of polarization cross-talks inside the instrument for four BB filters were measured in P94 & P95.

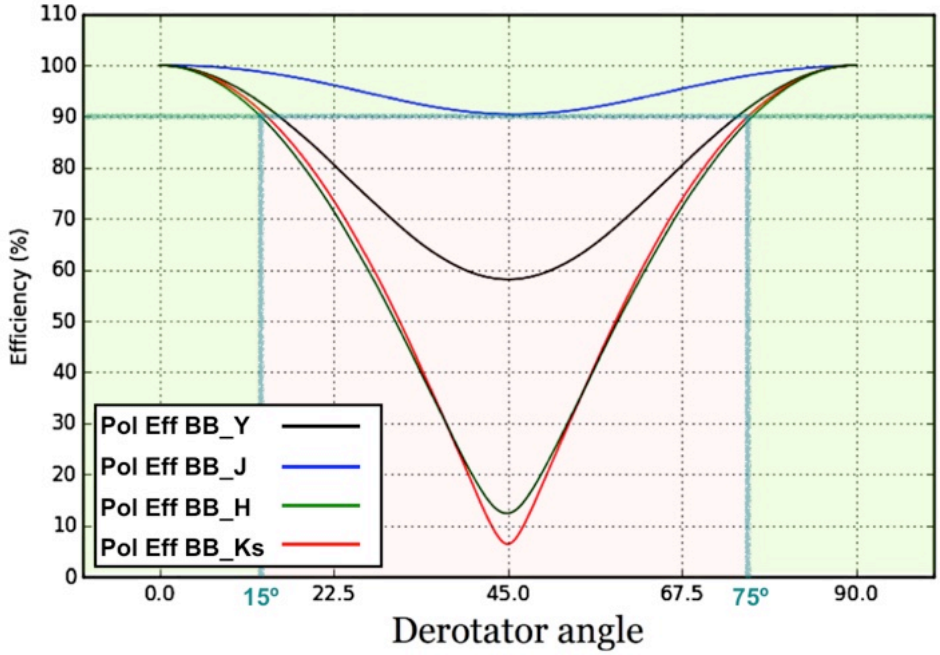

Figure 37: Measurements of the instrumental polarization efficiency (not accounting for the telescope) for four broad band filters. For best use of the DPI mode (relevant for field tracking while irrelevant for pupil tracking), one should avoid the pink zone where the efficiency drops below 90% (> 10% loss due to cross-talks). For that, one should make sure the derotator angle stays < 15° or > 75°. J-band is the least affected and therefore the most recommended filter, especially for long observations featuring a large parallactic angle variation. At J-band the efficiency is always > 90%.

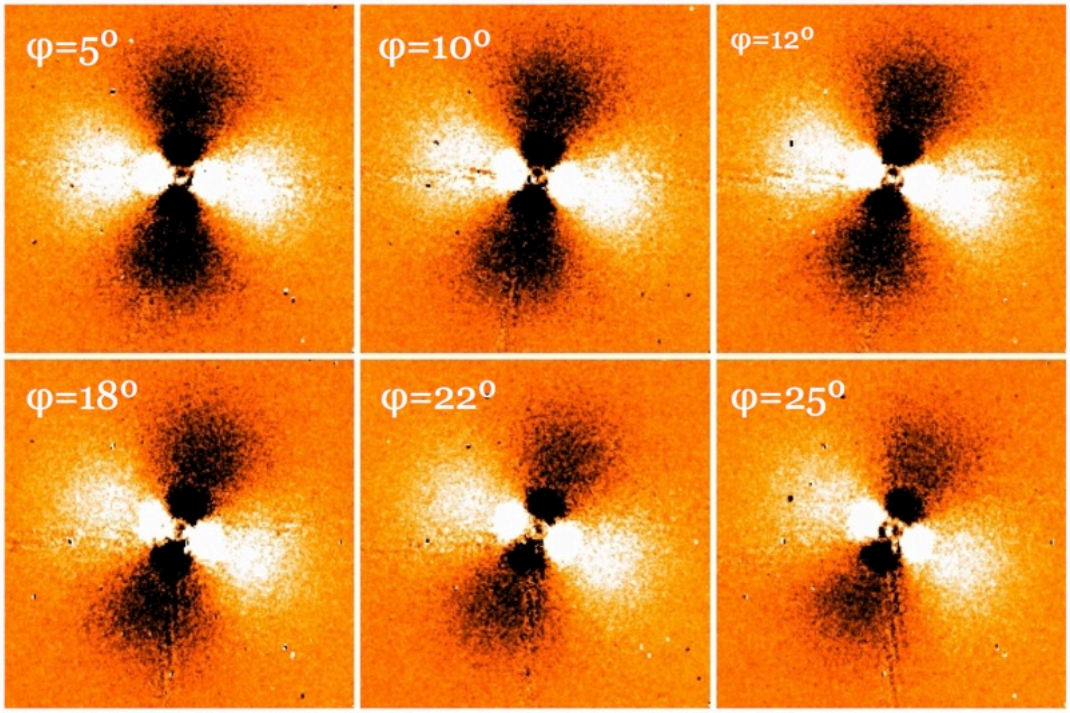

Figure 38a: Effect of the instrumental polarization (efficiency loss due to increased cross-talks at a varying derotator angle). The « butterfly pattern » rotates with time and its signal to noise ratio decreases significantly. This is the polarimetric signature of a bright face-on disk (H-band observations).

Figure 38: a shows the « butterfly » pattern of a bright face-on polarized disk. Its SNR and orientation varies in time. This is because of the departure, during the observation from the ideal (< 15º or > 75º) derotator position as it tracks the field, in H-band (as shown in Figure 37). This effect was even stronger before the end of April 2015 when we changed the half-wave-plate control law.

We recommend the following when using the DPI mode with field tracking (not relevant for pupil tracking):

- Use the BB filters as much as possible.
- J-band is the least affected filter (efficiency always > 90%).
- For Y, H and K-band DPI, try to keep the derotator angle < 15º or > 75º. This can be done by entering a derotator position angle in the science template (bottom parameter). You can use this formula:
  Derotator position angle = <parang – alt> or = 180 + <parang – alt>

  Narrow-band (NB) filters can be used in DPI with a waiver, but these filters tend to produce ghosts. The locations of these ghost images can be found on this SPHERE web page link.

  Where <parang – alt> is the mean value of the difference between the parallactic angle and altitude of the target during the template. If the amplitude of that difference is greater than 15º during the template, split the template in 2 shorter ones, and repeat the calculation.

- To help you check whether your observation, at a given time will be affected by efficiency problem, an Excel table is now available here: http://www.eso.org/sci/facilities/paranal/instruments/sphere/doc/IRDIS_DPI.html
- It calculates for a given declination and position angle (as entered in P2), in which regime of Figure 37 the derotator is and hence, which is the implication on the polarimetric efficiency. Time is given in local hour angle (HA; angle to the meridian in hour) and the efficiency regimes are “green” when < 20º from the ideal derotator angle, yellow when > 20º and < 30º, red otherwise: http://www.eso.org/sci/facilities/paranal/instruments/sphere/doc/IRDIS_DPI.html
- Since P100, DPI is also offered in Pupil tracking (coronagraphy or SAM).

7.1.9 Polarimetry in pupil-tracking mode: advantages and polarimetric efficiency

Polarimetry in pupil-tracking has several advantages over field-tracking. For coronagraphic observations, a higher contrast is achieved since the Lyot stop is aligned with the telescope spiders and therefore removes the spider diffraction pattern from the image. Polarimetric differential imaging can be combined to other star-subtraction techniques such as Angular Differential Imaging thanks to the natural field rotation. Last, the polarimetric efficiency is always high, without the need to tune the derotator offset as in field tracking (the derotator offset is actually not a user parameter in pupil-tracking as the Lyot stop needs to be aligned with the telescope pupil).

The polarimetric efficiency of measurements in pupil-tracking depends entirely on the parallactic and altitude angles of the observations. Figure 1 from van Holstein et al. (2017) shows the polarimetric efficiency for pupil-tracking in H-band as a function of parallactic and altitude angle. The maximum and minimum polarimetric efficiencies in this plot are 99.7% and 63.8%, respectively. The plots of the polarimetric efficiency in the other broadband filters show the same structure, but have different minimum values equal to 76.5%, 93.5% and 66.5% in Y-, J- and K_s-band. However, during real observations not all combinations of parallactic and altitude angle are possible. Therefore, the real

minimum polarimetric efficiency in H- and K_s-band will be around 75%, but will often be higher (see Fig. 32b). The negative effect of the lower polarimetric efficiency at high altitude angles is (partially) compensated by the lower air mass there.

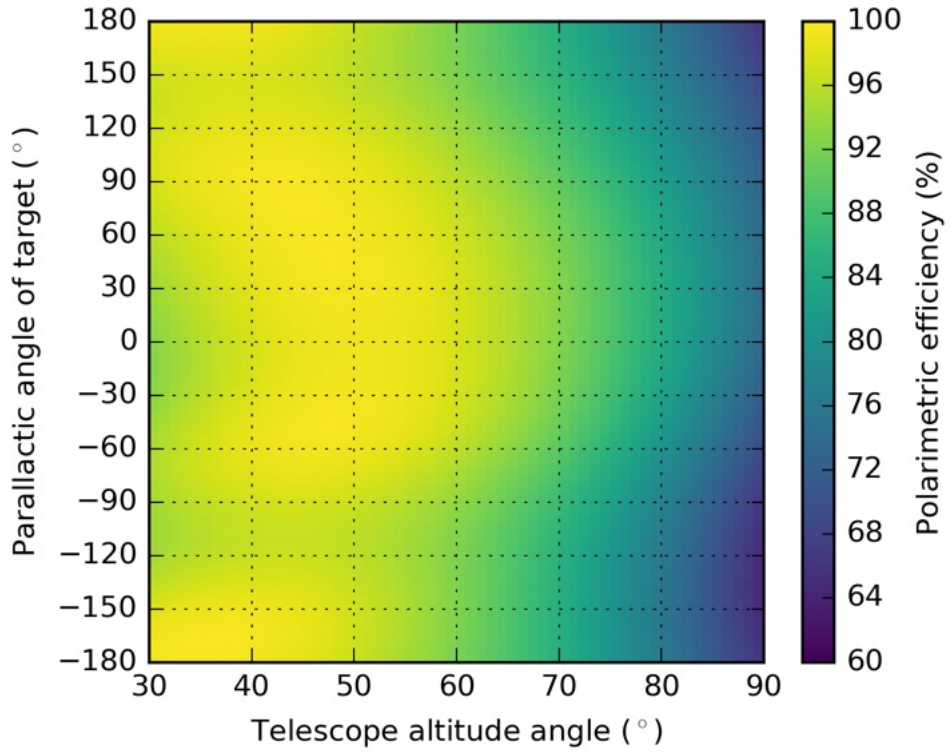

Figure 32b: *Polarimetric efficiency for pupil-tracking in H-band as a function of parallactic and altitude angle (van Holstein et al. 2017, SPIE)*

7.1.10 Observation templates and user-defined parameters

IRDIS observation templates	Observing modes
SPHERE_irdis_dpi_obs	IRDIS DPI

For IRDIS only observations in dual polarized imaging mode, there is a single template called SPHERE_IRDIS_dpi. Parameters defined by the observer are discussed in Section 9. They include setting:

- DIT, NDIT, NEXP. A DIT value of 0 indicates that the smallest possible DIT value (currently 0.83 seconds) is to be used.
- IRDIS Filter Combination and Neutral density filters.
- Stokes parameters to be measured (Q or Q and U).
- Number of polarimetric cycles
- The polarization gamma parameter. This parameter reflects the on-sky orientation (measured clockwise from North) of the measured polarization in the first image of a Q cycle.

7.1.11 Calibrations

Differential polarimetry is a proxy to achieve greater contrasts at small inner-working-angles. This is provided that the object of interest features polarized scattered light in the near IR (i.e debris and proto-planetary disks, etc.).
Calibrating IRDIS-DPI data involves on-sky and internal calibrations similar to the IRDIS CI and IRDIFS_DBI modes (see Section 7.1.2). Other night-time and day-time calibrations provided as part of the SPHERE calibration plan are detailed in Section 8.

IRDIS alone Long Slit Spectroscopy (LSS)

7.1.12 IRDIS/LSS: Observation templates and user-defined parameters

IRDIS observation template	Observing mode
SPHERE_irdis_lss_obs	IRDIS LSS

User-defined parameters are:

- DIT, NDIT, NEXP. A DIT value of 0 indicates that the smallest possible DIT value (currently 0.83 seconds) is to be used.
- Spectral resolution and range: LRS (R~350) / MRS (R~50).

The slit selection (for width and size of the central blocking mask) is made in the acquisition template that also ensures the appropriate on-slit target centering.
The complete list of user-defined parameters is presented in Section 9.

7.1.13 IRDIS/LSS: Purpose and properties

Scope of LSS:
IRDIS long slit spectroscopy mode (LSS) is designed for the spectral characterization of already detected objects either at low resolution (LRS, R ~ 50) over Y to Ks, or medium resolution (MRS, R ~ 350) over Y to H. It offers the unique combination of a classical Lyot coronagraph with long slit spectroscopy.

Configurations:
In practice, the slits and opaque coronagraphic masks have been merged into a single device that is placed in the coronagraph wheel of the CPI. The specifications of the three slits that are available for LSS are listed in Table 13. Since P101, a special apodizer optimized for the LSS mode is offered for better performance at small separations. It is called SLLC, for stop-less Lyot coronagraph. The goal of this apodizer is to improve the raw contrast performance in LSS at very small separations (0.2-0.5"). The very positive results have been demonstrated on the internal source and on-sky (Vigan et al. 2016a, A&A, 586, A144). Although the transmission of the apodizer is low (~30%), offering it to the users would be good for the characterization of bright companions at very small angular separations. To use the apodizer, just select the apodizer tick box in the ird_lss_acq template.

In addition to the slit+coronagraphic masks, two dispersive elements are placed in the IRDIS cryostat in the Lyot stop wheel: a prism for the LRS mode and a grism for the MRS mode (the dispersion curves for these two components are available in the Appendix). The combination of the three slits and the two dispersive elements provides 4 different configurations listed in Table 14.

As a consequence of using a slit, the observations in this mode are necessarily done in field–stabilized mode to maintain the object of interest inside the slit during the observations.

Target size and spectral resolution:
Positioning of the object with respect to the slit is of significant importance in IRDIS LSS because the diffraction limit is reached inside the slit. The actual spectral resolution for point-like sources is thus set by the diffraction limit rather than the slit width. The central star halo (the star PSF core is hidden behind the coronagraphic mask) can be considered as an extended object in the sense that the speckle field of the star will fully cover the slit, decreasing the effective resolution of its spectrum.

Important 1: the true north is actually –1.75 degrees for IRDIS. For this reason, the value of 1.75 has to be added to any position angle (PA-TN = PA+1.75 deg, where TN is true north).

Important 2: we strongly recommend to take sky frames after the science exposures to be able to correct for the background.

Because the object is unresolved inside the slit, the wavelength calibration can be impacted by the position of the object. Indeed, the wavelength calibration is performed by observing an extended source through the slit, which means that it is only fully valid for the star, or if the object is perfectly centered in the slit. If the object is not well centered, this will induce a systematic shift of the wavelength for the object with respect to that of the star. Also, note that the inaccurate positioning of the object inside the slit can induce differential flux losses (see e.g. Goto et al. 2003, SPIE, 4839) that might affect the spectral slope of the continuum of the object.

Table 13: Specifications of the LSS slits+coronagraphic focal masks available in the coronagraphic wheel to use in IRDIS LSS mode.

Slit name	***Width***	***Coronagraphic mask radius***
SLIT_WL	0.12”	0.2”
SLIT_NL	0.09”	0.2”

Table 14: Configurations available in IRDIS LSS mode.

Configuration	***Slit***	***Dispersive element***
S_LR_WL	SLIT_WL	PRISM
S_MR_WL	SLIT_WL	GRISM
S_MR_NL	SLIT_NL	GRISM

7.1.14 IRDIS/LSS: Calibrations

The calibration frames acquired automatically by the observatory include:

- **Internal background**, **Internal flat-field sequences:** a series of flat-field images is produced in all setups used during the night. In the LSS mode, a flat-field in the spectroscopic wide-band filters YJHKs (in LRS) or YJH (in MRS) are provided. It is also possible to calibrate the detector flat field using a flat acquired in the H broad-band filter if no wide-band flat field is available.
- **Wavelength calibration:** the SPHERE calibration unit provides the user with six laser emission lines covering the spectral range 988 to 2015 nm in LRS. In MRS, five emission lines are available for calibration, from 988 to 1730. This calibration is automatically obtained during day-time, after a spectroscopic observation has been done. It is however recommended that observers attach the wavelength calibration to their OB for improved accuracy. For this,

the SPHERE_irdis_lss_cal_wave template should be used. The time needed to execute this template will be charged to the user.

The following additional calibrations can also be requested, but will be charged to the observer:

- **Sky background:** the acquisition of sky background frames during the night may be necessary, especially in the LRS mode covering the K band where the sky background may be bright and variable. Such background file provides an efficient correction of the thermal background of the sky + instrument, the dark features and the static bad pixels. The SPHERE_irdis_lss_obs_sky template should be used.
- **Telluric standard observation:** allows calibrating the telluric absorption on a featureless stellar spectrum. This calibration is done on request and prepared by the user with the template SPHERE_irdis_lss_obs_telluric. If the chosen star is a spectro-photometric standard, use of the widest slit is recommended to avoid the slit losses.

ZIMPOL polarimetric imaging

7.1.15 ZIMPOL: Observation templates and user-defined parameters

observation template	Observing mode
SPHERE_zimpol_p1_obs	ZIMPOL polarimetric imaging P1
SPHERE_zimpol_p2_obs	ZIMPOL polarimetric imaging P2

User-defined parameters are:

- Detector readout mode and exposures: DIT, NDIT, NEXP. As the polarized signal is modulated between two CCDs (cf. Fig. 8), NDIT must be an even number.
- Polarization orientation and switching scheme. See section 7.1.18
- Derotator: fixed (P1) or field-stabilized (P2). In case of field-stabilized observations, the field orientation. See details in Section 7.1.16.
- Beam Splitter: This is selected in the acquisition template. Note that the grey beam splitter gives worse AO performance, since the light reaching the WFS decreases by 1.4 mag.
- Filters: ZIMPOL filters, excluding the filters located in the common FW0, which are not currently supported for polarimetry. The selected filters may or may not be the same for both arms (in FW1 and FW2). Note that if the dichroic beam splitter (between AO WFS and ZIMPOL) is set in the acquisition template, then the choice of ZIMPOL filters is restricted to the R band, narrowband R, H-alpha broad, H-alpha continuum or (for arm 2 only) H-alpha narrow. See Section 4.1.
- Stokes parameters to be measured (Q or Q and U).
- Number of polarimetric cycles.
- Polarization gamma parameter: Selects the on-sky orientation (measured in degrees clockwise from North) of the measured polarization in the first image of a Q cycle.
- ZIMPOL polarization compensator selector: Determines whether the derotator polarization compensator is in the beam (COMP) or not (OPEN).
- ZIMPOL polarization compensator tilt angle. Tilt of the compensator plate in degrees. It is recommended to leave this at the default value of 25 degrees.
- Observation type list. Defines the sequence of Object (O), Flux (F) and Star Center (C) measurements to be obtained.
- Detector X and Y offset for flux measurements. Indicates the offset (in mas) which is performed to offset the source from the coronagraphic mask for the flux measurement.

- Deformable mirror waffle parameters. These parameters control the amplitude and the pattern of the four symmetric echoes of the PSF core in the Star Center measurement. In case of observing an object with a known companion, changing these parameters may be useful to ensure that the position of the echoes do not coincide with the location of the companion.
- Field position: see Section 7.1.17.

A complete list of user-defined parameters is presented in Section 9.

Table 15: ZIMPOL P1/P2 modes in a nutshell.

P1 mode	Highest precision polarimetry mode without derotation: • best suited for absolute polarimetric calibration • arbitrary Q/U orientation selection with HWP2 • derotator and compensator always in the same fixed position
P2 mode	Polarimetry mode with derotation: • arbitrary Q/U orientation selection with HWP2 • stable field on detector with user-defined orientation • derotator, compensator and HWP-Z move during observations

7.1.16 ZIMPOL: P1 or P2 rotation modes for ZIMPOL polarimetry

Two field rotation modes are offered for ZIMPOL polarimetry. They provide two different observing strategies:

- **P1: No field derotation. This mode is only intended for experts as special algorithms will be required to reduce the data.** For bright targets the integration times can be short enough for observations without image derotation because the rotational smearing of the signal on the detector can be neglected. The rotator is fixed in vertical position. This has the advantage that all components are fixed except for HWP1, which needs to correct for the altitude dependence of the M3 polarization, and HWP2, which rotates the polarization position angle correctly into the orientation of the derotator and the ZIMPOL system. This mode will provide the highest polarimetric sensitivity and polarimetric calibration accuracy and is best suited for the search of planets around bright stars because nothing moves after HWP2.
- **P2: Active field derotation.** This mode is suited for long integration of fainter targets. Field derotation is activated and the polarization vector is rotated by HWP2 into the rotating derotator system and rotated back by HWPZ into the ZIMPOL system. Therefore, the field is fixed but the remaining instrument polarization of about p=0.5% can have some complex, hard to calibrate drifts due to the rotating components.

7.1.17 ZIMPOL: Dithering, mosaicking

7.1.17.1 Dithering

Dithering with the tip-tilt folding mirrors in front of the detector is possible. Dithering moves the image by several pixels on the detector so that effects of individual pixels can be averaged-out or corrected. The user can select a dithering pattern which is applied to both arms. A recommended pattern is a 9-point dithering pattern with shifts of 50 mas or 14 pixels (3.5 mas each) on the detector:

The dithering positions (in pixels) are setup in the observing template as follows, for instance:
[x,y] = [-14,-14], [-14,0], [-14,+14], [0,-14], [0,0], [0,+14], [+14,-14], [+14,0], [+14,+14]

This pattern can be restricted to a 3 point or 5 point dithering pattern or additional dithering positions can be added. When supplied as a list of dithering positions, each consecutive position is taken as an offset relative to the last position. The positions are not taken as absolute positions.

Note that a negative dithering offset in the X-direction will move the star to the right, while a negative offset in the Y-direction will move the star down. For instance, a dithering position of [-14 -14] in the first frame and a position of [0 0] in the second frame, then the star in the second frame will be displaced by 14 pixels to left and 14 pixels down with respect to the first one.

7.1.17.2 Off-axis positions

Using the tip-tilt mirrors to explore the full 8 arcsec diameter is currently not offered.

7.1.18 Observing sequences for ZIMPOL polarimetry

An individual exposure with ZIMPOL polarimetry includes at least two frames taken with opposite charge shifting phasing (double phase mode). This corrects for the charge shifting effects. This minimum unit can be called within several levels of sequences. The recommended sequences for ZIMPOL polarimetry are from low level to high level:
NDIT: number of frames taken (MUST BE an even number) per exposure or data cube.
NEXPO: Number of data cubes taken per higher order sequence.
STOKES sequence: Q or QU for a HWP2 cycle (Q switch), at 0 and 45 degrees, or double cycle (QU switch) with 0, 45, 22.5 and 67.5 degrees. The QU switch sequence should be used by default. Other settings are for experts.
NPOL: Number of STOKES cycles taken within a higher order sequence.
DITH.PATTERN.LIST: List of dithering positions, each xy pair being a relative offset wrt. the last position.
FIELD.ETA: List of image rotation angles (only for P2 mode).

Example: one can have a sequence with:

- 3 field orientation (list given with eta = 0, 30, 60).
- For each field orientation 3 dithering positions (e.g. list [-14, 0], [0, 0], [+14, 0])
- For each dithering position 2 (=NPOL) STOKES QU cycles.
- For each HWP position 1 exposure (NEXPO=1).
- Each exposure with 50 frames of 1.2s integration time.

This yields: 50 x 1 x 4 x 2 x 3 x 3 frames or 3600 frames with a net integration time of 3960s.

7.1.18.1 Recommendations for sequences

Large NDIT (>10) reduces the observing overhead. NDIT=20 should be preferred to, e.g., NEXPO=4, NDIT=5. NDIT is limited to 20 because too large fits files can also generate errors when written to disk.

STOKES Q or STOKES QU cycles should not be too long (less than a few minutes), because the HWP2 switch corrects well for many instrumental polarization effects if the 0 – 45 degree or 22.5 – 67.5 degree switch cycle is shorter than drifts in the instrument polarization. We recommend a HWP2 switch should be made every few minutes.

DITHERINGS can correct for detector effects. A reasonable number of dithering is 3 or 5. One should also consider that ZIMPOL has a second arm where the same data can be taken simultaneously with another detector.

7.1.18.2 Recommended sequences for different types of targets

ZIMPOL polarimetry in P2 mode for faint sources:
One STOKES QU cycle with NDIT=2, DIT=100s (total = 800s in 4 exposures including 8 frames). This mode is appropriate for faint sources observed in slow polarimetry and yields photon noise limited or readout ZIMPOL polarization accuracy including the correction for instrumental polarization. Second arm (with the same or another filter) can be used for the identification of bad pixels and other instrumental effects.

ZIMPOL polarimetry in P1 mode of very bright star with high sensitivity:
Short exposure DIT=1.2 sec with many frames (NDIT=50) per exposure, NEXPO=2 for a total of 100 frames between each HWP2 switch. A STOKES QU cycle, where one full polarization cycle has 400 frames, has an integration time of 8 minutes. 10 such cycles (NPOL=10) form then one observing block, which may be repeated several times during the night with slight offsets of the dithering position.

7.1.19 ZIMPOL: polarimetric calibrations

For ZIMPOL polarimetry the same principles for CCD detector calibrations apply. Therefore the ZIMPOL polarimetry calibration plan includes bias, dark and flat-field calibrations. One also needs a calibration of the polarimetric modulation-demodulation efficiency of ZIMPOL. The polarimetric calibration of the telescope and instrument is not required for most application because the ZIMPOL/SPHERE design has well-defined polarimetric properties. The telescope polarization is compensated to less than 1%, and the instrument polarization is self-calibrated with the half-wave plate (HWP2) switch. The zero-point of the polarization position angle will be available after commissioning to an accuracy of better than 5 degrees. Polarization cross-talks affect the measured fractional polarization p (or Q/I and U/I) by less than $\Delta p/p = 0.1$. These polarimetric properties are monitored by the observatory with the measurement and analysis of high polarization standard stars and zero polarization standard stars on a regular basis. The user should consider additional standard star measurements for science cases requiring a better accuracy in the polarimetric calibration. One can expect that the instrument will be characterized with higher precision, once more measurements become available.

- Modulation-demodulation efficiency calibration: the standard polarimetric calibration to be carried out for each polarimetric observation is the modulation-demodulation efficiency calibration. These frames can be obtained during day-time with a flat-field illumination of the detectors using a linear polarizer in the beam producing a fully (100%) polarized illumination of ZIMPOL. The polarization signal measured by ZIMPOL provides then polarization efficiency (e.g. about $\varepsilon \sim 0.8$ for fast polarimetry or $\varepsilon \sim 0.9$ for slow polarimetry) and the polarization signal in the science data must be corrected by the obtained frame ($Q_cal = Q_measured / \varepsilon$). The modulation-demodulation efficiency calibration depends on various parameters, most importantly on the modulation frequency, the used filter, and the location on the detector. Therefore, one must obtain for each polarimetric science frame a calibration taken in the same modulation mode (fast or slow) and with a similar broadband color filter. It is recommended to use for narrowband or line filter polarimetry a corresponding broadband filter calibration because they can be obtained with short exposures reducing the charge trap problem while the color dependence is sufficiently taken into account (see Section 8). The calibration frames for the modulation-demodulation efficiency are also affected by the charge trap problem. Therefore, it is recommended to take these frames only with short integrations (limited number of charge shifts). For narrowband and line filter data one can use broadband filter calibrations.
- Bias calibrations for polarimetry: bias subtraction for ZIMPOL is mainly based on the overscan pixel bias level. Fast polarimetry produces a fixed pattern along two columns

originating from the read-out process. To remove them it is important to have a set of bias calibration (e.g. 50 frames) available. It is useful to take similar calibrations for slow polarimetry as a detector quality check.

- Dark calibrations: can be useful for subtracting the dark current from long integrations. For most cases this calibration is not needed.
- Intensity flat-fields for polarimetry (polarization flats): well illuminated intensity flats are required to calibrate pixel to pixel sensitivity variations. Intensity flats should be taken with the same filters as the science observations. If a coronagraph on a substrate is selected then sensitivity features due to dust and inhomogeneities of the plate can be corrected with a flat-field with the same focal plane plate inserted. The charge traps are an issue for the flat-fielding in polarimetric mode and therefore one should use short integration times. Detector fringing is an issue for the flat-fielding of frames taken with the line filters.

ZIMPOL imaging

7.1.20 ZIMPOL Imaging: Observation templates and user-defined parameters

observation template	Observing mode
SPHERE_zimpol_i_obs	ZIMPOL non-polarimetric imaging

User-defined parameters are:

- Detector readout mode and exposures: DIT, NDIT, NEXP
- Derotator: field-stabilized or pupil-stabilized. In case of field-stabilized observations, the field orientation.
- Filter: ZIMPOL filters. The selected filters may or may not be the same for both arms (in FW1 and FW2). Note that if the dichroic beam splitter (between AO WFS and ZIMPOL) is selected in the acquisition template, then the choice of ZIMPOL filters is restricted within the R band: narrowband R, H-alpha broad, H-alpha continuum or (for arm 2 only) H-alpha narrow.
- Observation type list. Defines the sequence of Object (O), Flux (F) and Star Center (C) measurements to be obtained.
- Detector X and Y offset for flux measurements. Indicates the offset (in mas) which is performed to offset the source from the coronagraphic mask for the flux measurement.
- Deformable mirror waffle parameters. These parameters control the amplitude and the pattern of the four symmetric echoes of the PSF core in the Star Center measurement. In case of observing an object with a known companion, changing these parameters may be useful to ensure that the position of the echoes do not coincide with the location of the companion.
- Field position: see before.

The exhaustive list of user-defined parameters, as extracted from the Template Reference Manual, is presented in Section 9.

7.1.21 ZIMPOL Imaging: Purpose and properties

ZIMPOL provides an instrument mode for imaging without polarimetry. In principle, the polarimetric mode of ZIMPOL provides differential polarization signal and intensity images. But having a dedicated imaging mode ensures optimal imaging performance. The resulting data are less affected by instrumental effects (e.g. the HWP are out of the beam). Thus, if one seeks high quality imaging for targets where the polarimetric signal is not relevant then one should consider the imaging mode. Imaging provides in particular a pupil-stabilized observing mode and also features which are not available in polarimetric imaging.

The following list highlights the main advantages of the imaging mode:

- All polarimetric components are out of the beam. This enhances the throughput and reduces ghost effects and the scattered light level. Components which are not in the beam when compared to polarimetric imaging are: HWP1, HWP2, FLC modulator and eventually the polarization compensator and HWPZ.
- A pupil-stabilized observing mode is offered for imaging which enables angular differential imaging (ADI).
- No charge shifting is required on the CCD. Therefore, one has no problems with the charge traps which appear in polarimetric imaging.
- The Filters in the common filter wheel are also available for imaging.
- The format of the resulting data is simpler.

Only minor drawbacks are related to the imaging mode when compared with the polarimetric imaging mode:

- Currently only the fast readout mode with a high readout noise of 20 e-/pix is offered.
- The two channels of ZIMPOL are strongly polarization sensitive. The total efficiency of one arm depends more strongly on the telescope pointing direction and the instrument configuration than in polarimetric mode.

7.1.22 ZIMPOL Imaging:Calibrations

Typical day-time (bias, flats, distortion maps) and night-time (photometric standard stars and astrometric fields/stars) calibrations are provided by the observatory (see Section 8).

8. CALIBRATION PLAN SUMMARY

Night-time calibrations

Some observing modes require attached calibration to be taken during the night. Here we detail which ones are mandatory and will be charged to the user observing time, and which ones are part of the calibrations provided by the observatory.
Whenever a coronagraph is used, the SPHERE calibration plan recommends including Flux (F) and Star Center (C) observation types in observing templates both before and after the science observing template. The purpose of the first calibration (Flux - F) is to measure the unsaturated peak flux of the star by offsetting it from the coronagraph spot, in order to ensure accurate relative photometry, and thus contrast calibration. The second calibration (Star Center - C) applies a waffle pattern on the deformable mirror to produce echoes of the PSF hidden behind the coronagraphic mask at very specific locations. The goal of (Star Center - C) is to accurately measure the position of the star behind the coronagraph, which is critical for astrometric measurements of off-axis sources.

8.1.1 Night-time calibrations provided by the observatory

The SPHERE calibration plan includes taking photometric standard stars for all imaging modes using broadband filters. The calibration plan also includes observing reference astrometric fields (binary systems or star clusters with high precision astrometry available) without a coronagraph (including ND filters if needed to avoid detector saturation) on an infrequent basis (every ~90 days).

8.1.2 Optional night-time calibrations

Photometric standard stars in narrow band filters, or wavelength calibration for IRDIS_LSS, must be requested by the user and is charged to the observer. No spectro-photometric standards or telluric standard will be taken unless explicitly requested as special night-time calibrations. The time required to do so will be charged to the observer.

Day-time calibrations

In addition, all necessary day-time calibrations will be acquired by the observatory staff during the day following the night of the observations (or within the validity period indicated in the tables below). In the following tables, "Modes" refers to the instrument mode among IRDIFS, IRDIFS_EXT, IRDIS_DBI, IRDIS_CI, IRDIS_LSS, and ZIMPOL_I, ZIMPOL_P1, ZIMPOL_P2, when applicable. "Matching parameters" describes the most critical parameter for generating the automatic calibration. For instance, darks/backgrounds will have the same DIT as the science, flats will be taken in the same filter as the science, etc. On the other hand, ZIMPOL polarimetric calibrations will be done in corresponding broadband filters (see filter correspondence table below).

Table 16: Day-time calibrations for IRDIS.

Calibration	Modes	Matching parameter(s)	Validity
Background	all	DIT, Filter, (ND filter for DPI)	1 day
Lamp Flat	all	Filter, (w/ and w/o polarizer for DPI)	1 day
Distortion map	All, except IRDIS_LSS	Filters (YJHKs and Clear)	7 days
Wavelength calibration	IRDIS_LSS	Coro+Slit/Grism/Filter	1 day

Table 17: Day-time calibrations for IFS.

Calibration	Modes	Matching parameter(s)	Validity
Background	all	DIT, Filter	1 day
Lamp Flat	all	Prism	1 day
Wavelength calibration	all	Prism	1 day
Spectra registration	all	Prism	1 day
Distortion map	all	Filters (YJHKs and Clear)	7 days

Table 18: Day-time calibrations for ZIMPOL.

Calibration	Modes	Matching parameter(s)	Validity
Bias	all	readout mode	10 days
Dark	all	DIT, readout mode	on request
Imaging flat	all	Filter and ND (+dichroic), readout mode, focal plane mask on substrate (if used)	10 days
Polarimetric flat	ZIMPOL_P1, ZIMPOL_P2	Filter and ND (+dichroic), readout mode, focal plane mask on substrate (if used)	10 days
Modulation efficiency	ZIMPOL_P1, ZIMPOL_P2	Filter (+dichroic), readout mode, HWP=(+--)	10 days

NOTE: ZIMPOL distortion maps are every 2 weeks in V, N_R, N_I and CLEAR for monitoring purposes.

Table 19: Filter correspondence table for ZIMPOL calibrations.

Filter of Science	**Filter for imaging and polarimetric flat**	**Filter for modulation efficiency**
Ha_NB	Ha_NB	N_R
OI_630	OI_630	N_R
HeI	HeI	V
V_S	V_S	V
V_L	V_L	V
730_NB	730_NB	N_R
I_L	I_L	N_R
VBB (RI)	VBB (RI)	VBB (RI)
I_PRIM	I_PRIM	I_PRIM
R_PRIM	R_PRIM	R_PRIM
N_I	N_I	N_I
N_R	N_R	N_R
B_Ha	B_Ha	N_R
CntHa	CntHa	N_R
V	V	V
Cnt820	Cnt820	N_I
TiO_717	TiO_717	N_I
CH4_727	CH4_727	N_I
KI	KI	N_I
N_Ha	N_Ha	N_R
Cnt748	Cnt748	N_I

Astrometry

8.1.3 Instrumental distortion and detector orientation in IRDIFS and IRDIFS_EXT

Observations of the gobular cluster 47 Tuc have been used to calibrate the distortion, plate scale and true north orientation at the level of the IRDIS and IFS detectors. The cylindrical mirrors in the SPHERE common path are the main source for the optical distortion, hence these distortion effects are common to IRDIS and IFS, and they dominate the telescope distortion effects (Maire et al. 2016). The SPHERE distortion at first order is an anamorphism of 0.60±0.02% between the horizontal and vertical pixel scales. This effect -if uncorrected- translates into an astrometric error of 6 mas at 1″, which is larger than the astrometric specifications for SPHERE (5 mas).

The following steps are required for accurately calibrating IRDIFS data :

- IRDIS: there a very small anamorphic distortion between the x and y axes. It can be corrected by multiplying the Y coordinate by 1.0062+/-0.0002. This value has been calibrated during commissioning and was measured to be stable within the provided error.
- IFS: the IFS is affected by the same anamorphic distortion as IRIDS. However, because the IFS field is rotated by +100.56 (counter-clockwise), the corrections to be applied are 1.0059 in x and 1.0011 in y.
- Field orientation: once the anamorphism is corrected, the position angle on sky of any object can be determined using the following formulae:

Stabilization	Sub-system	Formula
Field	IRDIS	$PA_{sky} = PA_{detector} + POSANGLE + TN$
	IFS	$PA_{sky} = PA_{detector} + POSANGLE + TN + IFS_{offset}$
Pupil	IRDIS	$PA_{sky} = PA_{detector} + PARANGLE + TN + PUPIL_{offset}$
	IFS	$PA_{sky} = PA_{detector} + PARANGLE + TN + PUPIL_{offset} + IFS_{offset}$

With:

$PUPIL_{offset}$: 135.99 ± 0.11 deg (the sign was incorrect before version 15 of the manual)
IFS_{offset}: −100.48 ± 0.13 deg
TN: true North correction (see below)
POSANG: position angle offset (input in the observing template)
PARANGLE: parallactic angle

8.1.4 Plate scale and true north orientation

Basic astrometry, i.e. plate scale and true north orientation is provided by the observatory on a regular basis using a few reference calibrators. We selected as main reference fields 47 Tucanae, the Orion Trapezium B1–B4, NGC 3603, and NGC 6380 (Tab. 1 and Fig. 1), as well as a handful of long-period binaries (HIP 67745, HIP 68725, HIP 102979) with Hipparcos data and separations larger than the IFS field of view (separations ~2–5″). The catalogs of the stellar positions for these fields come from various sources: Washington Double Star (WDS) catalog for the binaries, literature for the Orion Trapezium B1–B429 , and private requests for 47 Tucanae (A. Bellini/STScI), NGC 6380 (E. Noyola/Univ. Texas Austin), and NGC 360330 (Z. Khorrami/OCA). Additional details are given in Maire et al. (2016).

The true north TN is -1.75º ± 0.08º and was shown to be stable within error bars (Maire et al. 2016). A synchronization problem affected all data obtained before July 13 2016. For data taken in field tracking mode before July 13 2016, a correction factor ϵ needs to be added to the true north using the formula

$$\epsilon = \mathrm{ATAN}(\mathrm{TAN}((\ \mathrm{TEL.ALT} - \mathrm{TEL.PARANG.START} - 2 \times \mathrm{INS4.DROT2.BEGIN}\ ) \times \pi/180)) \times 180/\pi$$

This incorrect synchronization also affected the science data taken before July 13 2016 in pupil-tracking mode, but to a smaller extent (it can however be as large as 0.1º to 0.2º) because the rotation speed of the derotator is slower in this mode. The formula for correcting this drift for pupil-tracking data is

ϵ = ATAN(TAN((TEL.ALT – 2 × INS4.DROT2.BEGIN) × π/180)) ×180/π

This correction factor needs to be added to the parallactic angle of each pupil-tracking frame in order to derotate the image accurately.

Beware that if you need to recalculate the parallactic angle (for instance to stamp each individual frame of a cube), the target coordinate at the epoch of observation (e.g. epoch J201X.XX) can be retrieved directly from the keyword INS4.DROT2.RA/DEC. The RA/DEC keywords are indeed given in J2000 (therefore not corrected for the precession/nutation at the epoch of observation) and rely on the coordinate on the guide star used by the telescope which is assumed to have no proper motion.

The IRDIS plate scale was evaluated in the H2 filter with the N_ALC_YJH_S coronagraph. The value is 12.255 ± 0.021 mas/pix. The plate scale can be adjusted for different filters using the following relations :

plate_scale(H3)=plate_scale(H2)–0.005
the plate_scale for J2/J3 is 0.004 mas/pix larger than for H2/H3
the plate_scale for Y2/Y3 is 0.024 mas/pix larger than for H2/H3
the plate scale for non-coronagraphic observations is 0.019+/-0.001 mas/pixel smaller than that for coronagraphic observations

The plate scale of the IFS is 7.46±0.02 mas/pix.

9. SPHERE TEMPLATE PARAMETERS

The instrument, detector and telescope are controlled by OBs, which are made up of templates. Templates are divided into three categories: acquisition, observation and calibration.
Usually, OBs consist of an acquisition template and one or more observation templates for nighttime observations and, in some limited cases, an additional nighttime calibration template.
Only one acquisition template is allowed in an OB, and therefore only one preset on sky. It is not possible e.g. to group in the same OB observation templates on the science object and calibration template on a standard star. The next sections provide a short summary of the templates offered from P95. These templates should cover most needs. If this is not the case, users must contact the User Support Department through the online ticketing system well before the start of observations.

SPHERE Acquisition Templates

Telescope presets can only be done via acquisition templates and all observing blocks must start with one. There are ten acquisition templates and they are to be used with nine different observation templates with the following associations:

SPHERE_irdifs_acq, SPHERE_irdifs_acq_rrm:
SPHERE_irdifs_obs
SPHERE_irdifs_ext_obs
SPHERE_irdis_acq, SPHERE_irdis_acq_rrm:
SPHERE_irdis_ci_obs
SPHERE_irdis_dbi_obs
SPHERE_irdis_dpi_acq:
SPHERE_irdis_dpi_obs
SPHERE_irdis_lss_acq:
    SPHERE_irdis_lss_obs
SPHERE_zimpol_i_acq, SPHERE_zimpol_i_acq_rrm:
    SPHERE_zimpol_i_obs
SPHERE_zimpol_p_acq, SPHERE_zimpol_p_acq_rrm:
    SPHERE_zimpol_p1_obs
    SPHERE_zimpol_p2_obs
SPHERE_gen_acq_GoTo_acq (mode independent, concatenation only)
SPHERE_gen_acq_starhop (mode independent, concatenation only)
SPHERE_gen_acq_hopback (mode independent, concatenation only)

The setups allowed by each template are shown in Tables 21–26 in terms of the parameters which may be set. For example, the SPHERE_irdifs_acq (see Table 20) allows the setting of IRDIS and IFS coronagraphs, derotator mode (field or pupil tracking), adaptive optics (AO or no AO) and position angle offset.
The parameter SEQ.AO.ST specifies weth the AO loop should be closed (T) or opened (F). Unless specific calibration purposes, the state will therefore be T (loop closed).

SPHERE Observation Templates

The templates SPHERE_irdifs_obs and SPHERE_irdifs_ext_obs both use IRDIS and IFS together. They should be used for modes IRDIFS (Y-J range with IFS and H-band range with IRDIS) and IRDIFS_EXT (Y-H range with IFS, K-band range with IRDIS) as described in section 1.7. Please note that SPHERE_iridfs_obs and SPHERE_irdifs_ext_obs templates cannot be mixed within a single OB; a new acquisition is necessary to go from the irdifs to the irdifs_ext sub-mode and vice-

versa. The parameters which can be set to define your observations are shown in Table 27 and 28. The minimum DIT allowed is actually 0.83 seconds, and setting DIT to anything less (e.g. zero) sets it to 0.83 s. The SEQ.OBSTYPE.LIST parameter allows you include obs_flux (F), star_center (C), and sky (S) along with your science observations (O) in the order you prescribe (see section 6.4). The DITs and NDITs for each of these component observations are set separately using different parameters (e.g. SEQ.IFS.DIT.STARCENTER, SEQ.IRDIS.DIT.STARCENTER). However, the dithering parameters (e.g. SEQ.IRDIS.DITH.PATTERN) control all components (FCOS).

Table 20: SPHERE_irdifs_acq

SPHERE_irdifs_acq.tsf			
To be specified:			
Parameter	Hidden	Range *(Default)*	Label
DPR.CATG	yes	SCIENCE CALIB ACQUISITION TECHNICAL *(ACQUISITION)*	Data product category
INS.COMB.ICOR	no	N_ALC_YJH_S N_ALC_Ks N_ALC_YJH_L N_CLC_SW_L N_NS_CLEAR N_ALC_YJ_S N_SAM_7H *(NODEFAULT)*	IR Coronagraph
INS.COMB.ROT	no	PUPIL FIELD *(NODEFAULT)*	Derotator Mode
INS.CPRT.POSANG	no	0.0..360.0 *(0.0)*	Derotator position angle (deg)
INS.MODE	no	IRDIFS IRDIFS_EXT *(NODEFAULT)*	Instrument Mode
SEQ.AO.ST	no	T F *(T)*	SAXO state
SEQ.DO.CENTERING	yes	T F *(F)*	Perform centering?
SEQ.DO.FOCUS	yes	T F *(F)*	Perform focus optimization?
SEQ.DTTS.BACKGND	yes	T F *(T)*	DTTS background flag
SEQ.IFS.ROM.THRESH	yes	0..43200 *(0)*	IFS DET level to change ROM
SEQ.INSTALL_CFG	yes	T F *(F)*	Install in system configuration for use?
SEQ.PRESET	yes	T F *(T)*	Telescope preset flag
SEQ.SKY.OFFSETALPHA	yes	0..60 *(5)*	Offset in RA for background measurement (arcsec)
SEQ.SKY.OFFSETDELTA	yes	0..60 *(5)*	Offset in DEC for background measurement (arcsec)
SEQ.TARGET.HMAG	no	-4..18 *(0)*	Target H magnitude
SEQ.TARGET.RMAG	no	-10..18 *(0)*	Target R magnitude
SEQ.VWFS.BACKGND	yes	T F *(F)*	VWFS background flag
TEL.AG.GUIDESTAR	no	NONE SETUPFILE CATALOGUE *(CATALOGUE)*	Telescope guide star selection
TEL.GS1.ALPHA	no	ra *(0.)*	RA of guide star
TEL.GS1.DELTA	no	dec *(0.)*	DEC of guide star
TEL.TARG.ADDVELALPHA	yes	-15..15 *(0.0)*	Differential tracking in RA
TEL.TARG.ADDVELDELTA	yes	-15..15 *(0.0)*	Differential tracking in DEC
TEL.TARG.ALPHA	no	ra *()*	RA
TEL.TARG.DELTA	no	dec *()*	DEC
TEL.TARG.EPOCH	no	-2000..3000 *(2000)*	Epoch
TEL.TARG.EQUINOX	no	-2000..3000 *(2000)*	Equinox
TEL.TARG.OFFSETALPHA	yes	*(0)*	RA offset
TEL.TARG.OFFSETDELTA	yes	*(0)*	DEC offset
TEL.TARG.PMA	no	-500..500 *(0)*	Proper motion in RA
TEL.TARG.PMD	no	-500..500 *(0)*	Proper motion in DEC
Fixed values:			
Parameter	Hidden	Value	Label

Table 21: SPHERE_irdis_acq

SPHERE_irdis_acq.tsf			
To be specified:			
Parameter	Hidden	Range *(Default)*	Label
DPR.CATG	yes	SCIENCE CALIB ACQUISITION TECHNICAL *(ACQUISITION)*	Data product category
INS.COMB.ICOR	no	N_ALC_YJH_S N_ALC_YJH_L N_ALC_Ks N_CLC_SW_L N_CLC_LW_L N_NS_CLEAR N_ALC_YJ_S N_SAM_7H *(NODEFAULT)*	IR Coronagraph
INS.COMB.ROT	no	FIELD PUPIL *(NODEFAULT)*	Derotator Mode
INS.CPRT.POSANG	no	0.0..360.0 *(0.0)*	Derotator position angle (deg)
SEQ.AO.ST	no	T F *(T)*	SAXO state
SEQ.DO.CENTERING	yes	T F *(F)*	Perform centering?
SEQ.DO.FOCUS	yes	T F *(F)*	Perform focus optimization?
SEQ.DTTS.BACKGND	yes	T F *(T)*	DTTS background flag
SEQ.INSTALL_CFG	yes	T F *(F)*	Install in system configuration for use?
SEQ.PRESET	yes	T F *(T)*	Telescope preset flag
SEQ.SKY.OFFSETALPHA	yes	0..60 *(5)*	Offset in RA for background measurement (arcsec)
SEQ.SKY.OFFSETDELTA	yes	0..60 *(5)*	Offset in DEC for background measurement (arcsec)
SEQ.TARGET.HMAG	no	-4..18 *(0)*	Target H magnitude
SEQ.TARGET.RMAG	no	-10..18 *(0)*	Target R magnitude
SEQ.VWFS.BACKGND	yes	T F *(F)*	VWFS background flag
TEL.AG.GUIDESTAR	no	NONE SETUPFILE CATALOGUE *(CATALOGUE)*	Telescope guide star selection
TEL.GS1.ALPHA	no	ra *(0.)*	RA of guide star
TEL.GS1.DELTA	no	dec *(0.)*	DEC of guide star
TEL.TARG.ADDVELALPHA	yes	-15..15 *(0.0)*	Differential tracking in RA
TEL.TARG.ADDVELDELTA	yes	-15..15 *(0.0)*	Differential tracking in DEC
TEL.TARG.ALPHA	no	ra *()*	RA
TEL.TARG.DELTA	no	dec *()*	DEC
TEL.TARG.EPOCH	no	-2000..3000 *(2000)*	Epoch
TEL.TARG.EQUINOX	no	-2000..3000 *(2000)*	Equinox
TEL.TARG.OFFSETALPHA	yes	*(0)*	RA offset
TEL.TARG.OFFSETDELTA	yes	*(0)*	DEC offset
TEL.TARG.PMA	no	-500..500 *(0)*	Proper motion in RA
TEL.TARG.PMD	no	-500..500 *(0)*	Proper motion in DEC
Fixed values:			
Parameter	Hidden	Value	Label

Table 22: SPHERE_irdis_dpi_acq

SPHERE_irdis_dpi_acq.tsf			
To be specified:			
Parameter	Hidden	Range *(Default)*	Label
DPR.CATG	yes	SCIENCE CALIB ACQUISITION TECHNICAL *(ACQUISITION)*	Data product category
INS.COMB.ICOR	no	N_ALC_YJH_S N_ALC_YJH_L N_ALC_Ks N_CLC_SW_L N_CLC_LW_L N_NS_CLEAR N_ALC_YJ_S N_SAM_7H *(NODE-FAULT)*	IR Coronagraph
INS.COMB.ROT	no	FIELD PUPIL *(FIELD)*	Derotator Mode
INS.CPRT.POSANG	no	0.0..360.0 *(0.0)*	Derotator position angle (deg)
SEQ.AO.ST	no	T F *(T)*	SAXO state
SEQ.DO.CENTERING	yes	T F *(F)*	Perform centering?
SEQ.DO.FOCUS	yes	T F *(F)*	Perform focus optimization?
SEQ.DTTS.BACKGND	yes	T F *(T)*	DTTS background flag
SEQ.INSTALL_CFG	yes	T F *(F)*	Install in system configuration for use?
SEQ.PRESET	yes	T F *(T)*	Telescope preset flag
SEQ.SKY.OFFSETALPHA	yes	0..60 *(5)*	Offset in RA for background measurement (arcsec)
SEQ.SKY.OFFSETDELTA	yes	0..60 *(5)*	Offset in DEC for background measurement (arcsec)
SEQ.TARGET.HMAG	no	-4..18 *(0)*	Target H magnitude
SEQ.TARGET.RMAG	no	-10..18 *(0)*	Target R magnitude
SEQ.VWFS.BACKGND	yes	T F *(F)*	VWFS background flag
TEL.AG.GUIDESTAR	no	NONE SETUPFILE CATALOGUE *(CATALOGUE)*	Telescope guide star selection
TEL.GS1.ALPHA	no	ra *(0.)*	RA of guide star
TEL.GS1.DELTA	no	dec *(0.)*	DEC of guide star
TEL.TARG.ADDVELALPHA	yes	-15..15 *(0.0)*	Differential tracking in RA
TEL.TARG.ADDVELDELTA	yes	-15..15 *(0.0)*	Differential tracking in DEC
TEL.TARG.ALPHA	no	ra *()*	RA
TEL.TARG.DELTA	no	dec *()*	DEC
TEL.TARG.EPOCH	no	-2000..3000 *(2000)*	Epoch
TEL.TARG.EQUINOX	no	-2000..3000 *(2000)*	Equinox
TEL.TARG.OFFSETALPHA	yes	*(0)*	RA offset
TEL.TARG.OFFSETDELTA	yes	*(0)*	DEC offset
TEL.TARG.PMA	no	-500..500 *(0)*	Proper motion in RA
TEL.TARG.PMD	no	-500..500 *(0)*	Proper motion in DEC
Fixed values:			
Parameter	Hidden	Value	Label

Table 23: SPHERE_irdis_lss_acq

SPHERE_irdis_lss_acq.tsf		
Parameter	Range *(Default)*	Label
INS.COMB.ICOR	N_S_LR_WL N_S_LR_WS N_S_MR_WL N_S_MR_NL *(NODEFAULT)*	Infrared IRDIS coronagraph combination
INS.CPRT.POSANG	0.0..360.0 *(0.0)*	Derotator position angle (deg)
SEQ.AO.ST	T F *(T)*	SAXO state
SEQ.TARGET.HMAG	0..18 *(0)*	Target H magnitude
SEQ.TARGET.RMAG	0..18 *(0)*	Target R magnitude
TEL.AG.GUIDESTAR	NONE SETUPFILE CATALOGUE *(CATALOGUE)*	Telescope guide star selection
TEL.GS1.ALPHA	ra *(0.)*	RA of guide star
TEL.GS1.DELTA	dec *(0.)*	DEC of guide star
TEL.TARG.ALPHA	ra *()*	RA
TEL.TARG.DELTA	dec *()*	DEC
TEL.TARG.EPOCH	-2000..3000 *(2000)*	Epoch
TEL.TARG.EQUINOX	QUERY-TARG getEquinoxList *(2000)*	Equinox
TEL.TARG.PMA	-500..500 *(0)*	Proper motion in RA
TEL.TARG.PMD	-500..500 *(0)*	Proper motion in DEC

Table 24: SPHERE_zimpol_i_acq

SPHERE_zimpol_i_acq.tsf			
To be specified:			
Parameter	Hidden	Range *(Default)*	Label
DPR.CATG	yes	SCIENCE CALIB ACQUISITION TECHNICAL *(ACQUISITION)*	Data product category
INS.COMB.VCOR	no	V_CLC_S_WF V_CLC_M_WF V_CLC_MT_WF V_CLC_L_WF V_CLC_XL_WF V_NC_WF V_SAM_7H *(V_CLC_M_WF)*	Visible coronagraph combination
INS.CPRT.MODE	no	FIELD PUPIL *(FIELD)*	Pupil derotator mode
INS.CPRT.POSANG	no	0.0..360.0 *(0.0)*	Derotator position angle (deg)
INS.ZISL.NAME	no	BS_GREY DIC_HA *(BS_GREY)*	Position of the ZIMPOL/WFS selector
SEQ.AO.ST	no	T F *(T)*	SAXO state
SEQ.APPLY.DTTPDV	yes	T F *(F)*	Apply DTTP delta voltages?
SEQ.DO.CENTERING	yes	T F *(F)*	Perform centering?
SEQ.DO.FOCUS	yes	T F *(F)*	Perform focus optimization?
SEQ.PRESET	yes	T F *(T)*	Telescope preset flag
SEQ.SKY.OFFSETALPHA	yes	0..60 *(5)*	Offset in RA for background measurement (arcsec)
SEQ.SKY.OFFSETDELTA	yes	0..60 *(5)*	Offset in DEC for background measurement (arcsec)
SEQ.TARGET.RMAG	no	-10..18 *(0)*	Target R magnitude
SEQ.VWFS.BACKGND	yes	T F *(F)*	VWFS background flag
TEL.AG.GUIDESTAR	no	NONE SETUPFILE CATALOGUE *(CATALOGUE)*	Telescope guide star selection
TEL.GS1.ALPHA	no	ra *(0.)*	RA of guide star
TEL.GS1.DELTA	no	dec *(0.)*	DEC of guide star
TEL.TARG.ADDVELALPHA	yes	-15..15 *(0.0)*	Differential tracking in RA
TEL.TARG.ADDVELDELTA	yes	-15..15 *(0.0)*	Differential tracking in DEC
TEL.TARG.ALPHA	no	ra ()	RA
TEL.TARG.DELTA	no	dec ()	DEC
TEL.TARG.EPOCH	no	-2000..3000 *(2000)*	Epoch
TEL.TARG.EQUINOX	no	-2000..3000 *(2000)*	Equinox
TEL.TARG.OFFSETALPHA	yes	*(0)*	RA offset
TEL.TARG.OFFSETDELTA	yes	*(0)*	DEC offset
TEL.TARG.PMA	no	-500..500 *(0)*	Proper motion in RA
TEL.TARG.PMD	no	-500..500 *(0)*	Proper motion in DEC
Fixed values:			
Parameter	Hidden	Value	Label

Table 25: SPHERE_zimpol_p_acq

SPHERE_zimpol_p_acq.tsf			
To be specified:			
Parameter	Hidden	Range *(Default)*	Label
DPR.CATG	yes	SCIENCE CALIB ACQUISITION TECHNICAL *(ACQUISITION)*	Data product category
INS.COMB.VCOR	no	V_CLC_S_WF V_CLC_M_WF V_CLC_MT_WF V_CLC_L_WF V_CLC_XL_WF V_NC_WF V_SAM_7H *(V_CLC_M_WF)*	Visible coronagraph combination
INS.CPRT.MODE	no	FIELD FIXED *(FIELD)*	Pupil derotator mode
INS.CPRT.POSANG	no	0.0..360.0 *(0.0)*	Derotator position angle (deg)
INS.ZISL.NAME	no	BS_GREY DIC_HA *(BS_GREY)*	Position of the ZIMPOL/WFS selector
SEQ.AO.ST	no	T F *(T)*	SAXO state
SEQ.APPLY.DTTPDV	yes	T F *(F)*	Apply DTTP delta voltages?
SEQ.DO.CENTERING	yes	T F *(F)*	Perform centering?
SEQ.DO.FOCUS	yes	T F *(F)*	Perform focus optimization?
SEQ.PRESET	yes	T F *(T)*	Telescope preset flag
SEQ.SKY.OFFSETALPHA	yes	0..60 *(5)*	Offset in RA for background measurement (arcsec)
SEQ.SKY.OFFSETDELTA	yes	0..60 *(5)*	Offset in DEC for background measurement (arcsec)
SEQ.TARGET.RMAG	no	-10..18 *(0)*	Target R magnitude
SEQ.VWFS.BACKGND	yes	T F *(F)*	VWFS background flag
TEL.AG.GUIDESTAR	no	NONE SETUPFILE CATALOGUE *(CATALOGUE)*	Telescope guide star selection
TEL.GS1.ALPHA	no	ra *(0.)*	RA of guide star
TEL.GS1.DELTA	no	dec *(0.)*	DEC of guide star
TEL.TARG.ADDVELALPHA	yes	-15..15 *(0.0)*	Differential tracking in RA
TEL.TARG.ADDVELDELTA	yes	-15..15 *(0.0)*	Differential tracking in DEC
TEL.TARG.ALPHA	no	ra *()*	RA
TEL.TARG.DELTA	no	dec *()*	DEC
TEL.TARG.EPOCH	no	-2000..3000 *(2000)*	Epoch
TEL.TARG.EQUINOX	no	-2000..3000 *(2000)*	Equinox
TEL.TARG.OFFSETALPHA	yes	*(0)*	RA offset
TEL.TARG.OFFSETDELTA	yes	*(0)*	DEC offset
TEL.TARG.PMA	no	-500..500 *(0)*	Proper motion in RA
TEL.TARG.PMD	no	-500..500 *(0)*	Proper motion in DEC
Fixed values:			
Parameter	Hidden	Value	Label

Table 26: SPHERE_gen_acq_starhop

SPHERE_gen_acq_starhop.tsf			
To be specified:			
Parameter	Hidden	Range *(Default)*	Label
SEQ.TARGET.RMAG	no	-10..18 *(0)*	Target R magnitude
TEL.AG.GUIDESTAR	no	NONE SETUPFILE CATALOGUE *(CATALOGUE)*	Telescope guide star selection
TEL.GS1.ALPHA	no	ra *(0.)*	RA of guide star
TEL.GS1.DELTA	no	dec *(0.)*	DEC of guide star
TEL.TARG.ALPHA	no	ra *()*	RA
TEL.TARG.DELTA	no	dec *()*	DEC
TEL.TARG.EPOCH	no	-2000..3000 *(2000)*	Epoch
TEL.TARG.EQUINOX	no	-2000..3000 *(2000)*	Equinox
TEL.TARG.PMA	no	-500..500 *(0)*	Proper motion in RA
TEL.TARG.PMD	no	-500..500 *(0)*	Proper motion in DEC
Fixed values:			
Parameter	Hidden	Value	Label

Table 27: SPHERE_gen_acq_hopback

SPHERE_gen_acq_hopback.tsf			
To be specified:			
Parameter	Hidden	Range *(Default)*	Label
SEQ.DIRECTION	no	AUTO POS NEG *(AUTO)*	AUTO move to the other star. POS move to original star, NEG mov to the second star
Fixed values:			
Parameter	Hidden	Value	Label

Table 28: SPHERE_irdifs_obs

SPHERE_irdifs_obs.tsf		
Parameter	Range *(Default)*	Label
DET.IFS.DIT	0 2 4 8 16 32 64 *(0)*	IFS Detector Integration Time
DET.IFS.NDIT	1..1000 *(1)*	IFS Number of DIT
DET.IRDIS.DIT	0 2 4 8 16 32 64 *(0)*	IRDIS Detector Integration Time
DET.IRDIS.NDIT	1..1000 *(1)*	IRDIS Number of DIT
INS.COMB.IFLT	DB_H23 DB_H34 DB_NDH23 BB_H *(NO DEFAULT)*	IRDIS filter combination
INS.COMB.IND.FLUX	ND_N_0.0 ND_N_1.0 ND_N_2.0 ND_N_3.5 *(NODEFAULT)*	Infrared neutral density filters combination (flux)
INS.COMB.IND	ND_N_0.0 ND_N_1.0 ND_N_2.0 ND_N_3.5 *(NODEFAULT)*	Infrared neutral density filters combination
INS.COMB.ROT	PUPIL FIELD *(NODEFAULT)*	Derotator and ADC modes combination
INS.CPRT.POSANG	0.0..360.0 *(0.0)*	Derotator position angle (deg)
SEQ.IFS.DIT.FLUX	0 2 4 8 16 32 64 *(0)*	IFS Integration Time (flux)
SEQ.IFS.NDIT.FLUX	1..1000 *(1)*	IFS Number of integrations (flux)
SEQ.IFS.NDIT.SKY	1..1000 *(1)*	IFS Number of integrations (sky)
SEQ.IFS.NDIT.STARCENTER	1..1000 *(1)*	IFS Number of integrations (star center)
SEQ.IFS.NEXPO	1..100 *(1)*	IFS exposures per dithering position
SEQ.IRDIS.DIT.FLUX	0 2 4 8 16 32 64 *(0)*	IRDIS Integration Time (flux)
SEQ.IRDIS.DITH.NPATTERN	1..100 *(1)*	IRDIS dithering pattern repetitions
SEQ.IRDIS.DITH.PATTERN	1x1 2x2 4x4 6x6 8x8 10x10 *(4x4)*	IRDIS dithering pattern sequence
SEQ.IRDIS.NDIT.FLUX	1..1000 *(1)*	IRDIS Number of integrations (flux)
SEQ.IRDIS.NDIT.SKY	1..1000 *(1)*	IRDIS Number of integrations (sky)
SEQ.IRDIS.NDIT.STARCENTER	1..1000 *(1)*	IRDIS Number of integrations (star center)
SEQ.IRDIS.NEXPO	1..100 *(1)*	IRDIS exposures per dithering position
SEQ.OBSTYPE.LIST	F C O S *(NODEFAULT)*	Observation type (F, C, O, S)
SEQ.TARG.OFFSETALPHA .LIST	0..60 *(NODEFAULT)*	Sky RA offset list (arcsec)
SEQ.TARG.OFFSETDELTA .LIST	0..60 *(NODEFAULT)*	Sky DEC offset list (arcsec)
SEQ.TARG.OFFSETX	0..400 *(400)*	Detector X offset (mas)
SEQ.TARG.OFFSETY	0..400 *(400)*	Detector Y offset (mas)
SEQ.WAFFLE.AMPLITUDE	0..0.05 *(0.02)*	DM waffle pattern amplitude
SEQ.WAFFLE.ORIENTATION	x + *(x)*	DM waffle pattern orientation
Fixed values:		
SEQ.IFS.DITH.NPATTERN	1	IFS dithering pattern repetitions
SEQ.IFS.DITH.PATTERN	1x1	IFS dithering pattern sequence

Table 29: SPHERE_irdifs_ext_obs

SPHERE_irdifs_ext_obs.tsf		
Parameter	Range *(Default)*	Label
DET.IFS.DIT	0 2 4 8 16 32 64 *(0)*	IFS Detector Integration Time
DET.IFS.NDIT	1..1000 *(1)*	IFS Number of DIT
DET.IRDIS.DIT	0 2 4 8 16 32 64 *(0)*	IRDIS Detector Integration Time
DET.IRDIS.NDIT	1..1000 *(1)*	IRDIS Number of DIT
INS.COMB.IND.FLUX	ND_N_0.0 ND_N_1.0 ND_N_2.0 ND_N_3.5 *(NODEFAULT)*	Infrared neutral density filters combination (flux)
INS.COMB.IND	ND_N_0.0 ND_N_1.0 ND_N_2.0 ND_N_3.5 *(NODEFAULT)*	Infrared neutral density filters combination
INS.COMB.ROT	PUPIL FIELD *(NODEFAULT)*	Derotator and ADC modes combination
INS.CPRT.POSANG	0.0..360.0 *(0.0)*	Derotator position angle (deg)
SEQ.IFS.DIT.FLUX	0 2 4 8 16 32 64 *(0)*	IFS Integration Time (flux)
SEQ.IFS.NDIT.FLUX	1..1000 *(1)*	IFS Number of integrations (flux)
SEQ.IFS.NDIT.SKY	1..1000 *(1)*	IFS Number of integrations (sky)
SEQ.IFS.NDIT.STARCENTER	1..1000 *(1)*	IFS Number of integrations (star center)
SEQ.IFS.NEXPO	1..100 *(1)*	IFS exposures per dithering position
SEQ.IRDIS.DIT.FLUX	0 2 4 8 16 32 64 *(0)*	IRDIS Integration Time (flux)
SEQ.IRDIS.DITH.NPATTERN	1..100 *(1)*	IRDIS dithering pattern repetitions
SEQ.IRDIS.DITH.PATTERN	1x1 2x2 4x4 6x6 8x8 10x10 *(4x4)*	IRDIS dithering pattern sequence
SEQ.IRDIS.NDIT.FLUX	1..1000 *(1)*	IRDIS Number of integrations (flux)
SEQ.IRDIS.NDIT.SKY	1..1000 *(1)*	IRDIS Number of integrations (sky)
SEQ.IRDIS.NDIT.STARCENTER	1..1000 *(1)*	IRDIS Number of integrations (star center)
SEQ.IRDIS.NEXPO	1..100 *(1)*	IRDIS exposures per dithering position
SEQ.OBSTYPE.LIST	F C O S *(NODEFAULT)*	Observation type (F, C, O, S)
SEQ.TARG.OFFSETALPHA.LIST	0..60 *(NODEFAULT)*	Sky RA offset list (arcsec)
SEQ.TARG.OFFSETDELTA.LIST	0..60 *(NODEFAULT)*	Sky DEC offset list (arcsec)
SEQ.TARG.OFFSETX	0..400 *(400)*	Detector X offset (mas)
SEQ.TARG.OFFSETY	0..400 *(400)*	Detector Y offset (mas)
SEQ.WAFFLE.AMPLITUDE	0..0.2 *(0.05)*	DM waffle pattern amplitude
SEQ.WAFFLE.ORIENTATION	x + *(x)*	DM waffle pattern orientation
Fixed values:		
Parameter	Value	Label
INS.COMB.IFLT	DB_K12 BB_K *(NODEFAULT)*	IRDIS filter combination
SEQ.IFS.DITH.NPATTERN	1	IFS dithering pattern repetitions
SEQ.IFS.DITH.PATTERN	1x1	IFS dithering pattern sequence

Table 30: SPHERE_irdis_dbi_obs

SPHERE_irdis_dbi_obs.tsf		
Parameter	Range *(Default)*	Label
DET.IRDIS.DIT	0 2 4 8 16 32 64 *(0)*	IRDIS Detector Integration Time
DET.IRDIS.NDIT	1..1000 *(1)*	IRDIS Number of DIT
INS.COMB.IFLT	DB_Y23 DB_J23 DB_H23 DB_H32 DB_H34 DB_K12 DB_NDH23 DB_NDH32 *(DB_H23)*	IRDIS filter combination
INS.COMB.IND.FLUX	ND_N_0.0 ND_N_1.0 ND_N_2.0 ND_N_3.5 *(NODEFAULT)*	Infrared neutral density filters combination (flux)
INS.COMB.IND	ND_N_0.0 ND_N_1.0 ND_N_2.0 ND_N_3.5 *(NODEFAULT)*	Infrared neutral density filters combination
INS.COMB.ROT	FIELD PUPIL *(NODEFAULT)*	Derotator and ADC modes combination
INS.CPRT.POSANG	0.0..360.0 *(0.0)*	Derotator position angle (deg)
SEQ.IRDIS.DIT.FLUX	0 2 4 8 16 32 64 *(0)*	IRDIS Integration Time (flux)
SEQ.IRDIS.DITH.NPATTERN	1..100 *(1)*	IRDIS dithering pattern repetitions
SEQ.IRDIS.DITH.PATTERN	1x1 2x2 4x4 6x6 8x8 10x10 *(4x4)*	IRDIS dithering pattern sequence
SEQ.IRDIS.NDIT.FLUX	1..1000 *(1)*	IRDIS Number of integrations (flux)
SEQ.IRDIS.NDIT.SKY	1..1000 *(1)*	IRDIS Number of integrations (sky)
SEQ.IRDIS.NDIT.STARCENTER	1..1000 *(1)*	IRDIS Number of integrations (star center)
SEQ.IRDIS.NEXPO	1..100 *(1)*	Number of exposures
SEQ.OBSTYPE.LIST	F C O S *(NODEFAULT)*	Observation type (F, C, O, S)
SEQ.TARG.OFFSETALPHA .LIST	0..60 *(NODEFAULT)*	Sky RA offset list (arcsec)
SEQ.TARG.OFFSETDELTA .LIST	0..60 *(NODEFAULT)*	Sky DEC offset list (arcsec)
SEQ.TARG.OFFSETX	0..400 *(400)*	Detector X offset (mas)
SEQ.TARG.OFFSETY	0..400 *(400)*	Detector Y offset (mas)
SEQ.WAFFLE.AMPLITUDE	0..0.2 *(0.05)*	DM waffle pattern amplitude
SEQ.WAFFLE.ORIENTATION	x + *(x)*	DM waffle pattern orientation

Table 31: SPHERE_irdis_ci_obs

SPHERE_irdis_ci_obs.tsf		
To be specified:		
Parameter	Range *(Default)*	Label
DET.IRDIS.DIT	0 2 4 8 16 32 64 *(0)*	IRDIS Detector Integration Time
DET.IRDIS.NDIT	1..1000 *(1)*	IRDIS Number of DIT
INS.COMB.IFLT	BB_Y BB_J BB_H BB_Ks NB_HeI NB_CntJ NB_PaB NB_CntH NB_FeII NB_CntK1 NB_H2 NB_BrG NB_CO NB_CntK2 *(NODEFAULT)*	IRDIS filter combination
INS.COMB.IND.FLUX	ND_N_0.0 ND_N_1.0 ND_N_2.0 ND_N_3.5 *(NODEFAULT)*	Infrared neutral density filters combination (flux)
INS.COMB.IND	ND_N_0.0 ND_N_1.0 ND_N_2.0 ND_N_3.5 *(NODEFAULT)*	Infrared neutral density filters combination
INS.COMB.ROT	FIELD PUPIL *(NODEFAULT)*	Derotator and ADC modes combination
INS.CPRT.POSANG	0.0..360.0 *(0.0)*	Derotator position angle (deg)
SEQ.IRDIS.DIT.FLUX	0 2 4 8 16 32 64 *(0)*	IRDIS Integration Time (flux)
SEQ.IRDIS.DITH.NPATTERN	1..100 *(1)*	IRDIS dithering pattern repetitions
SEQ.IRDIS.DITH.PATTERN	1x1 2x2 4x4 6x6 8x8 10x10 *(4x4)*	IRDIS dithering pattern sequence
SEQ.IRDIS.NDIT.FLUX	1..1000 *(1)*	IRDIS Number of integrations (flux)
SEQ.IRDIS.NDIT.SKY	1..1000 *(1)*	IRDIS Number of integrations (sky)
SEQ.IRDIS.NDIT.STARCENTER	1..1000 *(1)*	IRDIS Number of integrations (star center)
SEQ.IRDIS.NEXPO	1..100 *(1)*	Number of exposures
SEQ.OBSTYPE.LIST	F C O S *(NODEFAULT)*	Observation type (F, C, O, S)
SEQ.TARG.OFFSETALPHA.LIST	0..60 *(NODEFAULT)*	Sky RA offset list (arcsec)
SEQ.TARG.OFFSETDELTA.LIST	0..60 *(NODEFAULT)*	Sky DEC offset list (arcsec)
SEQ.TARG.OFFSETX	0..400 *(400)*	Detector X offset (mas)
SEQ.TARG.OFFSETY	0..400 *(400)*	Detector Y offset (mas)
SEQ.WAFFLE.AMPLITUDE	0..0.2 *(0.05)*	DM waffle pattern amplitude
SEQ.WAFFLE.ORIENTATION	x + *(x)*	DM waffle pattern orientation

Table 32: SPHERE_irdis_dpi_obs

SPHERE_irdis_dpi_obs.tsf			
To be specified:			
Parameter	Hidden	Range *(Default)*	Label
DET.IRDIS.DIT	no	0 2 4 6 8 12 16 24 32 48 64 96 *(0)*	IRDIS DIT (Object)
DET.IRDIS.NDIT	no	1..1000 *(1)*	IRDIS NDIT (Object)
DPR.CATG	yes	SCIENCE CALIB ACQUISITION TECHNICAL *(SCIENCE)*	Data product category
INS.COMB.IFLT	no	DP_0_BB_Y DP_0_BB_J DP_0_BB_H DP_0_BB_Ks DP_0_NB_HeI DP_0_NB_CntJ DP_0_NB_PaB DP_0_NB_CntH DP_0_NB_FeII DP_0_NB_CntK1 DP_0_NB_H2 DP_0_NB_BrG DP_0_NB_CO DP_0_NB_CntK2 *(NODEFAULT)*	IRDIS filter combination
INS.COMB.IND.FLUX	no	ND_N_0.0 ND_N_1.0 ND_N_2.0 ND_N_3.5 *(NODEFAULT)*	IR ND filter (Flux)
INS.COMB.IND	no	ND_N_0.0 ND_N_1.0 ND_N_2.0 ND_N_3.5 *(NODEFAULT)*	IR ND filter (Object)
INS.COMB.ROT	no	FIELD PUPIL *(FIELD)*	Derotator Mode
INS.CPRT.POSANG	no	0.0..360.0 *(0.0)*	Derotator position angle (deg)
SEQ.IRDIS.DIT.FLUX	no	0 2 4 6 8 12 16 24 32 48 64 96 *(0)*	IRDIS DIT (Flux)
SEQ.IRDIS.DITH.NPATTERN	no	1..100 *(1)*	IRDIS DITHER REPEATS
SEQ.IRDIS.DITH.PATTERN	no	1x1 2x2 4x4 6x6 8x8 10x10 *(4x4)*	IRDIS DITHER PATTERN
SEQ.IRDIS.DITH.STOP.POS	yes	*(0)*	
SEQ.IRDIS.NDIT.FLUX	no	1..1000 *(1)*	IRDIS NDIT (Flux)
SEQ.IRDIS.NDIT.SKY	no	1..1000 *(1)*	IRDIS NDIT (Sky)
SEQ.IRDIS.NDIT.STARCENTER	no	1..1000 *(1)*	IRDIS NDIT (Center)
SEQ.IRDIS.NEXPO	no	1..100 *(1)*	Number of exposures
SEQ.IRDIS.POL.STOKES	no	Q QU *(QU)*	Stoke parameter measure
SEQ.IRDIS.ROM.THRESH	yes	0..43200 *(0)*	IRDIS DIT threshold for ROM (s)
SEQ.OBSTYPE.LIST	no	F C O S *(NODEFAULT)*	Observation type (F, C, O, S)
SEQ.POL.NCYCLE	no	1..100 *(1)*	Number of polarimetric cycles
SEQ.POL.OFFSET.GAMMA	no	-360..360 *(0)*	Polarization: gamma parameter (degrees)
SEQ.TARG.OFFSETALPHA.LIST	no	-60..60 *(NODEFAULT)*	Sky RA offset list (arcsec)
SEQ.TARG.OFFSETDELTA.LIST	no	-60..60 *(NODEFAULT)*	Sky DEC offset list (arcsec)
SEQ.TARG.OFFSETX	no	-500..500 *(400)*	Detector X offset (mas) for (flux)
SEQ.TARG.OFFSETY	no	-500..500 *(400)*	Detector Y offset (mas) for (flux)
SEQ.WAFFLE.AMPLITUDE	no	0..0.2 *(0.05)*	DM waffle pattern amplitude (star center)
SEQ.WAFFLE.ORIENTATION	no	x + *(x)*	DM waffle pattern orientation (star center)

Table 33: SPHERE_irdis_lss_obs

SPHERE_irdis_lss_obs.tsf		
Parameter	Range *(Default)*	Label
DET.IRDIS.DIT	0 2 4 8 16 32 64 *(0)*	IRDIS Detector Integration Time
DET.IRDIS.NDIT	1..1000 *(1)*	IRDIS Number of DIT
INS.COMB.IND	ND_N_0.0 ND_N_1.0 ND_N_2.0 ND_N_3.5 *(NODEFAULT)*	Infrared neutral density filters combination
INS.CPRT.POSANG	0.0..360.0 *(0.0)*	Derotator position angle (deg)
SEQ.IRDIS.NEXPO	1..100 *(1)*	Number of exposures

Table 34: SPHERE_zimpol_p1_obs

SPHERE_zimpol_p1_obs.tsf		
Parameter	Range *(Default)*	Label
DET.ZIMPOL.DIT	0..1200 *(1.3)*	Integration time
DET.ZIMPOL.NDIT	1..1000 *(2)*	Number of integrations
DET.ZIMPOL.READOUT	FastPolarimetry SlowPolarimetry *(FastPolarimetry)*	ZIMPOL read-out mode
DET.ZIMPOL.SHUTTER	Enabled Disabled *(Disabled)*	ZIMPOL detector shutter
INS.ZCSL.NAME	OPEN COMP *(COMP)*	ZIMPOL polarization compensator selector
INS.ZCTT.POS	-90.0..90.0 *(25.0)*	ZIMPOL polarization compensator, tilt angle
INS.ZIFW0.NAME	OPEN P_VIS PQ_VIS Q_VIS ND_1.0 ND_2.0 ND_4.0 Ha_NB OI_630 HeI V_S V_L 730_NB I_L *(OPEN)*	ZIMPOL common filter wheel
INS.ZIFW1.NAME	OPEN VBB I_PRIM R_PRIM N_I N_R B_Ha CntHa V Cnt820 TiO_717 CH4_727 KI *(N_R)*	Arm 1 filter
INS.ZIFW2.NAME	OPEN VBB I_PRIM R_PRIM N_I N_R B_Ha CntHa V Cnt820 N_Ha Cnt748 PUPIM *(N_R)*	Arm 2 filter
SEQ.ZIMPOL.DITH.PATTERN.LIST	-14..14 *(-14 -14 0 0 +14 +14)*	List of pixel coordinates for dithering
SEQ.ZIMPOL.FIELD.POS	0 1 2 3 4 5 6 7 8 9 *(0)*	Field position on ZIMPOL detector
SEQ.ZIMPOL.NEXPO	1..100 *(1)*	Number of exposures per dithering position
SEQ.ZIMPOL.NPOL	1..100 *(1)*	ZIMPOL - Number of polarimetric cycles
SEQ.ZIMPOL.POL.GAMMA	0..360 *(0)*	ZIMPOL - Polarization: gamma parameter.
SEQ.ZIMPOL.POL.PCOMLOOP	T F *(F)*	Initial computation of PCOM tilt angle
SEQ.ZIMPOL.POL.STOKES	Q QU QnoSwitch *(QU)*	Defines if we measure (+Q,-Q) or (+Q,-Q,+U,-U)

Table 35: SPHERE_zimpol_p2_obs

SPHERE_zimpol_p2_obs.tsf		
Parameter	Range *(Default)*	Label
DET.ZIMPOL.DIT	0..1200 *(1.3)*	Integration time
DET.ZIMPOL.NDIT	1..1000 *(2)*	Number of integrations
DET.ZIMPOL.READOUT	FastPolarimetry SlowPolarimetry *(FastPolarimetry)*	ZIMPOL read-out mode
DET.ZIMPOL.SHUTTER	Enabled Disabled *(Disabled)*	ZIMPOL detector shutter
INS.ZCSL.NAME	OPEN COMP *(COMP)*	ZIMPOL polarization compensator selector
INS.ZCTT.POS	-90.0..90.0 *(25.0)*	ZIMPOL polarization compensator, tilt angle
INS.ZIFW0.NAME	OPEN P_VIS PQ_VIS Q_VIS ND_1.0 ND_2.0 ND_4.0 Ha_NB OI_630 HeI V_S V_L 730_NB I_L *(OPEN)*	ZIMPOL common filter wheel
INS.ZIFW1.NAME	OPEN VBB I_PRIM R_PRIM N_I N_R B_Ha CntHa V Cnt820 TiO_717 CH4_727 KI *(N_R)*	Arm 1 filter
INS.ZIFW2.NAME	OPEN VBB I_PRIM R_PRIM N_I N_R B_Ha CntHa V Cnt820 N_Ha Cnt748 PUPIM *(N_R)*	Arm 2 filter
SEQ.ZIMPOL.DITH.PATTERN.LIST	-14..14 *(-14 -14 0 0 +14 +14)*	List of pixel coordinates for dithering
SEQ.ZIMPOL.FIELD.POS	0 1 2 3 4 5 6 7 8 9 *(0)*	Field position on ZIMPOL detector
SEQ.ZIMPOL.FIELD.POSANG	0..360 *(0.0)*	Field orientation on detector
SEQ.ZIMPOL.NEXPO	1..100 *(1)*	Number of exposures per dithering position
SEQ.ZIMPOL.NPOL	1..100 *(1)*	ZIMPOL - Number of polarimetric cycles
SEQ.ZIMPOL.POL.GAMMA	0..360 *(0)*	ZIMPOL - Polarization: gamma parameter.
SEQ.ZIMPOL.POL.STOKES	Q QU QnoSwitch *(QU)*	Defines if we measure (+Q,-Q) or (+Q,-Q,+U,-U)

Table 36: SPHERE_zimpol_i_obs

SPHERE_zimpol_i_obs.tsf		
Parameter	Range *(Default)*	Label
DET.ZIMPOL.DIT	0..1200 *(1.3)*	Integration time
DET.ZIMPOL.NDIT	1..1000 *(1)*	Number of integrations
DET.ZIMPOL.READOUT	StandardImaging SnapShotImaging *(StandardImaging)*	ZIMPOL read-out mode
DET.ZIMPOL.SHUTTER	Enabled Disabled *(Disabled)*	ZIMPOL detector shutter
INS.CPRT.MODE	FIELD PUPIL *(FIELD)*	Pupil derotator mode
INS.ZIFW0.NAME	OPEN P_VIS PQ_VIS Q_VIS ND_1.0 ND_2.0 ND_4.0 Ha_NB OI_630 HeI V_S V_L 730_NB I_L *(OPEN)*	ZIMPOL common filter wheel
INS.ZIFW1.NAME	OPEN VBB I_PRIM R_PRIM N_I N_R B_Ha CntHa V Cnt820 TiO_717 CH4_727 KI *(N_R)*	Arm 1 filter
INS.ZIFW2.NAME	OPEN VBB I_PRIM R_PRIM N_I N_R B_Ha CntHa V Cnt820 N_Ha Cnt748 PUPIM *(N_R)*	Arm 2 filter
SEQ.ZIMPOL.DITH.PATTERN.LIST	-14..14 *(-14 -14 0 0 +14 +14)*	List of pixel coordinates for dithering
SEQ.ZIMPOL.FIELD.POS	0 1 2 3 4 5 6 7 8 9 *(0)*	Field position on ZIMPOL detector
SEQ.ZIMPOL.FIELD.POSANG	0..360 *(0.0)*	Field orientation on detector
SEQ.ZIMPOL.NEXPO	1..100 *(1)*	Number of exposures per dithering position

Table 37: SPHERE_GoTo_acq

SPHERE_GoTo_acq.tsf			
To be specified:			
Parameter	Hidden	Range *(Default)*	Label
DPR.CATG	yes	SCIENCE CALIB ACQUISITION TECHNICAL *(ACQUISITION)*	Data product category
SEQ.AO.ST	no	T F *(T)*	SAXO state
SEQ.PRESET	yes	T F *(T)*	Telescope preset flag
SEQ.SKY.OFFSETALPHA	yes	0..60 *(5)*	Offset in RA for background measurement (arcsec)
SEQ.SKY.OFFSETDELTA	yes	0..60 *(5)*	Offset in DEC for background measurement (arcsec)
SEQ.TARGET.HMAG	no	-4..18 *(0)*	Target H magnitude
SEQ.TARGET.RMAG	no	-10..18 *(0)*	Target R magnitude
TEL.AG.GUIDESTAR	no	NONE SETUPFILE CATALOGUE *(CATALOGUE)*	Telescope guide star selection
TEL.GS1.ALPHA	no	ra *(0.)*	RA of guide star
TEL.GS1.DELTA	no	dec *(0.)*	DEC of guide star
TEL.TARG.ADDVELALPHA	yes	-15..15 *(0.0)*	Differential tracking in RA
TEL.TARG.ADDVELDELTA	yes	-15..15 *(0.0)*	Differential tracking in DEC
TEL.TARG.ALPHA	no	ra *()*	RA
TEL.TARG.DELTA	no	dec *()*	DEC
TEL.TARG.EPOCH	no	-2000..3000 *(2000)*	Epoch
TEL.TARG.EQUINOX	no	-2000..3000 *(2000)*	Equinox
TEL.TARG.OFFSETALPHA	yes	*(0)*	RA offset
TEL.TARG.OFFSETDELTA	yes	*(0)*	DEC offset
TEL.TARG.PMA	no	-500..500 *(0)*	Proper motion in RA
TEL.TARG.PMD	no	-500..500 *(0)*	Proper motion in DEC
Fixed values:			
Parameter	Hidden	Value	Label

Table 38: SPHERE_irdifs_acq_rrm

SPHERE_irdifs_acq_rrm.tsf			
To be specified:			
Parameter	Hidden	Range *(Default)*	Label
DPR.CATG	yes	SCIENCE CALIB ACQUISITION TECHNICAL *(ACQUISITION)*	Data product category
INS.COMB.ICOR	no	N_ALC_YJH_S N_ALC_Ks N_ALC_YJH_L N_CLC_SW_L N_NS_CLEAR N_ALC_YJ_S N_SAM_7H *(NODEFAULT)*	IR Coronagraph
INS.COMB.ROT	no	PUPIL FIELD *(NODEFAULT)*	Derotator Mode
INS.CPRT.POSANG	no	0.0..360.0 *(0.0)*	Derotator position angle (deg)
INS.MODE	no	IRDIFS IRDIFS_EXT *(NODEFAULT)*	Instrument Mode
SEQ.AO.ST	no	T F *(T)*	SAXO state
SEQ.DO.CENTERING	yes	T F *(F)*	Perform centering?
SEQ.DO.FOCUS	yes	T F *(F)*	Perform focus optimization?
SEQ.DTTS.BACKGND	yes	T F *(T)*	DTTS background flag
SEQ.IFS.ROM.THRESH	yes	0..43200 *(0)*	IFS DET level to change ROM
SEQ.INSTALL_CFG	yes	T F *(F)*	Install in system configuration for use?
SEQ.PRESET	yes	T F *(T)*	Telescope preset flag
SEQ.RRM.REGISTER	no	T F *(T)*	Register OB in RRM system
SEQ.RRM.VISITOR	no	T F *(T)*	Allow RRM activation in Visitor mode
SEQ.SKY.OFFSETALPHA	yes	0..60 *(5)*	Offset in RA for background measurement (arcsec)
SEQ.SKY.OFFSETDELTA	yes	0..60 *(5)*	Offset in DEC for background measurement (arcsec)
SEQ.TARGET.HMAG	no	-4..18 *(0)*	Target H magnitude
SEQ.TARGET.RMAG	no	-10..18 *(0)*	Target R magnitude
SEQ.VWFS.BACKGND	yes	T F *(F)*	VWFS background flag
TEL.AG.GUIDESTAR	no	NONE SETUPFILE CATALOGUE *(CATALOGUE)*	Telescope guide star selection
TEL.GS1.ALPHA	no	ra *(0.)*	RA of guide star
TEL.GS1.DELTA	no	dec *(0.)*	DEC of guide star
TEL.TARG.ADDVELALPHA	yes	-15..15 *(0.0)*	Differential tracking in RA
TEL.TARG.ADDVELDELTA	yes	-15..15 *(0.0)*	Differential tracking in DEC
TEL.TARG.ALPHA	no	ra *()*	RA
TEL.TARG.DELTA	no	dec *()*	DEC
TEL.TARG.EPOCH	no	-2000..3000 *(2000)*	Epoch
TEL.TARG.EQUINOX	no	-2000..3000 *(2000)*	Equinox
TEL.TARG.OFFSETALPHA	yes	*(0)*	RA offset
TEL.TARG.OFFSETDELTA	yes	*(0)*	DEC offset
TEL.TARG.PMA	no	-500..500 *(0)*	Proper motion in RA
TEL.TARG.PMD	no	-500..500 *(0)*	Proper motion in DEC
Fixed values:			
Parameter	Hidden	Value	Label

Table 39: SPHERE_irdis_acq_rrm

SPHERE_irdis_acq_rrm.tsf			
To be specified:			
Parameter	Hidden	Range *(Default)*	Label
DPR.CATG	yes	SCIENCE CALIB ACQUISITION TECHNICAL *(ACQUISITION)*	Data product category
INS.COMB.ICOR	no	N_ALC_YJH_S N_ALC_YJH_L N_ALC_Ks N_CLC_SW_L N_CLC_LW_L N_NS_CLEAR N_ALC_YJ_S N_SAM_7H *(NODEFAULT)*	IR Coronagraph
INS.COMB.ROT	no	FIELD PUPIL *(NODEFAULT)*	Derotator Mode
INS.CPRT.POSANG	no	0.0..360.0 *(0.0)*	Derotator position angle (deg)
SEQ.AO.ST	no	T F *(T)*	SAXO state
SEQ.DO.CENTERING	yes	T F *(F)*	Perform centering?
SEQ.DO.FOCUS	yes	T F *(F)*	Perform focus optimization?
SEQ.DTTS.BACKGND	yes	T F *(T)*	DTTS background flag
SEQ.INSTALL_CFG	yes	T F *(F)*	Install in system configuration for use?
SEQ.PRESET	yes	T F *(T)*	Telescope preset flag
SEQ.RRM.REGISTER	no	T F *(T)*	Register OB in RRM system
SEQ.RRM.VISITOR	no	T F *(T)*	Allow RRM activation in Visitor mode
SEQ.SKY.OFFSETALPHA	yes	0..60 *(5)*	Offset in RA for background measurement (arcsec)
SEQ.SKY.OFFSETDELTA	yes	0..60 *(5)*	Offset in DEC for background measurement (arcsec)
SEQ.TARGET.HMAG	no	-4..18 *(0)*	Target H magnitude
SEQ.TARGET.RMAG	no	-10..18 *(0)*	Target R magnitude
SEQ.VWFS.BACKGND	yes	T F *(F)*	VWFS background flag
TEL.AG.GUIDESTAR	no	NONE SETUPFILE CATALOGUE *(CATALOGUE)*	Telescope guide star selection
TEL.GS1.ALPHA	no	ra *(0.)*	RA of guide star
TEL.GS1.DELTA	no	dec *(0.)*	DEC of guide star
TEL.TARG.ADDVELALPHA	yes	-15..15 *(0.0)*	Differential tracking in RA
TEL.TARG.ADDVELDELTA	yes	-15..15 *(0.0)*	Differential tracking in DEC
TEL.TARG.ALPHA	no	ra *()*	RA
TEL.TARG.DELTA	no	dec *()*	DEC
TEL.TARG.EPOCH	no	-2000..3000 *(2000)*	Epoch
TEL.TARG.EQUINOX	no	-2000..3000 *(2000)*	Equinox
TEL.TARG.OFFSETALPHA	yes	*(0)*	RA offset
TEL.TARG.OFFSETDELTA	yes	*(0)*	DEC offset
TEL.TARG.PMA	no	-500..500 *(0)*	Proper motion in RA
TEL.TARG.PMD	no	-500..500 *(0)*	Proper motion in DEC
Fixed values:			
Parameter	Hidden	Value	Label

Table 40: SPHERE_zimpol_i_acq_rrm

SPHERE_zimpol_i_acq_rrm.tsf			
To be specified:			
Parameter	Hidden	Range *(Default)*	Label
DPR.CATG	yes	SCIENCE CALIB ACQUISITION TECHNICAL *(ACQUISITION)*	Data product category
INS.COMB.VCOR	no	V_CLC_S_WF V_CLC_M_WF V_CLC_MT_WF V_CLC_L_WF V_CLC_XL_WF V_NC_WF V_SAM_7H *(V_CLC_M_WF)*	Visible coronagraph combination
INS.CPRT.MODE	no	FIELD PUPIL *(FIELD)*	Pupil derotator mode
INS.CPRT.POSANG	no	0.0..360.0 *(0.0)*	Derotator position angle (deg)
INS.ZISL.NAME	no	BS_GREY DIC_HA *(BS_GREY)*	Position of the ZIMPOL/WFS selector
SEQ.AO.ST	no	T F *(T)*	SAXO state
SEQ.APPLY.DTTPDV	yes	T F *(F)*	Apply DTTP delta voltages?
SEQ.DO.CENTERING	yes	T F *(F)*	Perform centering?
SEQ.DO.FOCUS	yes	T F *(F)*	Perform focus optimization?
SEQ.PRESET	yes	T F *(T)*	Telescope preset flag
SEQ.RRM.REGISTER	no	T F *(T)*	Register OB in RRM system
SEQ.RRM.VISITOR	no	T F *(T)*	Allow RRM activation in Visitor mode
SEQ.SKY.OFFSETALPHA	yes	0..60 *(5)*	Offset in RA for background measurement (arcsec)
SEQ.SKY.OFFSETDELTA	yes	0..60 *(5)*	Offset in DEC for background measurement (arcsec)
SEQ.TARGET.RMAG	no	-10..18 *(0)*	Target R magnitude
SEQ.VWFS.BACKGND	yes	T F *(F)*	VWFS background flag
TEL.AG.GUIDESTAR	no	NONE SETUPFILE CATALOGUE *(CATALOGUE)*	Telescope guide star selection
TEL.GS1.ALPHA	no	ra *(0.)*	RA of guide star
TEL.GS1.DELTA	no	dec *(0.)*	DEC of guide star
TEL.TARG.ADDVELALPHA	yes	-15..15 *(0.0)*	Differential tracking in RA
TEL.TARG.ADDVELDELTA	yes	-15..15 *(0.0)*	Differential tracking in DEC
TEL.TARG.ALPHA	no	ra *()*	RA
TEL.TARG.DELTA	no	dec *()*	DEC
TEL.TARG.EPOCH	no	-2000..3000 *(2000)*	Epoch
TEL.TARG.EQUINOX	no	-2000..3000 *(2000)*	Equinox
TEL.TARG.OFFSETALPHA	yes	*(0)*	RA offset
TEL.TARG.OFFSETDELTA	yes	*(0)*	DEC offset
TEL.TARG.PMA	no	-500..500 *(0)*	Proper motion in RA
TEL.TARG.PMD	no	-500..500 *(0)*	Proper motion in DEC
Fixed values:			
Parameter	Hidden	Value	Label

Table 41: SPHERE_zimpol_p_acq_rrm

SPHERE_zimpol_p_acq_rrm.tsf			
To be specified:			
Parameter	Hidden	Range *(Default)*	Label
DPR.CATG	yes	SCIENCE CALIB ACQUISITION TECHNICAL *(ACQUISITION)*	Data product category
INS.COMB.VCOR	no	V_CLC_S_WF V_CLC_M_WF V_CLC_MT_WF V_CLC_L_WF V_CLC_XL_WF V_NC_WF V_SAM_7H *(V_CLC_M_WF)*	Visible coronagraph combination
INS.CPRT.MODE	no	FIELD FIXED *(FIELD)*	Pupil derotator mode
INS.CPRT.POSANG	no	0.0..360.0 *(0.0)*	Derotator position angle (deg)
INS.ZISL.NAME	no	BS_GREY DIC_HA *(BS_GREY)*	Position of the ZIMPOL/WFS selector
SEQ.AO.ST	no	T F *(T)*	SAXO state
SEQ.APPLY.DTTPDV	yes	T F *(F)*	Apply DTTP delta voltages?
SEQ.DO.CENTERING	yes	T F *(F)*	Perform centering?
SEQ.DO.FOCUS	yes	T F *(F)*	Perform focus optimization?
SEQ.PRESET	yes	T F *(T)*	Telescope preset flag
SEQ.RRM.REGISTER	no	T F *(T)*	Register OB in RRM system
SEQ.RRM.VISITOR	no	T F *(T)*	Allow RRM activation in Visitor mode
SEQ.SKY.OFFSETALPHA	yes	0..60 *(5)*	Offset in RA for background measurement (arcsec)
SEQ.SKY.OFFSETDELTA	yes	0..60 *(5)*	Offset in DEC for background measurement (arcsec)
SEQ.TARGET.RMAG	no	-10..18 *(0)*	Target R magnitude
SEQ.VWFS.BACKGND	yes	T F *(F)*	VWFS background flag
TEL.AG.GUIDESTAR	no	NONE SETUPFILE CATALOGUE *(CATALOGUE)*	Telescope guide star selection
TEL.GS1.ALPHA	no	ra *(0.)*	RA of guide star
TEL.GS1.DELTA	no	dec *(0.)*	DEC of guide star
TEL.TARG.ADDVELALPHA	yes	-15..15 *(0.0)*	Differential tracking in RA
TEL.TARG.ADDVELDELTA	yes	-15..15 *(0.0)*	Differential tracking in DEC
TEL.TARG.ALPHA	no	ra *()*	RA
TEL.TARG.DELTA	no	dec *()*	DEC
TEL.TARG.EPOCH	no	-2000..3000 *(2000)*	Epoch
TEL.TARG.EQUINOX	no	-2000..3000 *(2000)*	Equinox
TEL.TARG.OFFSETALPHA	yes	*(0)*	RA offset
TEL.TARG.OFFSETDELTA	yes	*(0)*	DEC offset
TEL.TARG.PMA	no	-500..500 *(0)*	Proper motion in RA
TEL.TARG.PMD	no	-500..500 *(0)*	Proper motion in DEC
Fixed values:			
Parameter	Hidden	Value	Label

10. DATA REDUCTION

Obtaining calibration files from the ESO archive

Darks and flats are taken every morning after SPHERE observations, in the appropriate filters and with the appropriate exposure times for the science data. Moreover, to check the health of the instrument, calibrations are also taken on a weekly basis using standard setups (see chapter on the calibration plan). One can download necessary calibration files from the ESO Data Archive (archive.eso.org/eso/eso_archive_main.html). For example, to download IRDIS calibrations from the archive page, one can enter the *Start* and *End* UT dates for the data they want. Furthermore, one can select *SPHERE/VLT* under *Imaging, CALIB* under *Category, Dark* under *Data Product Info:Type.* If desired one can also choose the exposure time under *Instrumental Setup: Exptime.* Pressing the *Search* button displays the calibrations available for download. **To pin point calibrations more rapidly and avoid downloading unnecessary files, one can use the SPHERE specific form which allows to narrow down the searches with help of header keywords**:

archive.eso.org/wdb/wdb/eso/sphere/form

The data reduction procedures are described in the SPHERE pipeline manual. For a short summary we outline the principal steps for each instrument:

IFS reduction cascade summary

1. **Correction using a dark frame taken with the IFS shutter closed and all internal lamps off. In this step hot pixels and cosmic ray hits are removed and the background subtracted. The IFS background is dominated by thermal emission, which depends on the temperature of the instrument.**
2. **Correction for the wavelength-dependent detector flat-field (pixel-to-pixel response variations). This needs at least three detector flats taken at different wavelengths, possibly another one taken in white light. These are taken with IFS shutter closed and one of its internal calibration sources switched on.**
3. **Wavelength calibration using a pixel description table that holds the wavelengths assigned to each pixel, its illumination fraction, and spectrum ID. This table is made in two steps: First, spectra are detected on an external flat-field frame with IFS shutter open and the external white light calibration source switched on. Then, a wavelength solution is found on a frame where again IFS shutter is open and 3 or 4 of the monochromatic external calibration sources are switched on. Wavelength calibration is obtained using an integrating sphere and laser lines at 0.9877, 1.1237, 1.3094, and 1.5451 (µm).**
4. **Application of an IFU flat. This corrects for throughput variations between individual lens-lets (spaxels). It is derived from the same flat-field as used in the first step 3.**
5. **Construction of a cube of evenly spaced monochromatic planes. This is actually the endpoint of the automated pipeline. Note that it does not combine several cubes. The results can be fed to (manually operated) data analysis recipes or dedicated software packages.**

IRDIS reduction cascade summary

10.1.1 DBI, classical imaging

Data reduction of DBI and classical imaging mode data is as follows:

1. **Correction using a dark frame.**

2. **Application of the internal flat-field.**
3. **Determination of the position of the optical axis in each of the two simultaneous images. To do this, a dedicated calibration is used where a waffle pattern is applied to SPHERE's high-order deformable mirror. This causes four off-axis peaks to appear (even in coronagraphic images), the positions of which are detected and measured. Their centers of illumination are then used as center of rotation and to align the two frames.**
4. **The combination of all input frames. This includes optionally de-rotation, spectral differencing, and angular differencing.**

10.1.2 IRDIS DPI

The DPI mode of IRDIS works essentially the same way as the other imaging modes. The official SPHERE pipeline does not currently provide any (polarimetric) analysis recipes. However, there is now a highly-automated end-to-end pipeline to reduce IRDIS polarimetric data called IRDAP (IRDIS Data reduction for Accurate Polarimetry) which is publicly available at https://irdap.readthedocs.io. IRDAP's core feature is the correction of instrumental polarization effects based on the fully validated Mueller matrix model describing the instrument and telescope as described in van Holstein et al. (2019). IRDAP handles both field- and pupil-tracking data (even for non-optimal HWP laws), and for the latter can additionally perform angular differential imaging (ADI).

10.1.3 Long slit spectroscopy

Data reduction of LSS mode data is as follows:

1. **Correction using dark.**
2. **Application of internal flat.**
3. **Wavelength calibration, taken the same way as for IFS.**
4. **Combination of all input frames. Output is a frame that has wavelengths assigned to each pixel. The extraction of a spectrum, e.g. a correction for telluric absorption that is measured in the same way on a calibration star, is left to the user.**

ZIMPOL reduction cascade summary

Because of the stripe mask on the ZIMPOL detector, all recipes include a pre-processing step that re-orders the image rows into logical and viewable images. All recipes provide these pre-processed data as optional output.

10.1.4 Imaging

The principal calibration steps for imaging are:

1. **Subtraction of the bias level. The default method is a subtraction of the mean value for the overscan pixels. A bias frame subtraction can be used if a fixed read-out noise pattern is present.**
2. **Possibly a subtraction of a dark frame of matching exposure time or interpolated to a matching exposure time. For short integration times (e.g. <30 s) this is not needed. Noise in the dark frame may add noise to the science image.**
3. **Flat-fielding with flat field calibration frames taken with the same filter (and the same focal plane coronagraph plate if a coronagraph on a substrate is used).**

4. **Combination of all frames using optionally some filtering of outliers. The combination includes back-shifting of dithered images and optionally also the derotation of the frames (see Schmid et al. 2018; 2018A&A...619A...9S).**

The ZIMPOL QuickLook RTD (real time display) shows the pre-processed, overscan bias subtracted image of the first frame in an exposure.

10.1.5 Polarimetry

The principle calibration steps for polarimetry are:

1. **Subtraction of the bias level. For slow polarimetry a subtraction of the mean value for the overscan pixels provides good results. For fast polarimetry, a bias frame subtraction should be used to remove the fixed read-out column feature.**
2. **Dark current correction as for imaging**
3. **Correction for the modulation-demodulation efficiency. This is derived from frames illuminated evenly by the 100% polarized flat field calibration source and corrects for the pixel-dependent efficiency to in shifting charges back and forth during integration, thus measuring polarization. The modulation-demodulation efficiency calibration is only applied to the polarization frame.**
4. **Flatfielding as for imaging. The flatfielding is only applied to the intensity frame.**
5. **Combination of all frames as for imaging (with dithering and rotation corrections) and derivation of the intensity image and Q, or U polarization state.**

The ZIMPOL QuickLook RTD shows the pre-processed, overscan bias subtracted intensity frame (top) and the polarimetrically combined fractional polarization frame (bottom) for the two first frames of an exposure.

AO performance monitoring

The AO system of SPHERE generates parameter files accessible through the archive. These file are multi-extension fits files containing binary tables and images. One file is generated every time a new acquisition template is run. It stores every 20s the strehl, atmospheric parameters estimated by the real time calculator (turbulent wind speed, Fried parameter, seeing) and other AO internal parameters (flux on the visible wavefront sensor and infra-red DTTS camera) and every 2s the image of the DTTS camera (for coronagraphic near-infrared observations).This information can be useful for atmospheric and performance monitoring and the DTTS image can be used to monitor the photometry. These files are accessible in the dedicated SPHERE archive query form http://archive.eso.org/wdb/wdb/eso/sphere/form by entering OBJECT,AO in the DPR TYPE field (User defined input) in addition to the night of observation.

11. OVERHEADS

The most important contributors to overheads are:

a. **Target acquisition: this strongly dominates the overheads when staying on the same target less than 1hr.**
b. **Detector: overheads associated to the detector operations.**

Additionally, the HW setup changes (including dithering, filter or HWP swapping) also contribute, depending on the observing sequence. The observing overheads can be estimated by creating test Observing Blocks in the P2 demo environment (https://www.eso.org/p2demo).

Target acquisition

Target acquisition (whenever a new target is pointed at) includes the telescope preset (= 6 min, see, e.g. http://www.eso.org/sci/facilities/paranal/cfp/cfp95/overheads.html), AO loop closing (including the measurement of flux, performance, and the check of the selected setup). Given the small fields of view of the 3 instruments accurate coordinates and proper motions of all targets are mandatory. In case the initial pointing is not accurate enough to guarantee that the AO sensors detect the star within its ~2'' FoV, larger FoV images should be obtained by the operator. This could easily cost an additional 2 minutes.

If the coronagraph set-up has been changed (or if the previous check is older than typically one hour), it is recommended to repeat the coronagraph centering.

Observing Blocks (OBs) typically last 1 hour. Hence, in Service Mode, single OBs or the first OB in a concatenation must take into account the overhead for centering given in Table 42: IRDIS and IFS detector properties.. In Visitor Mode, the overhead mentioned in Table 42: IRDIS and IFS detector properties. should be taken into account every hour.

Table 42: Target acquisition execution times for all acquisition templates, including the 6 min of telescope preset, along with typical execution times for star center (C), and flux (F).

Action	**Approximate duration**
Acquisition	10 min **(including 6 min of telescope preset)**
Coronagraph centering	+ 5 min
Star Center – C	+ 3.5 min
Flux – F	+ 3.5 min

IRDIS and IFS observation overheads

The formula to compute execution time for IRDIS and IFS, including overheads, are:

time_IFS = (O_START_IFS + NDIT_IFS * (DIT_DELAY_IFS + DIT_IFS + ROT_IFS) + O_EXP_IFS) * NEXP_IFS
time_IRD = ((T_START_IRD + NDIT_IRD * (DIT_DELAY_IRD + DIT_IRD + ROT_IRD) + O_EXP_IRD) * NEXPO_IRD + O_DITH_IRD) * NDITHER * NPATTERN

The total execution for an IRDIFS sequence is :

time_obs = MAX(time_IFS, time_IRD)

In these formulas, DIT_IFS and DIT_IRD are the detector integration times for IFS and IRDIS, NDIT_IFS and NDIT_IRD the number of DITs, NEXP_IFS the number of IFS exposures, NDITHER the number of dithering positions for IRDIS, NEXPO_IRD the number of exposures per dithering position, ROT_IFS and ROT_IRD the readout times, DIT_DELAY_IFS and DIT_DELAY_IRD an additional readout delay, and O_* various detector and mechanical overheads for IFS and IRDIS. The value of these overheads are given in the table below.
Note that the minimum DIT for IRDIS is 0.838 s for IRDIS, while it is 1.65 s for IFS. You have to take this different into account when trying to match the execution time of IRDIFS observations.

Table 43: Overheads for IFS and IRDIS observations

Operation	**IFS**	**IRDIS**
O_START	0.3	0.3
DIT_DELAY	0.2	0.1
ROT	1.65	0.838
O_EXP	1.1	1.1
O_DITH_IRD		1.77

ZIMPOL observation overheads

The formula to compute typical ZIMPOL execution times, including overheads is:
(DIT + O_DIT) * NDIT * NEXPO * CYCLE * NPOL * NDITH * NETA + O_EXPO * NEXPO * CYCLE * NPOL * NDITH * NETA + O_NPOL * CYCLE * NPOL * NDITH * NETA + O_DITH * NDITH * NETA + O_ETA * NETA
Where DIT is the detector integration time, O_DIT, the DIT overhead, NDIT, the number of DITs, NEXPO, the number of exposures per position, O_EXPO, the exposure overhead, NPOL, the number of polarimetric cycles (CYCLE = 1 for QnoSwitch, 2 for Q, 4 for QU), NDITH, the number of dithering positions, O_DITH the overhead associated with dithering, NETA, the number of field angles, O_NETA, the overhead associated with derotator setting.

Table 44: ZIMPOL approximate overheads.

Mode	FastPol	SlowPol	StdI
O_DIT	0.1	0.1	0.1
O_EXPO	3	13	3

Table 45: HW setup overheads in ZIMPOL observations.

Operation	Overhead
O_NPOL	5
O_DITH	5
O_ETA	5

Typical examples (CYCLE = 2, Q):

	DIT	**NDIT**	**NEXPO**	**NPOL**	**NDITH**	**NETA**	**OST**	**Duration**		**Effic.**
								(s)	**(min)**	
SlowPol	50	2	2	2	1	3	2400	2852	47	0.84
FastPol	1.2	50	1	2	3	3	2160	2688	45	0.8
StdI	5	6	2	N/A	40	N/A	2400	2888	48	0.83

APPENDIX

A1. Detector properties

A1.1 IRDIS and IFS detectors

IRDIS and IFS are equipped with a 2Kx2K Hawaii-2RG arrays manufactured by Teledyne Imaging Sensors. The detectors are operated with cryogenic preamplifiers located next to the focal plane and operating at temperatures of ~80 K. The data acquisition system is the ESO New Generation Controller (NGC). The controller reads all the 32 video channels of each of the two Hawaii-2RG detectors in parallel. Users are advised to pay special attention to the saturation limits to avoid persistence in subsequent frames. Although historically we advised users to stay below the 0.1% linearity limit (20K) given in Table 42, we will allow exposures to the 1% linearity limit (35K), (see Figure 39). This is because with changing seeing, predicted detector counts are often exceeded, but we would like to avoid aborting observation blocks to change the DIT when within the 1% linearity limit. For the DITs below 2s, we still need to observe the 0.1% linearity limit. IRDIFS persistence falls to background levels in 10s after mild saturation (see Figure 39).

Table 42: IRDIS and IFS detector properties.

	IRDIS	**IFS**
Detector arrays	2k x 2k (2k x 1k read) Hawaii-2RG	2k x 2k Hawaii-2RG
Readout mode	Non destructive sampling (NonDest)	Non destructive sampling (NonDest)
Readout noise	4 (long DIT) - 10 (short DIT) e^- rms/pix/readout	4 (long DIT) - 10 (short DIT) e^- rms/pix/readout
Dark current	Negligible	Negligible
Gain	1.75 e^-/ADU	1.8 e^-/ADU
Quantum efficiency	>95% from Y to K	>95% from Y to H
MINDIT/readout time	0.83s	1.66s
Linearity and saturation	0.1% up to 10^5 e^- 20000 ADU linearity 40000 ADU saturation	0.1% up to 10^5 e^- 20000 ADU linearity 40000 ADU saturation

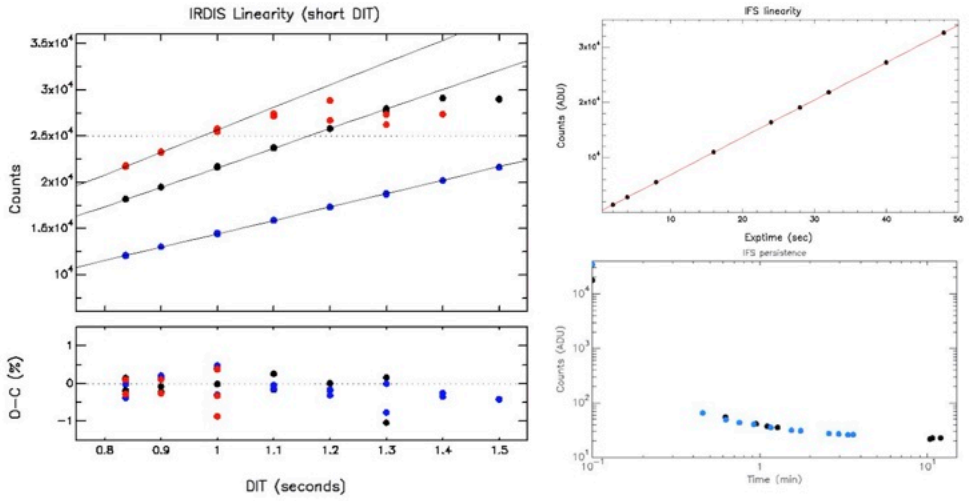

Figure 39: IRDIFS linearity and persistence

A1.2 ZIMPOL detectors

The ZIMPOL detectors CCD1 and CCD2 consist of 4k x 2k pixel, back-illuminated, frame transfer CCDs (e2v CCD 44-82 bi) with 15 µm x 15 µm pixels. They have two read-out registers which work in parallel, each reading out half a line. The 2k x 2k CCD is in all modes operated like a 1k x 1k pixel CCD with 2 x 2 pixel binning allowing faster read-out and providing an effective pixel size of 30 µm x 30 µm. The saturation limit is at 65000 while linearity is at 63000 ADUs.

Table 47: ZIMPOL detector and readout mode properties.

	Fast polarimetry	**Slow polarimetry**	**Standard Imaging**
Science application	high precision polarimetry of targets with intermediate brightness (R ~ 3-7 mag) in broad band filters	photon noise limited polarimetry of faint targets, or bright star observations of the outer PSF or in narrow band filters	Standard imaging, when polarization information is not needed
Modulation: frequency, time	967 Hz, 1.03 ms	27 Hz, 37ms	N/A
Row shift time (binned row)	54.7 µs	72.3 µs	N/A
Detector field of view*	3.5"×3.5", 1024 × 512 pix	3.5"× 3.5", 1024 × 512 pix	3.5"×3.5", 1024 × 512 pix
Integration times: min-max	1.2 – 100 s	10 – 1000 s	1.2 – 1000 s
Frame transfer time	56 ms	74 ms	66 ms
Max. frame rate	0.86 Hz	0.1 Hz	0.86 Hz
Shutter use	Not offered	Not offered	Not offered
Readout: noise, frequency	20 e^-, 625 kHz	3 e^-, 100 kHz	20 e^-, 625 kHz
Gain, well depth	10.5 e^-/ADU, 670 ke^-	1.5 e^-/ADU, 100 ke^-	10.5 e^-/ADU, 670 ke^-
Dark current	0.2 e^-/(s pix)	0.015 e^-/(s pix)	0.2 e^-/(s pix)

* *Effective field of view for one polarization mode I_0 or I_{90}.*

A2. System throughput

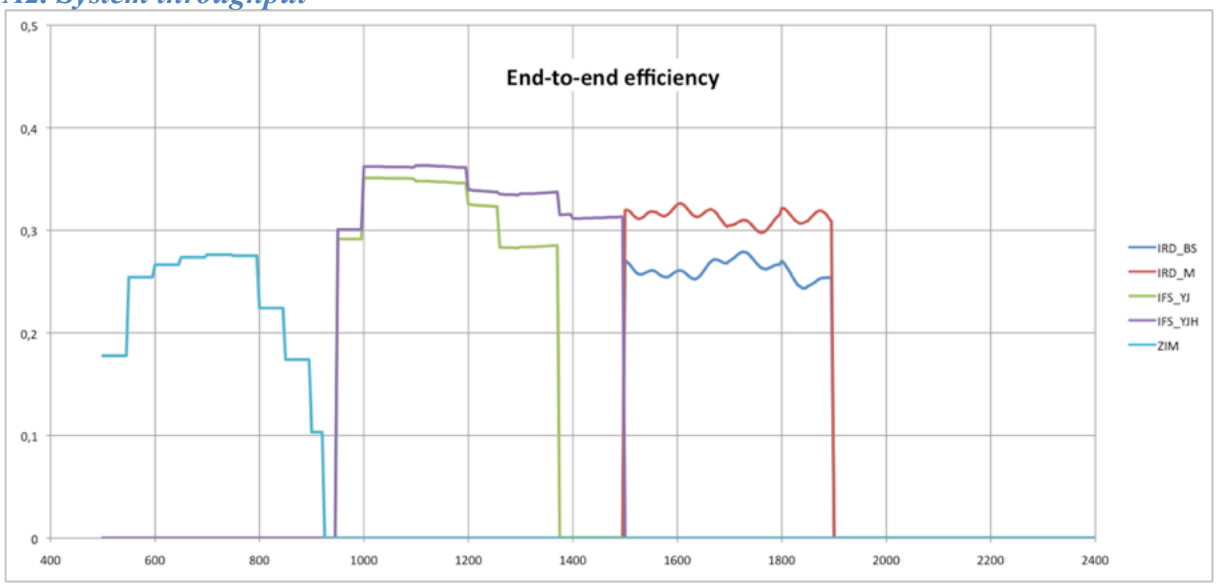

Figure 40: Transmission from SPHERE entrance to the science detectors, including the detector efficiency, assuming i) no coronagraph, ii) ZIMPOL path goes through the GREY beamsplitter (80% to ZIMPOL), and iii) the H dichroic separating the flux between IFS (up to 1450 nm) and IRDIS. Note that IRDIS cannot observe in K band in this setup.

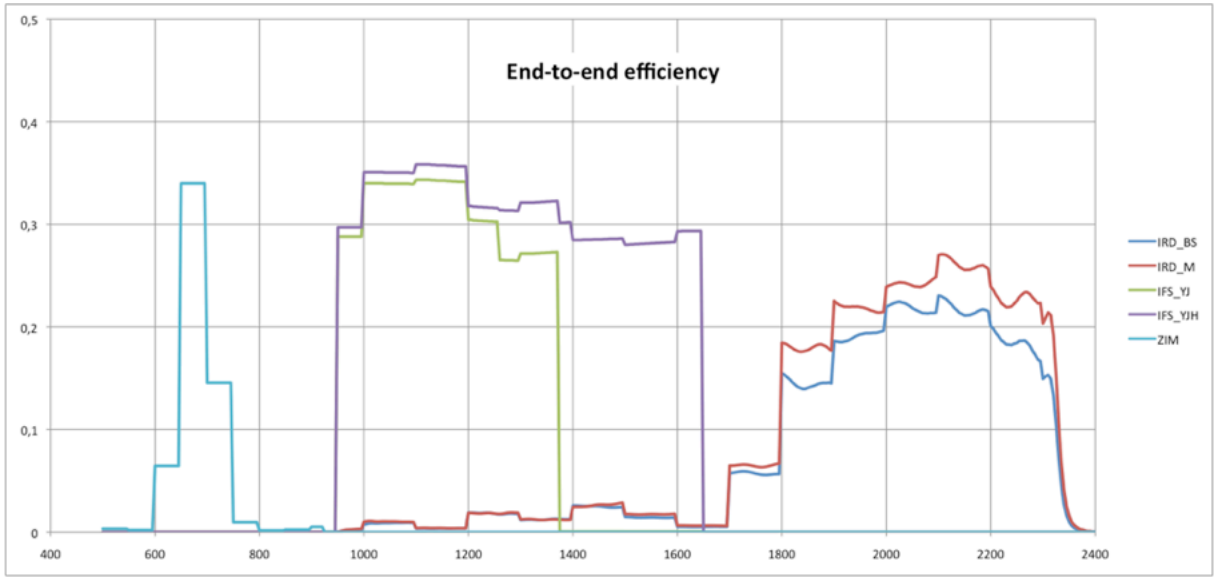

Figure 41: Transmission (as above) with different beamsplitters. In visible: separation between WFS and ZIMPOL uses a dichroic sending more light to ZIMPOL but in R band only; in NIR: the IFS/IRDIS dichroic 'K' feeds IFS with the its full Y-H range, with lower efficiency for IRDIS in K band only.

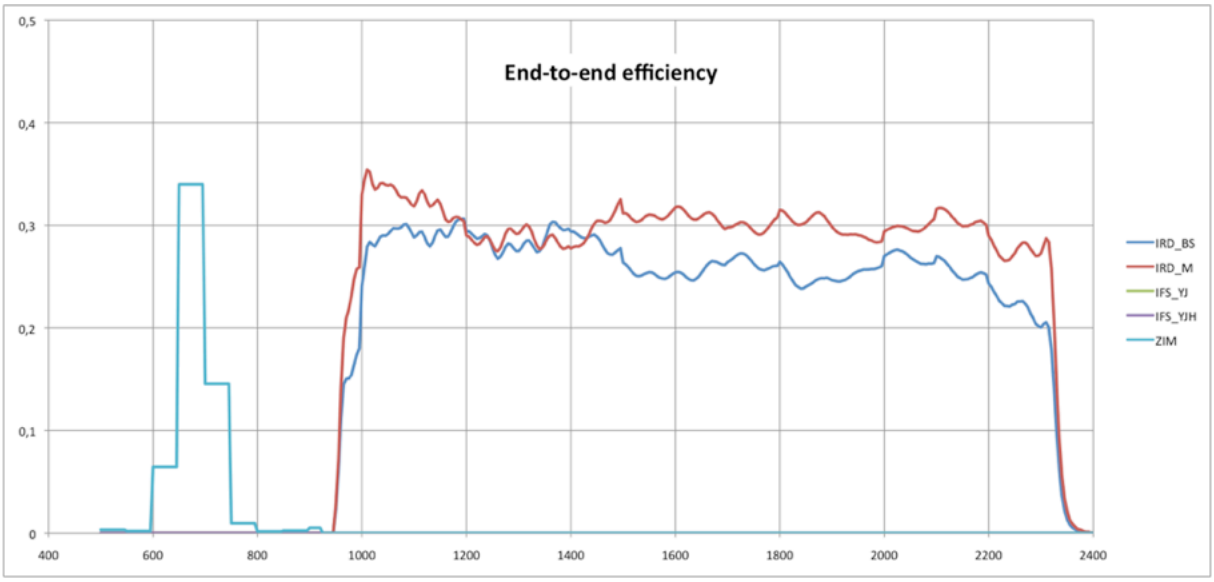

Figure 42: Transmission (as above) in IRDIS alone configuration where all the NIR light is sent to IRDIS.

A3. Neutral densities

Since neutral densities prevent most photons from reaching the detector, their use in science templates should be avoided when possible. Instead, a coronagraph should be considered when trying to prevent saturation. If accurate photometry or astrometry of the primary target is desired, Star center and Flux observations should be considered.
The transmission curves of the VIS and NIR neutral density filters are available here :
https://www.eso.org/sci/facilities/paranal/instruments/sphere/inst/filters.html

A3.1 CPI

The transmissions as a function of wavelength of the neutral density filter of CPI are displayed in Figure 43. These ND filters are common to IRDIS and IFS.

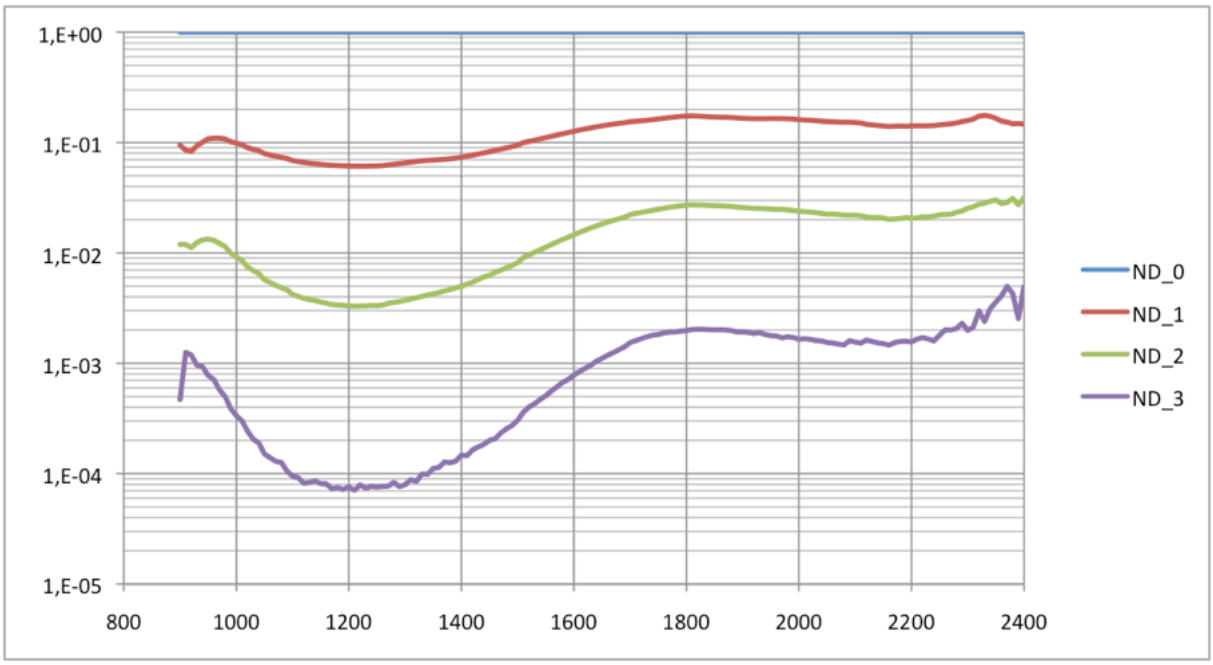

Figure 43: Transmission CPI NIR densities as a function of wavelength (nm).

A3.2 IFS

A filter wheel is mounted within IFS. These filters allow appropriate exposure levels for the IFS internal flat-field lamp. The wheel hosts three neutral density filters (ND1, ND2, ND3). The filters are identical to those in the CPI. They are inclined with respect to the optical axis, to avoid ghosts. This causes a small shift of the optical path.

A3.3 IRDIS

When observing with IRDIS-H in parallel to IFS, it might be useful to reduce the flux seen by IRDIS without affecting IFS data. This can be achieved by using the filter BBF-ND-H (consisting of H + a neutral density filter) instead of BBF-H.

A3.4 ZIMPOL

The transmission as a function of wavelength of the neutral density filters ND1, ND2 and ND4 mounted in filter wheel FW0 are shown in Figure 44.

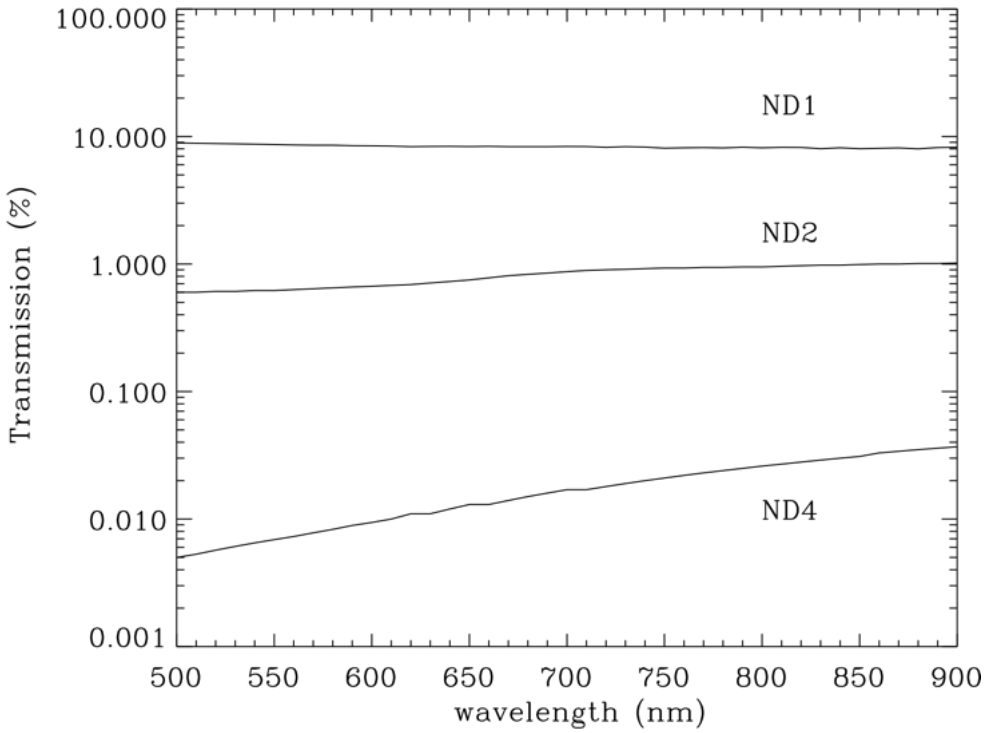

Figure 44: Spectral transmission of the ZIMPOL neutral density filters ND1, ND2 and ND3 (as provided by the manufacturer).

A4. IRDIS beam-splitter

The IRDIS internal beam-splitter separates the flux between the left and the right detector halves. The left (right) half is illuminated by light that is reflected (transmitted) by the splitter. The beam-splitter introduces flux differences between the two detector halves of less than 10% while slightly larger differences are observed for polarized light.

A5. IRDIS filters

IRDIS requires four types of filters: wideband filters (WBF), broadband filters (BBF), narrowband filters covering specific atomic or molecular lines (NBF), and dual band filters used pair wise for dual-band imaging (DBF). WBF, BBF, and NBF are referred to as common filters because they are located in a filter wheel situated in front of the beam separation optics. The DBFs are organized in pairs, located after the beam separation optics. Figure 46, Figure 47 and Figure 48 illustrate the various IRDIS filter transmissions. The numerical values for the transmission curves are at this SPHERE web page link.

The filters available as a function of observing mode are:

- **CI can use any filter (except DBF).**
- **DPI can use any of the BBF and NBF.**
- **DBI can use only the DBF.**

The transmission curves of all IRDIS filters are available here :
https://www.eso.org/sci/facilities/paranal/instruments/sphere/inst/filters.html

The IRDIS narrow band filters suffer from stronger ghosts, which can be seen here:
https://www.eso.org/sci/facilities/paranal/instruments/sphere/inst/sphere-irdis-narrow-band-psfs-and-ghosts.html

Moreover, in general with IRDIS, when a bright star is visible in the top right corner of the detector a faint ghost is visible about 7 arcseconds lower. The ghost does not rotate around the primary as would any off-axis point source in the sky plane. Its position follows the position of the secondary star with a translation vector of length of 7.1" and position angle 181.8º (e.g. 180º + true north of ~1.75º). The ghost was observed both in broad band H and in H2 H3. The contrast between the secondary star and the ghost is about 5 magnitudes (1%; see Figure 45.)

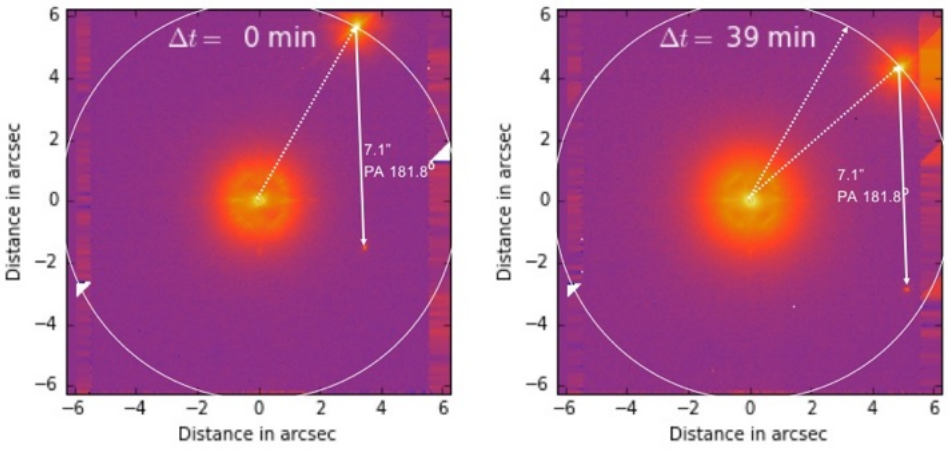

Figure 45: IRDIS ghost appears when there is a bright source on upper right corner of detector.

The DBF are used in conjunction with BBF (acting as blocking filters). In templates, the user is not asked for setting individual wheels but only pre-defined relevant combinations, as presented in Table 45.

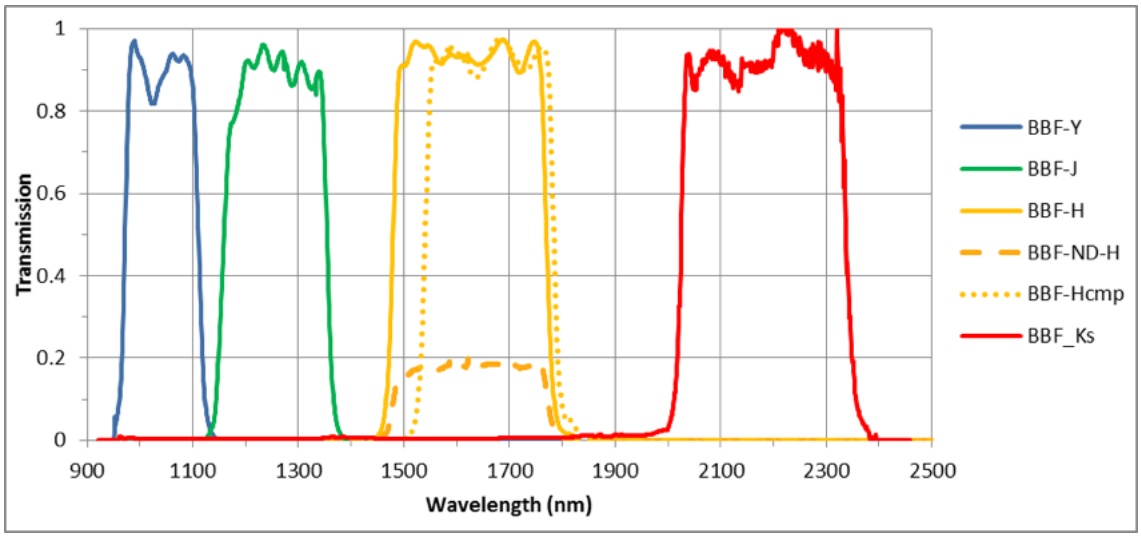

Figure 46: IRDIS BB filters.

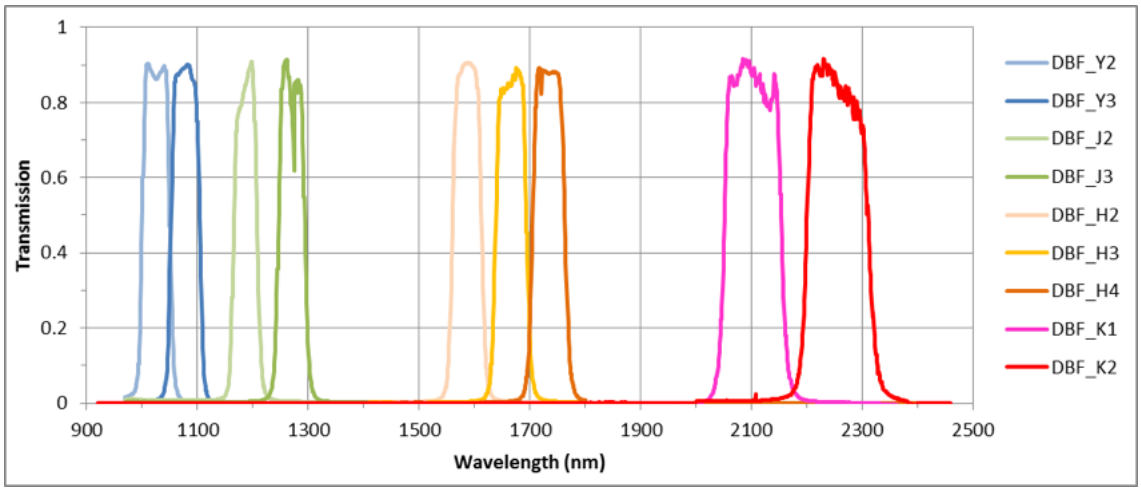

Figure 47: IRDIS DB filters.

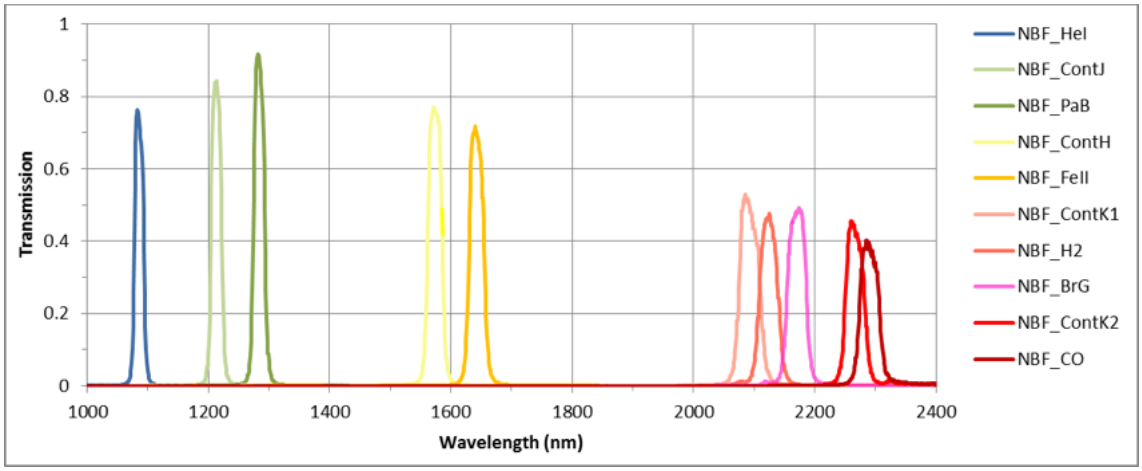

Figure 48: IRDIS NB filters.

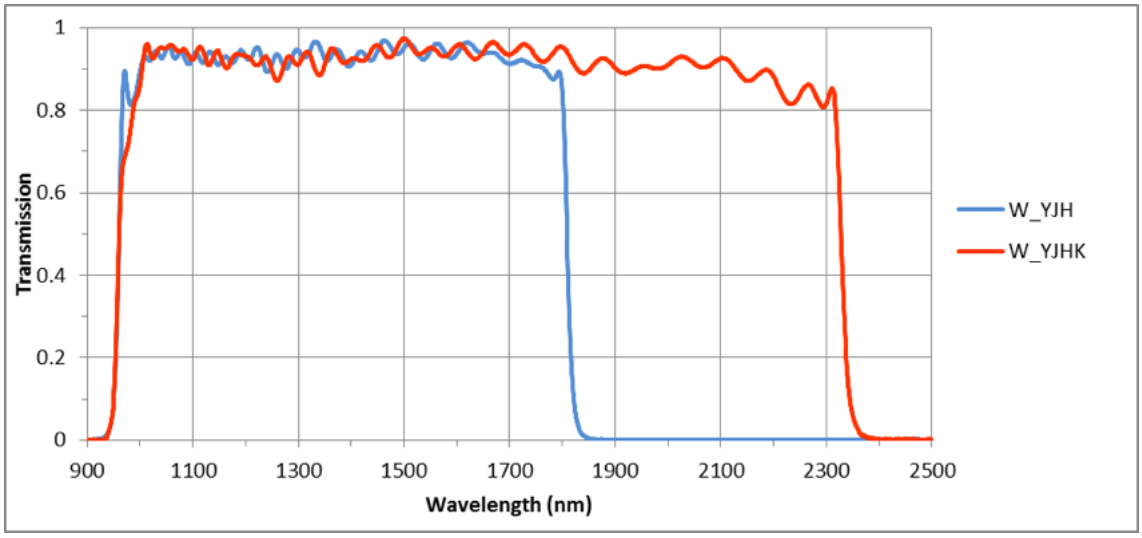

Figure 49: IRDIS wideband filter.

Table 48: IRDIS relevant filter combinations.

Name	Mode	λ_c (nm)	$\Delta\lambda$	IRFW1	IRFW2	Modes
DBI						
DB_Y23	*DBI, Y2-Y3*	*1022 - 1076*	*49 - 50*	B_Y	D_Y23	DBI, CI
DB_J23	*DBI, J2-J3*	*1190 - 1273*	*42 - 46*	B_J	D_J23	DBI, CI
DB_H23	*DBI, H2-H3*	*1593 - 1667*	*52 - 54*	B_H	D_H23	DBI, CI
DB_H32	*DBI, H3-H2*	*1667 - 1593*	*54 - 52*	B_H	D_H32	DBI, CI
DB_H34	*DBI, H3-H4*	*1667 - 1733*	*54 - 57*	B_Hcmp2	D_H34	DBI, CI
DB_K12	*DBI, K1-K2*	*2110 - 2251*	*102 - 109*	B_Ks	D_K12	DBI, CI
DBI + ND filter						
DB_NDH23	*Including ND 0.5*			B_ND-H	D_H23	DBI, CI
DB_NDH32	*Including ND 0.6*			B_ND-H	D_H32	DBI, CI
Broadband						
BB_Y	*Full Y band*	*1043*	*140*	B_Y	CLEAR	DPI, CI
BB_J	*Full J band*	*1245*	*240*	B_J	CLEAR	DPI, CI
BB_H	*Full H band*	*1625*	*290*	B_H	CLEAR	DPI, CI
BB_Ks	*Full Ks band*	*2182*	*300*	B_Ks	CLEAR	DPI, CI
Narrowband						
NB_HeI	*HeI (1083nm)*	*1085*	*14*	N_HeI	CLEAR	DBI, CI
NB_ContJ	*ContJ (1211nm)*	*1213*	*17*	N_ContJ	CLEAR	DBI, CI
NB_PaB	*PaB (1282nm)*	*1283*	*18*	N_PaB	CLEAR	DBI, CI
NB_ContH	*ContH (1574nm)*	*1573*	*23*	N_CntH	CLEAR	DBI, CI
NB_FeII	*FeII (1644nm)*	*1642*	*24*	N_FeII	CLEAR	DBI, CI
NB_ContK1	*ContK1 (2098nm)*	*2091*	*34*	N_CntK1	CLEAR	DBI, CI
NB_H2	*H2 (2122nm)*	*2124*	*31*	N_H2	CLEAR	DBI, CI
NB_BrG	*BrG (2167nm)*	*2170*	*31*	N_BrG	CLEAR	DBI, CI
NB_CO	*CO (2294nm)*	*2290*	*33*	N_CO	CLEAR	DBI, CI
NB_ContK2	*ContK2 (2267nm)*	*2266*	*32*	N_ContK2	CLEAR	DBI, CI
Spectroscopy						
S_LR	*YJHKs*	*1644*	*1370*	W_YJHKs	CLEAR	LSS
S_MR	*YJH*	*1384.5*	*851*	W_YJH	CLEAR	LSS

A6. NIR Coronagraphs

NIR coronagraphs include classical Lyot coronagraphs (CLC) and apodized Lyot coronagraphs (ALC). The available coronagraphs combinations for particular wavelengths and optical elements are summarized in Table 49. The value N_NS_CLEAR indicates that no coronagraph will be used. Since only ALC coronagraphs are offered in service mode, when “Coron” is chosen on the Exposure Time Calculators (ETCs), the choice of coronagraph and returned performances are implicitely the ones corresponding to ALCs.

Table 49: List of NIR coronagraph combinations with filters and slit. The most common combinations are highlighted in green.

Instrument mode	Wavelength/ Filter	Service mode	Visitor mode	
		Recommended* Coronagraph	Small IWA** Coronagraph	Large IWA Coronagraph
IRDIFS or IRDIS alone	IFS-YJ, DB_H23, DB_H34, DB_ND23, DB_NDH23, BB_H	N_ALC_YJH_S (IWA~0''.15)	N_ALC_YJ_S (IWA~0''.08)	N_ALC_YJH_L (IWA~0''.2)
IRDIFS-EXT	IFS-YJH, DB_K12, BB_Ks	N_ALC_YJH_S (IWA~0''.15)	N_ALC_YJ_S (IWA~0''.08)	N_CLC_SW_L (IWA~0''.35)
IRDIS alone	DB_Y23, BB_Y, NB_Hel	N_ALC_YJH_S (IWA~0''.15)	N_ALC_YJ_S (IWA~0''.08)	N_ALC_YJH_L (IWA~0''.2)
IRDIS alone	DB_J23, BB_J, NB_CntJ, NB_PaB	N_ALC_YJH_S (IWA~0''.15)	N_ALC_YJ_S (IWA~0''.08)	N_ALC_YJH_L (IWA~0''.2)
IRDIS alone	BB_H, NB_CntH, NB_FeII	N_ALC_YJH_S (IWA~0''.15)	N_ALC_YJ_S (IWA~0''.08)	N_ALC_YJH_L (IWA~0''.2)
IRDIS alone	DB_K12, BB_Ks	N_ALC_Ks (IWA~0''.2)	N/A	N_CLC_LW_L (IWA~0''.35)
IRDIS alone	NB_CntK1, NB_BrG, NB_CntK2, NB_H2, NB_CO	N_ALC_Ks (IWA~0''.2)	N/A	N_CLC_LW_L (IWA~0''.35)
IRDIS LSS	N_S_LR_WL, N_S_MR_WL	Not offered in service mode	N/A	N_S_LR_WL, N_S_MR_WL, N_S_APO_LR_WL, N_S_APO_MR_WL, N_S_APO_MR_NL (IWA~0''.2)

Three special coronagraphs (only available in visitor mode, for expert users) are not included in the table. For shorter wavelengths, ALC configurations are optimized depending on band and focal mask:* ***ALC_Y, ALC_YJ_S, ALC_YJ_L**.*

A6.1 ALC coronagraphs

The optimal transmission profile of the apodizer depends on the size (in λ/D) of the focal mask. Practically, a given focal mask has a given size in microns, not in units of λ/D. This means that, when observing in broadband filters, a given apodizer and focal mask combination is optimal only at a particular wavelength. The performance of the coronagraph decreases rapidly at longer wavelengths but slowly at shorter wavelengths. The ALC combinations include

- 2 apodizers, APO1 and APO2, optimized for 4 and 5.2 (λ/D) focal masks,
- 3 focal masks, ALC1, ALC2, ALC3, with diameters of 145, 185 and 240 (mas).

The ALC Lyot stop has good transmission (92%) with a large outer radius (96% of VLT pupil). The transmission and resolution are limited by the entrance apodizer. Optimal approved combinations of

apodizer-mask-Lyot stop have been preselected, and cannot be changed for now. These combinations are described in Table 50: Definition of the coronagraph combination.

Table 50: Definition of the coronagraph combination

Coronagraph combination name	Applicable band	Apodizer	Lyot Mask and diameter in mas
N_ALC_YJH_S	YJH	APO1	ALC2 (185mas)
N_ALC_YJH_L	YJH	APO2	ALC3 (240mas)
N_ALC_YJ_S	YJ	APO1	ALC1 (145mas)
N_ALS_YJ_L	YJ	APO2	ALC2 (185mas)
N_ALC_Ks	YJHKs	APO1	ALC3 (240mas)

A characterization of the transmission profile of N_ALC_YJH coronagraph (radius 92.5mas) was measured with IRDIS (H2/H3 filter) and the IFS (Y to J mode) by placing a star behind the coronagraph and offsetting it from the center of the mask.
Numerical end-to-end simulations confirm accurately the measurements of the transmission and are shown in the Figure 50. The vertical axis corresponds to the ratio between the star flux at a given separation and the star flux measured at large separation outside the influence radius of the coronagraphic mask. For the IFS, we measured a small chromatic dependence of the transmission profile which is not reproduced by the simulation (possibly ADC residuals or normalization effects) so we provide a single transmission curve from Y to J.
The measured inner working angle (IWA defined as the separation that yields a transmission of 50%) are 95mas and 99mas for the IFS YJ and IRDIS H2 respectively. About 90% of the flux is recovered at a separation of 130mas from the mask center in all configurations.
In case of a detection close to the coronagraph IWA or to provide contrast curves inside 200mas, correcting for the transmission profile of the coronagraph is required (see Guerri et al. 2011).

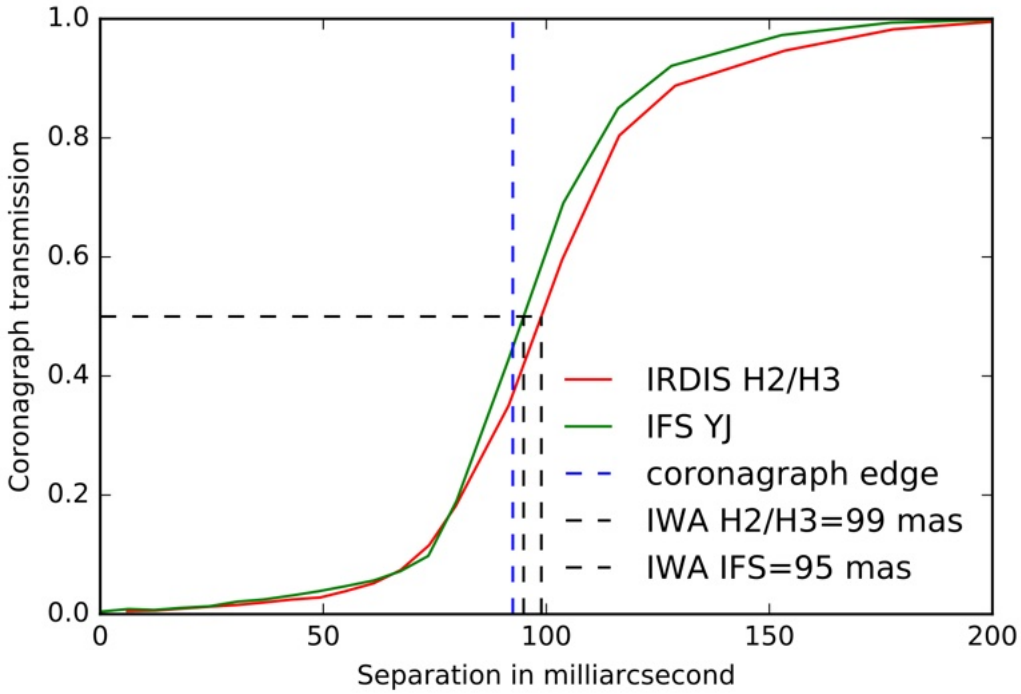

Figure 50 Transmission profile for the N_ALC_JYH_S coronagraph

A7. IFS dispersive components

There are two alternative dispersive elements in IFS. Both are Amici prisms designed either for the Y-J or the Y-H band. The prisms are associated with filters that define the pass-band of each spectrum, avoiding overlap of consecutive spectra along the dispersion direction. Prism parameters are listed in Table 51.

Table 51: IFS prisms parameters.

Parameter	Y-J	Y-H
Spectral length (pixels)	35.4	35.3
Wavelength range (µm)	0.96-1.34	0.97-1.66
Average dispersion (nm/pixel)	10.52	19.15
Average spectral resolution (per FWHM)	55.1	34.5

A8. IRDIS dispersive components

A8.1 LSS

LSS requires a long slit located in the coronagraphic focal plane and a dispersive component (prism or grism) that is located in the IRDIS pupil plane. The corresponding focal plane and pupil plane combinations for LSS are listed in Table 14 (see also Table 49). Naming conventions for named LR_N_L to MR_W_S are:

- LR for low resolution and MR for medium resolution,
- N for narrow (90 mas) and W for wide (120 mas) slit width, both larger than the PSF,
- L for large (400 mas) and S for small (200 mas) size of the central blocking mask.

A8.2 Prism

LRS mode uses a double prism designed for zero deviation close to the center of the spectral range and close to linear dispersion function. The wavelength λ to pixel y relation for the prism is fit by:

$$\lambda = \lambda_0 + c_1*(y-y_0)/100 + c_2*((y-y_0)/100)^2 + c_3*((y-y_0)/100)^3 + c_4*((y-y_0)/100)^4$$

The laser line is at λ_0=1545.07 nm and its position determines y_0. Fit parameters are: c_1 = -9.1293 for channel M or c_1= -9.12795 for channel BS; c_2, c_3 and c_4 are equal for both channels. The relative orientation of the double prisms introduces a higher variance in λ_0 and c_1 than for the grism.

A8.3 Grism

The pixel–wavelength relation is linear for the grism. Fitting parameter c_1 = -1.13878 +/- 0.00022 (nm/pixel) is related to the focal length of the camera mirror. As the two mirrors are slightly different, this term is slightly different for the two channels. In the fit, y_0 corresponds to a constant offset and varies with slit position. The two parameters, y_0 and λ_0, are determined as above.

A9. Visible Coronagraphs

The coronagraphs in the visible are all classical Lyot coronagraphs (CLC). The selection of a coronagraph includes setting of different devices: the focal mask and the pupil stop. The CLC focal masks, which have various diameters, are suspended or deposited on substrates (with no suspending wire), and include a field stop (either full ZIMPOL FoV or restricted to inner 1'' FoV for window mode). Relevant combinations are listed in Table 52. Naming conventions are:

- CLC, NC: for the type of coronagraph (Classical Lyot Coronagraph or no coronagraph).
- S, M, L, XL: for the size of the focal mask from small to very large (93, 155, 310 and 1240 mas, respectively).
- WF: for the wide field stop.

Table 52: List of visible coronagraph combinations. Recommended configurations are highlighted in green.

Mode	Filter	Recommended* Coronagraph	Medium/large/ extra large IWA Coronagraph
ZIMPOL_P1	RI, R_PRIM, I_PRIM, V, N_R, N_I, KI, TiO_717, CH4_727, Cnt748, Cnt820, CntHa, N_Ha, B_Ha	V_CLC_M_WF	V_CLC_S_WF/ V_CLC_L_WF/ V_CLC_XL_WF
ZIMPOL_P2	RI, R_PRIM, I_PRIM, V, N_R, N_I, KI, TiO_717, CH4_727, Cnt748, Cnt820, CntHa, N_Ha, B_Ha	V_CLC_M_WF	V_CLC_S_WF/ V_CLC_L_WF/ V_CLC_XL_WF
ZIMPOL_I	RI, R_PRIM, I_PRIM, V, V_S, V_L, N_R, 730_NB, N_I, I_L, KI, TiO_717, CH4_727, Cnt748, Cnt820, HeI, OI_630, CntHa, B_Ha, N_Ha, Ha_NB	V_CLC_M_WF	V_CLC_S_WF/ V_CLC_L_WF/ V_CLC_XL_WF

Not in the table is the **V_CLC_MT_WF mask (155 mas), which includes a grid of dots that is useful for calibration purposes and/or accurate astrometric reference.*

The selection depends on the required halo rejection, none-saturation capability and IWA:

- **No coronagraph (V_NC_WF or V_NC_NF):** Should be used when the science goal concerns the target itself or its immediate environment at the resolution limit. The N_NC_NF option uses a field stop of 1" (useful for – not yet offered- windowed read-out modes), whereas the full field-of-view is accessible with the V_NV_WF option. Saturation effects are limited thanks to the high CCD pixel-well and by the short DIT possible especially in window mode. Neutral density filters can be inserted unless observing with filters mounted on the FW0. If saturation occurs, the charge leakage is quite limited close to the saturated peak and over the columns. Observations performed so far indicate that artefacts introduced by saturations are very small.
- CLC with increasing mask diameter between 93 and 1240 (mas).
- Special case of V_CLC_MT_WF: this on-substrate 155 mas mask also includes a grid of dots that is useful for calibration purposes and/or accurate astrometric reference.

A10. ZIMPOL filters

ZIMPOL has three filter wheels, FW0 located in front of the polarization modulator and beam splitter, FW1 located in arm 1 of ZIMPOL and FW2 located in arm 2 of ZIMPOL. FW0 contains besides filters for imaging also polarization calibration components and neutral density filters. Recommendations are:

Filters located in FW0 can be used for imaging and they provide the same band-pass in both arms. FW0 cannot be combined with neutral density filters, as they are located in the same wheel. It is not recommended that the FW0 filter be used for polarimetric measurements because they may introduce polarimetric effects that are difficult to calibrate. The combination of FW0 filters with FW1 or FW2 filters is not supported.

Filters located in FW1 and FW2 can be used for imaging, differential imaging and polarization. Different filters can be used in FW1 and FW2, but one needs to be aware that the detector operation (e.g. exposure time) is identical in both arms. The combination of a narrowband filter with a broadband filter may therefore cause an underexposed image in one arm and an overexposed image in the other arm.

The list of relevant combinations, and their names are listed in Table 53. Note that if the dichroic beam splitter is used between ZIMPOL and WFS then only a small wavelength range in the R-band can be observed. This reduces the useful filters to those highlighted in green in Table 53: Measured band-pass of ZIMPOL filters. We list wavelengths (nm), where the transmission is 50% of its maximum, the 50% width and its central wavelength..
The transmission curves of all ZIMPOL filters are available here :
www.eso.org/sci/facilities/paranal/instruments/sphere/inst/filters.html

Table 53: Measured band-pass of ZIMPOL filters. We list wavelengths (nm), where the transmission is 50% of its maximum, the 50% width and its central wavelength.

Filter	λ_{min}	λ_{max}	FWHM	λ_0
RI	590.1	880.6	290.5	735.4
R_PRIM	552	700.6	148.6	626.3
I_PRIM	713.3	866	152.7	789.7
V	513.7	594.3	80.6	554
V_S	513	550.2	37.2	531.6
V_L	560.9	602	41.1	581.5
N_R	617.5	674.2	56.7	645.9
730_NB	705.5	760.4	54.9	733
N_I	776.5	857	80.5	816.8
I_L	842.4	898.8	56.4	870.6
KI	759.6	780.8	21.2	770.2
TiO_717	706.9	726.6	19.7	716.8
CH4_727	720	740.5	20.5	730.3
Cnt748	737.1	757.7	20.6	747.4
Cnt820	807.4	827.2	19.8	817.3
HeI	585.3	590.7	5.4	588
OI_630	626.8	632.2	5.4	629.5
CntHa	642.8	646.9	4.1	644.9
B_Ha	652.9	658.4	5.5	655.6
N_Ha	655.85	656.82	0.97	656.34
Ha_NB	656.04	657.02	0.98	656.49

NOTE: The filters highlighted in green are compatible with the dichroic beamsplitter.

A11. Polarimetric calibration components

ZIMPOL is optimized for the measurement of linear polarization. Here we present a short summary of the critical polarimetric calibration components, the reader is invited to read Bazzon et al. 2012 (SPIE 8446, 93B) for further details about the polarimetric concept.
The most important components for the polarimetric calibration are the linear polarizer and HWPZ. Less important are the quarter-wave plate and the circular polarizer. Note that:

- **The achromatic (dichroic glass) polarizer is made of structured absorptive nanoparticles. It provides a contrast <10^{-3} between 600-900 nm and 10^{-2} between 500-600 nm.**
- **Circular polarization is measured with an achromatic quarter-wave plate made out of MgF_2 and quartz. The retardance error is less than ±6% between 500-900 nm.**
- **The circular polarizer is a combination of a linear polarizer with the fast axis at 45° (±0.5°) followed by a quarter-wave plate with the fast axis at 0°. Both components are of the same. Since the quarter-wave plate is not perfectly achromatic the circular polarizer has a small leakage of linear polarization of several %.**

The reference orientation for the polarimetric alignment is given by the polarizing beam-splitter of ZIMPOL. The transmitted beam (CCD 1) has a linear polarization parallel to the ZIMPOL bench and the reflected beam (CCD 2) an orientation perpendicular

A12. Waffle spots

When a coronagraph is used with IRIDS or ZIMPOL, the position of the star behind the coronagraph can be known by applying a waffle pattern to the DM. This is critical because most post-processing techniques rely on the accurate registration of the star. The pattern creates four replicas of the PSF, called satellite spots, at a separation of about 14 λ/D. The orientation of this pattern can be chosen, between an x shape (position angle of the spots of 45º, 135º, 225º and 315º as shown in Figure 51) or a + shape (position angle of 0º, 90º, 180º and 270º). These spots can be used to find the star center by intersecting the line joining opposite spots, as illustrated in Figure 51. Non coronagraphic observations of a star with the waffle pattern on were obtained to calibrate the accuracy of this technique as illustrated in Figure 52. The star center as estimated from the intersection of the two lines joining opposite satellite spots and from a direct 2d fit on the PSF core agrees within better than 2.5mas.

From period 106, the waffle amplitudes will be set automatically by the template based on the brightness of the star and the filter and DIT. Thus the WAFFLE pattern amplitude (WPA) in observation templates should be left as “AUTO” by default, unless the observer has an atypical goal in mind. The WPA represents the percentage of the full DM stroke to be applied. A WPA of 0.05 makes the spot peaks equal to 1.3% of the star peak at H band, but the ratio scales quadratically with the WPA. Thus spot_peak = 0.013 . star_peak . $(WPA/0.05)^2$. When set to “AUTO”, the WPA will be calculated as $WPA = f \cdot 10^{0.2(Hmag-4)} \cdot DIT^{(-0.5)}$, where f scales with the filter as in the table below.

Filter name	Factor f
DB_Y23	0.05
DB_J23	0.05
DB_H23	0.09
BB_Ks	0.12
BB_H	0.07
DB_K12	0.15

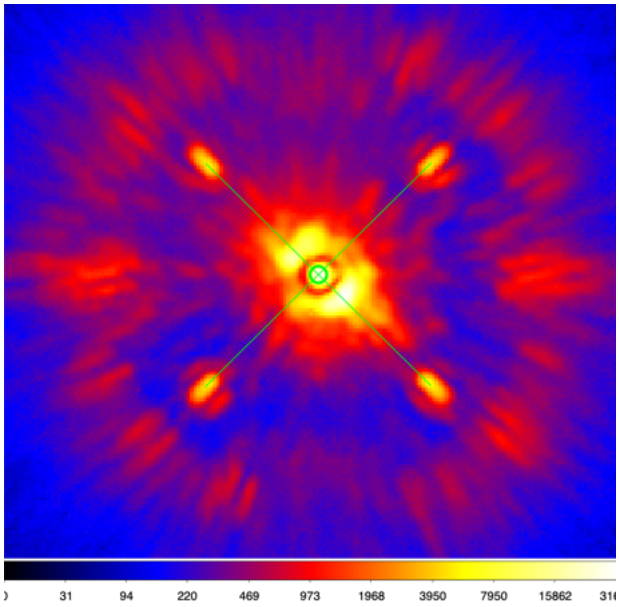

Figure 51. Irdis image in broad-band H, with the N_ALC_YJH coronagraph, with the waffle pattern applied to the DM, creating four satellite spots. These spots are elongated with broad-band filters and point source with narrow-band filters. The green lines start and end points were computed by fitting a 2D Gaussian on each spot, they intersect on the star center, indicated by a green thick circle.

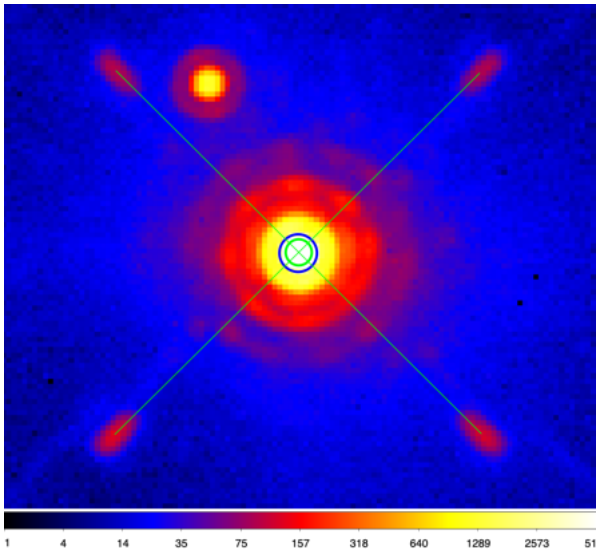

Figure 52 Non coronagraphic image of a star (happening to have a binary companion) in broad-band H with Irdis, after applying a waffle pattern to the DM for calibration purposes. The green thick circle indicates the intersection of the green lines, while the blue thick circle indicates the star position (Gaussian fit). Both agree within 2.5mas.